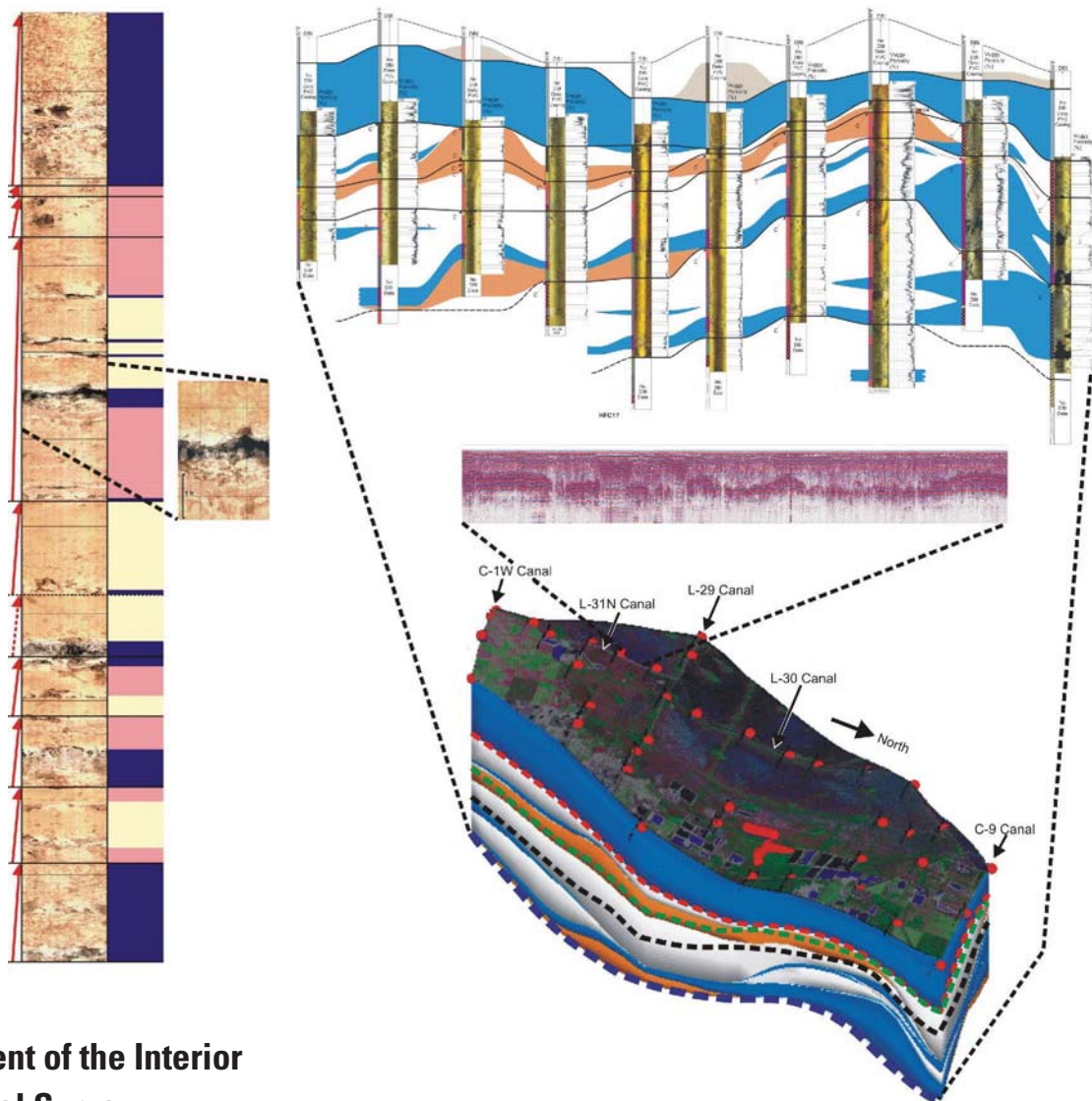# Characterization of Aquifer Heterogeneity Using Cyclostratigraphy and Geophysical Methods in the Upper Part of the Karstic Biscayne Aquifer, Southeastern Florida

Water-Resources Investigations Report 03-4208

U.S. Department of the Interior
U.S. Geological Survey

Prepared in cooperation with the

South Florida Water Management District

Characterization of Aquifer Heterogeneity Using Cyclostratigraphy and Geophysical Methods in the Upper Part of the Karstic Biscayne Aquifer, Southeastern Florida

By Kevin J. Cunningham, Janine L. Carlson, G. Lynn Wingard, Edward Robinson, *and* Michael A. Wacker

U.S. Geological Survey

Water-Resources Investigations Report 03-4208

≋ USGS
science for a changing world

Tallahassee, Florida
2004

U.S. DEPARTMENT OF THE INTERIOR
GALE A. NORTON, Secretary

U.S. GEOLOGICAL SURVEY
Charles G. Groat, Director

CONTENTS

PLATES

[Plates are in pocket]

FIGURES

List of Appendix IV Figures (on CD)

TABLES

Conversion Factors, Acronyms, Abbreviated Units, and Datums

Multiply	By	To obtain
inch (in.)	2.54	centimeter
foot (ft)	0.3048	meter
foot per day (ft/d)	0.3048	meter per day
foot per nanosecond (ft/ns)	0.3048	meter per nanosecond
mile (mi)	1.609	kilometer
mile per hour (mi/hr)	1.609	kilometer per hour

Acronyms

BIPS	Borehole image processing system
CMP	Common mid-point
DS	Depositional sequence
ENP	Everglades National Park
GWFC	Ground-water flow class
GPR	Ground-penetrating radar
HFC	High-frequency cycle
NWIS	National Water Information System
PVC	Polyvinyl chlorinated
RADAN	Radar data analyzer
SFWMD	South Florida Water Management District
SIR	Subsurface interface radar
USGS	U.S. Geological Survey
WCA	Water Conservation Area

Other Abbreviated Units

dB	decibel
mg/L	milligram per liter
MHz	megahertz
ns	nanosecond

Vertical coordinate information is referenced to the National Geodetic Vertical Datum of 1929 (NGVD 1929); horizontal coordinate information is referenced to the North American Datum of 1927 (NAD 1927), unless otherwise noted.

Characterization of Aquifer Heterogeneity Using Cyclostratigraphy and Geophysical Methods in the Upper Part of the Karstic Biscayne Aquifer, Southeastern Florida

By Kevin J. Cunningham[1], Janine L. Carlson[2], G. Lynn Wingard[3], Edward Robinson[4] *and* Michael A. Wacker[1]

ABSTRACT

This report identifies and characterizes candidate ground-water flow zones in the upper part of the shallow, eogenetic karst limestone of the Biscayne aquifer in the Lake Belt area of north-central Miami-Dade County using cyclostratigraphy, ground-penetrating radar (GPR), borehole geophysical logs, and continuously drilled cores. About 60 miles of GPR profiles were used to calculate depths to shallow geologic contacts and hydrogeologic units, image karst features, and produce qualitative views of the porosity distribution. Descriptions of the lithology, rock fabrics, and cyclostratigraphy, and interpretation of depositional environments of 50 test coreholes were linked to the geophysical interpretations to provide an accurate hydrogeologic framework. Molluscan and benthic foraminiferal paleontologic constraints guided interpretation of depositional environments represented by rock-fabric facies. Digital borehole images were used to characterize and quantify large-scale vuggy porosity. Preliminary heat-pulse flowmeter data were coupled with the digital borehole image data to identify candidate ground-water flow zones.

Combined results show that the porosity and permeability of the karst limestone of the Biscayne aquifer have a highly heterogeneous and anisotropic distribution that is mostly related to secondary porosity overprinting vertical stacking of rock-fabric facies within high-frequency cycles (HFCs). This distribution of porosity produces a dual-porosity system consisting of diffuse-carbonate and conduit flow zones. The nonuniform ground-water flow in the upper part of the Biscayne aquifer is mostly localized through secondary permeability, the result of solution-enlarged carbonate grains, depositional textures, bedding planes, cracks, root molds, and paleokarst surfaces. Many of the resulting pore types are classified as touching vugs.

GPR, borehole geophysical logs, and whole-core analyses show that there is an empirical relation between formation porosity, permeability, formation electrical conductivity, and GPR reflection amplitudes—as porosity and permeability increase, formation electrical conductivity increases and reflection amplitude decreases. This relation was observed throughout the entire vertical and lateral section of the upper part of the Biscayne aquifer in the study area. Further, upward-shallowing brackish- or freshwater-capped cycles of the upper part of the Fort Thompson Formation show low-amplitude reflections near their base that correspond to relatively higher porosity and permeability. This distribution is related to a systematic vertical stacking of rock-fabric facies within the cycle.

[1]U.S. Geological Survey, Miami, Florida
[2]Colorado School of Mines, Golden, Colorado
[3]U.S. Geological Survey, Reston, Virginia
[4]University of the West Indies, Kingston, Jamaica

Inferred flow characteristics of the porosity distribution within the upper part of the Biscayne aquifer were used to identify four ground-water flow classes, with each characterized by a discrete pore system that affects vertical and horizontal ground-water flow: (1) a low-permeability peat, muck, and marl ground-water flow class; (2) a horizontal conduit ground-water flow class; (3) a leaky, low-permeability ground-water flow class; and (4) a diffuse-carbonate ground-water flow class. At the top of the Biscayne aquifer, peat, muck, and marl can combine to form a relatively low-permeability layer of Holocene sediment that water moves through slowly. Most horizontal conduit flow is inferred to occur along touching vugs in portions of the following rock-fabric facies: (1) touching-vug pelecypod floatstone and rudstone, (2) sandy touching-vug pelecypod floatstone and rudstone, (3) vuggy wackestone and packstone, (4) laminated peloid grainstone and packstone, (5) peloid grainstone and packstone, and (6) peloid wackestone and packstone. Gastropod floatstone and rudstone, mudstone and wackestone, and pedogenic limestone rock-fabric facies are the main hosts for leaky, low-permeability units. This study provides evidence that the limestone that spans the base of the Miami Limestone and top of the Fort Thompson Formation has the potential to retard the vertical leakance of ground water; however, although the limestone contained in this zone has a relatively low-porosity and low-permeability matrix, common semivertical and irregular pores that transect or join to transect this zone produce what appears to be a very leaky unit. Diffuse-carbonate flow occurs in stratal units containing rock-fabric facies that generally are characterized by intergrain and separate-vug pores, and where flow is principally through a small-scale network of vug-to-matrix-to-vug connections. Rock-fabric facies that host diffuse flow are: (1) skeletal grainstone and packstone, (2) pelecypod floatstone and rudstone, (3) sandy skeletal grainstone and packstone, (4) sandy pelecypod floatstone and rudstone, and (5) quartz sandstone and skeletal sandstone.

At the borehole scale, there is a correspondence between vuggy porosity and depositional environments, depositional textures, and vertical position of rock-fabric facies within the context of HFCs. In the upper part of the Fort Thompson Formation, zones of touching vugs (vug-to-vug connections) that have a sheet-like geometry occur just above flooding surfaces within HFCs. The correlation between vuggy porosity and geologic parameters allows for prediction of

hydraulic parameters prior to drilling and for construction of a geologically realistic, conceptual framework for numerical models. A benefit from this research will be the use of results for helping to define the field-scale pore system within the Biscayne aquifer.

INTRODUCTION

During the past century, the Everglades and its watershed have been altered substantially by human activities, including the development of a highly managed hydrologic system in southern Florida. This hydrologic system of canals, levees, and pumping stations was developed to meet increasing demand for water supply as a result of a rapidly growing urban population and intensive agricultural activities. As a consequence, much of the Everglades, the Biscayne aquifer, and major estuarine systems in southern Florida presently do not receive sufficient quantity or distribution of water during times when it is most needed. Adequate water supply is essential to the restoration of the Everglades and its watershed.

In southeastern Florida, ground-water supply is augmented by surface storage of water in large-scale water-conservation areas (WCA's; fig. 1) and Everglades National Park (ENP). Surface water seeps into the Biscayne aquifer from the wetlands, then moves as ground water beneath a system of levees and canals on the eastern perimeter of the wetlands, flowing toward agricultural, urban, and coastal areas to the east. Sustainable ground-water levels east of the wetlands are critical for maintaining water levels at water-supply wells and preventing saltwater intrusion at the coast.

Managing the water levels in the WCA's and ENP is critical for establishing rates and volumes of water seeping from these areas to the Biscayne aquifer. A realistic, conceptual hydrogeologic model of the Biscayne aquifer, especially its karst limestone, is needed to accurately model the movement of ground water and determine a water budget to meet natural, agricultural, and urban needs.

Numerous studies have shown that two or more subaquifers that are separated by semiconfining units comprise the karst limestone of the Biscayne aquifer (Klein and Sherwood, 1961; Guardiario, 1996; Brown and Caldwell Environmental Engineers and Consultants, 1998; Cunningham and Wright, 1998; Kaufmann and Switanek, 1998; Nemeth and others, 2000; Sonenshein, 2001; Cunningham, 2004). Geophysical and
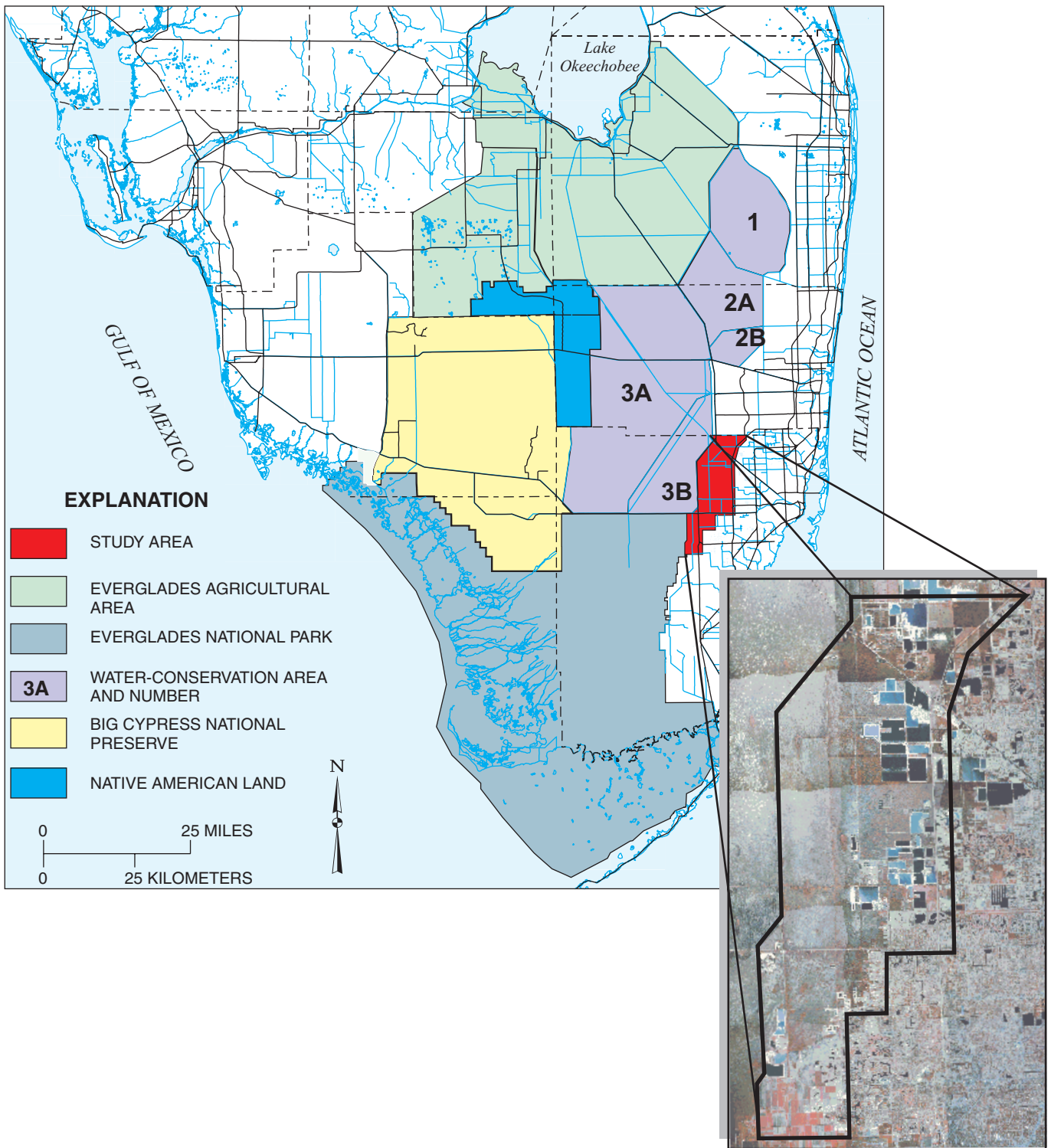
Figure 1. Location of study area, Federal and State lands, and agricultural areas in southern Florida.

geologic characterization, and mapping of the distribution of these subaquifers and semiconfining units are needed to fully identify their hydraulic properties and provide a basis for future studies.

In 1998, the U.S. Geological Survey (USGS), in cooperation with the South Florida Water Management District (SFWMD), initiated a study to provide a regional-scale hydrogeologic framework of a shallow semiconfining unit within the Biscayne aquifer of southeastern Florida. Initially, the primary objective was to characterize and delineate a low-permeability zone in the upper part of the Biscayne aquifer that spans the base of the Miami Limestone and uppermost part of the Fort Thompson Formation. Delineation of this zone, previously reported by numerous investigators (Klein and Sherwood, 1961; Shinn and Corcoran, 1988; Guardiario, 1996; Brown and Caldwell Environmental Engineers and Consultants, 1998; Cunningham and Wright, 1998; Genereux and Guardiario, 1998; Kaufman and Switanek, 1998; Nemeth and others, 2000; Sonenshein, 2001) in Miami-Dade County, was to aid development of a conceptual hydrogeologic model to be used as input into the SFWMD Lake Belt ground-water model. The approximate area encompassed by the ground-water model domain is shown as the "study area" in figures 1 and 2. Subsequent analysis of the preliminary data suggested hydraulic compartmentalization occurred within the Biscayne aquifer, and that there was a need to characterize and delineate ground-water flow zones and relatively low-permeability zones within the upper part of the Biscayne aquifer. Consequently, preliminary results suggested that the historical understanding of the porosity and preferential pathways for Biscayne aquifer ground-water flow required considerable revision.

Purpose and Scope

This report identifies and characterizes candidate ground-water flow zones in the upper part of the shallow, eogenetic karst limestone of the Biscayne aquifer using GPR, cyclostratigraphy, borehole geophysical logs, continuously drilled cores, and paleontology.

About 60 mi of GPR profiles (fig. 2) were acquired and are used to calculate the depth to shallow geologic contacts and hydrogeologic units, image karst features, and produce a qualitative perspective of the porosity distribution. Descriptions of lithology, rock fabric, cyclostratigraphy, and depositional environments of 50 test coreholes (fig. 2) were linked to

geophysical data to provide a more refined hydrogeologic framework. Interpretation of depositional environments was constrained by analysis of depositional textures and molluscan and benthic foraminiferal paleontology. Digital borehole images were used to help quantify large-scale vuggy porosity. Vuggy-porosity terminology used in this report is defined by Lucia (1995). Preliminary heat-pulse flowmeter data were coupled with the digital borehole image data to identify potential ground-water flow zones.

Previous Studies

Numerous studies have addressed topics relevant to the goals of this study. These include studies that describe permeability contrasts within the Biscayne aquifer in southeastern Florida, geophysical methods that have either characterized the hydrogeology of the Biscayne aquifer or provided useful discussions of techniques for characterization of the physical properties of carbonate strata, and quantification of vuggy porosity using borehole geophysical logs.

The presence of low-permeability zones near the top of the Biscayne aquifer was first suggested by Klein and Sherwood (1961), who proposed that two thin layers of dense limestone retard downward infiltration of surface water in WCA 3A and WCA 3B (fig. 1), causing a high head differential across Levee 30 at the edge of WCA 3B (fig. 2). Several studies that evaluated a dense, low-permeability zone that spans the base of the Miami Limestone and the top of the Fort Thompson Formation presented evidence for one or more hydrogeologic units limiting ground-water flow within the Biscayne aquifer (Shinn and Corcoran, 1988; Guardiario, 1996; Brown and Caldwell Environmental Engineers and Consultants, 1998; Cunningham and Wright, 1998; Genereux and Guardiario, 1998; Kaufman, and Switanek, 1998; Nemeth and others, 2000; Sonenshein, 2001). Borehole flowmeter measurements by Guardiario (1996) showed that this unit along the Levee 31W Canal at the eastern boundary of ENP (fig. 2) acts as a semiconfining unit, supporting vertical head differences and restricting vertical movement of water. At a nearby site, canal drawdown experiments were used with borehole flowmeter measurements to establish a high-resolution hydraulic-conductivity profile of the Biscayne aquifer (Genereux and Guardiario, 1998). Results revealed the presence of a low hydraulic conductivity zone at the top of the Fort Thompson Formation (Genereux and Guardiario, 1998, fig. 5).
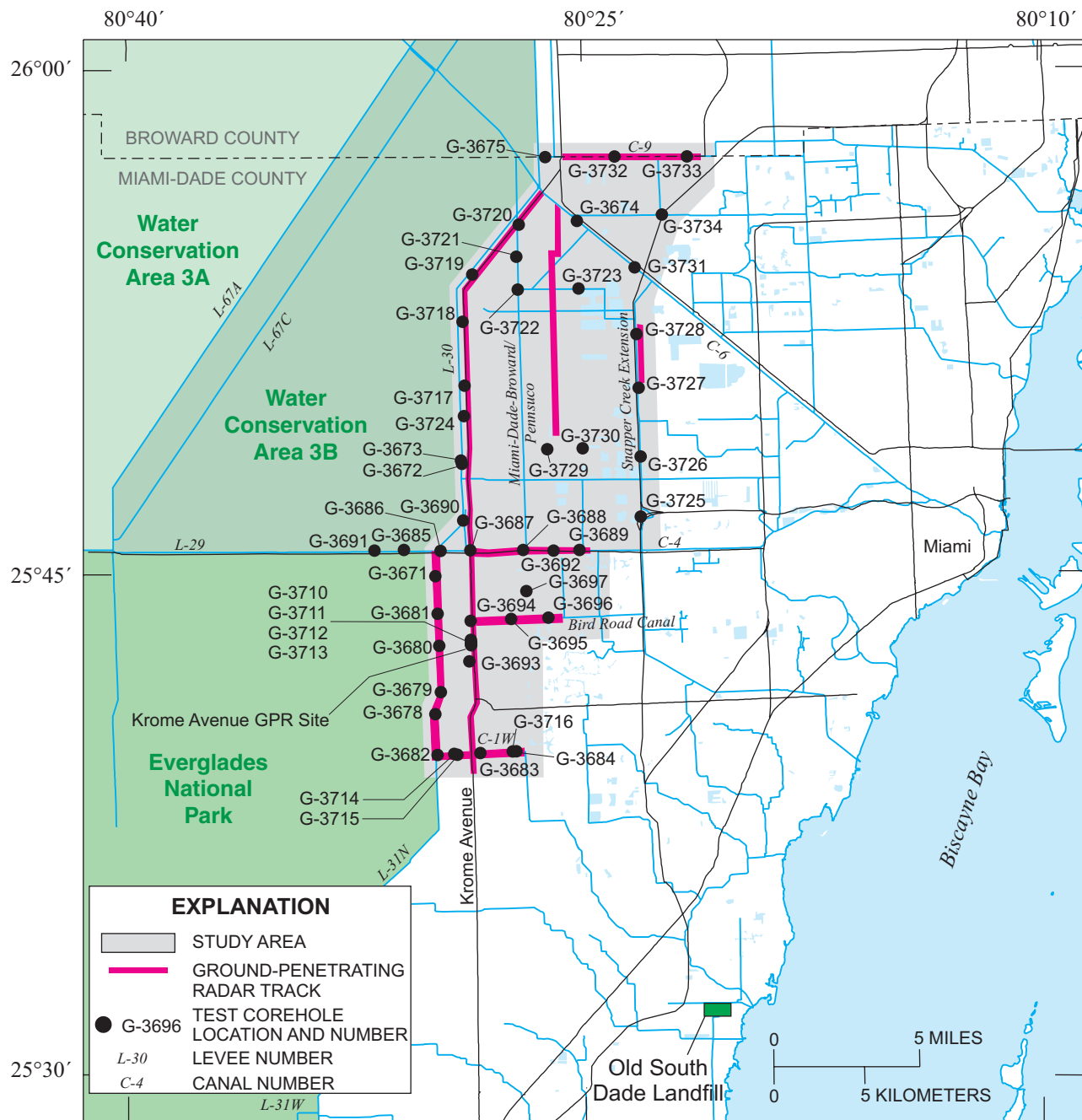
Figure 2. Location of study area, canals, levees, and Old South Dade Landfill (OSDLF) in Miami-Dade County, tracks of ground-penetrating radar, and test coreholes drilled for this study.

This latter low hydraulic conductivity zone (Genereux and Guardiario, 1998) is presumably equivalent to the low hydraulic conductivity zone that spans the lower part of the Miami Limestone and upper Fort Thompson Formation in north-central Miami-Dade County. The zone also has been identified as a semiconfining unit at the Old South Dade Landfill in Miami-Dade County (fig. 2; Shinn and Corcoran, 1988; Brown and Caldwell Environmental Engineers and Consultants, 1998;

Cunningham and Wright, 1998). Vertical head differences in surface water and ground water measured by Sonenshein (2001) indicate that this zone can restrict vertical flow between surface water and ground water in the wetlands west of Levee 30 in Miami-Dade County (fig. 2). Recent ground-water modeling of the Biscayne aquifer in the vicinity of the study area (fig. 2) has incorporated this zone as a low hydraulic conductivity unit (Nemeth and others, 2000; Sonenshein, 2001).

Although GPR is most commonly used in geologic studies of siliciclastic strata (for example, Beres and Haeni, 1991; Smith and Jol, 1992; van Overmeeren, 1998) and crystalline rocks (for example, Grasmueck, 1996; Lane and others, 2000), its use in studying karst-carbonate rocks is becoming more common (Ballard, 1983; Beck and Wilson, 1988; Barr, 1993; Benson, 1995; McMechan and others, 1998; Cunningham, 2000; Cunningham and Aviantara, 2001; Cunningham, 2004). However, the integrated use of GPR and digital borehole images in analyzing karst-carbonate rocks is a new application (Cunningham, 2000; Cunningham and Aviantara, 2001). Additionally, no published examples were found that demonstrate the use of GPR to delineate the distribution of porosity within a carbonate high-frequency cyclostratigraphy. Lithologic and hydraulic features that have been inferred from GPR profiles include sediment type and thickness (Beres and Haeni, 1991), karst features (Barr, 1993; Benson, 1995; McMechan and others, 1998), subaerial-exposure surfaces (Kruse and others, 2000), depth to water table, and clay bed occurrence (Johnson, 1992; Barr, 1993). McMechan and others (1998) used GPR to image a near-surface paleocave system in Lower Ordovician Ellenberger dolomites of central Texas. Martinez and others (1998) showed that small-scale (less than 1 centimeter, 0.39 in.) lithologic heterogeneity that affects permeability can be identified with GPR imaging behind Pennsylvanian cyclic limestone outcrops of Kansas and can provide quantitative data for use in fluid-flow modeling. Dagallier and others (2000) showed that GPR could be used to identify the internal organization of lithologic units within Jurassic limestone in France. Kruse and others (2000) found that GPR was an effective method to map the altitude and structure of shallow limestone cap rock in the prairie, cypress swamp, and hardwood hammock of the Fakahatchee Strand State Preserve in southwestern Florida. Beres and others (2001) demonstrated that GPR is an excellent tool for identifying and delineating shallow subsurface cavities in karstic Jurassic limestone in Switzerland.

The relation between the spatial distribution of porosity within high-frequency carbonate cycles and amplitude of reflections on GPR profiles has been demonstrated and is reported separately in Cunningham (2004). Results of that study have improved the understanding of the distribution of porosity in the young (Pleistocene) platform carbonates that comprise the unconfined surficial Biscayne aquifer, and provide a framework to guide collection of future hydraulic measurements.

Kindinger (2002) has shown the utility of seismic-reflection profiles in better defining the hydrogeologic framework of the middle and lower parts of the Biscayne aquifer. Kindinger (2002) collected more than 68 line-mi of seismic-reflection data from eight major canals to develop a better understanding of the geology and hydrogeology of the Lake Belt area, which approximates the study area herein. About 80 percent of the data were considered useful to this investigation and generally were usable to an altitude of about 100 ft below NGVD 29. The Fort Thompson Formation portion of the usable data shows several continuous horizons and numerous vertical to semivertical features that are inferred to represent shallow solution pipes or large vugs. Many solution pipes and collapse structures were inferred from the profiles within the Tamiami Formation (Kindinger, 2002).

Many recent studies have verified that digital electronic images of borehole walls can be useful in quantifying vuggy porosity (Hickey, 1993; Newberry and others, 1996; Hurley and others, 1998; 1999) in petroleum reservoirs and fractures in aquifers (Williams and Johnson, 2000). By quantifying vuggy porosity in borehole images, these researchers could identify fluid-flow zones. Cunningham and others (2004) report in detail the development of a method for quantifying vuggy porosity seen in digital borehole images collected in the limestone of the Biscayne aquifer.

Acknowledgments

METHODS OF INVESTIGATION

A combination of multidisciplinary techniques was used to produce an improved visualization of the pore system within a cyclic hydrogeologic framework of the upper part of the Biscayne aquifer. This approach included the integration of GPR methods, core analyses, borehole geophysical logs, cyclostratigraphy, quantification of vuggy porosity in borehole images, and paleontology.

Ground-Penetrating Radar Surveys

When combined with hydrogeologic data, GPR can contribute substantially to the characterization of hydrogeologic properties of shallow limestone aquifers. Numerous GPR profiles were collected (about 60 mi) and used to characterize the hydrogeologic framework of the upper part of the Biscayne aquifer.

Two types of GPR field surveys were conducted for this study: (1) continuous measurement common-offset reflection surveys, and (2) common mid-point (CMP) velocity surveys (Annan and Davis, 1976; Davis and Annan, 1989). The common-offset reflection surveys were performed to produce two-dimensional profiles of the GPR reflections, and the CMP surveys to calculate radar velocities propagating through the solid and fluid material comprising the Biscayne aquifer. All GPR data were collected using a subsurface interface radar (SIR) System-10A+ with a dual 100-MHz antenna fixed-offset array. A time-varying gain was used during collection of each GPR profile. The common-offset reflection surveys were collected while towing the antennas 55 ft behind a truck with a connecting rope and cable at a rate of about 0.5 mi/hr. The separation between the center point of antennas was 35 in. Processing of profiles included a horizontal filter pass and, for some profiles, a constant-velocity migration of the continuous survey data using radar data analyzer (RADAN) for WinNT software. Visual representation of the GPR data was accomplished using RADAN for WinNT software and RADAN-to-bitmap conversion utility. Descriptions of radar-reflection configuration patterns were based on comparison to seismic examples in Mitchum and others (1977).

Radar propagation velocities were calculated using depths to reflectors that could be determined from: (1) positive correlation of profile reflections with core-sample lithologies and borehole images, and (2) CMP survey data. Calculation of velocities (v) from comparison of profile reflections with core-sample lithologies and borehole images was established by dividing the one-way travel time (t) to a reflection by the depth (d) of its corresponding lithologic contact as verified in core or images. The equation $t/d = v$ results in the velocity (v) between the land surface and selected lithologic contact. The method presented in Telford and others (1990) was used to determine velocities using CMP surveys.

Drilling, Well Completion, Core Analysis, and Geophysical Logging

Nearly all of the 50 test coreholes were drilled following GPR data acquisition (table 1 and fig. 2). Test coreholes were located along the GPR profile tracts where they would be most useful for verification of GPR attributes. Collection of continuous 3.4- or 4-in. diameter cores was preferred to the normal rotary method, which produces small cutting samples collected over relatively wide depth intervals. The test coreholes were drilled by either Amdrill Inc., employing a wireline coring method, or by U.S. Drilling Inc., using a conventional coring method (table 1). Borehole geophysical logs were collected by the USGS in 45 of the 50 test coreholes drilled during this study and included induction resistivity, natural gamma ray, spontaneous potential, single-point resistivity, caliper, and digital borehole image logs (app. I). Borehole geophysical logs were not collected at the G-3694 and G-3697 test coreholes (fig. 2) due to problems with locating the well or destruction of the well after drilling. The borehole geophysical-logging tools were run in boreholes filled with clear freshwater. Each borehole was cased with 3.5- or 5-in. solid polyvinyl chlorinated (PVC) surface casing set to a depth between 4 and 19 ft below land surface (app. I). Data were acquired in digital format and archived in the USGS National Water Information System (NWIS) database. The digital borehole image logs were acquired using an RaaX BIPS digital optical logging tool. A Mount Sopris Model HFP-2293 heat-pulse flowmeter was used to assess borehole fluid movement in the G-3710 test corehole. A technique described by Paillet (2000) to estimate vertical groundwater borehole flow was utilized with the flowmeter measurements collected in the G-3710 test corehole. This method has been previously applied to southern Florida aquifers (Paillet and Reese, 2000). Most geophysical logs collected as part of this study are provided in appendix I.

Table 1. List of all test coreholes drilled during this study

[Well locations are shown in figure 2; all wells are located in Miami-Dade County, Florida; Wells G-3671 to G-3697 were drilled by Amdrill, Inc., using wireline-core drilling method and 3.5-inch solid polyvinyl chloride construction material, unless otherwise noted. Wells G-3710 to 3734 were drilled by U.S. Drilling, Inc., using conventional-core drilling method and 5.5-inch solid polyvinyl chloride construction material, unless otherwise noted. Latitudes and longitudes referenced to North American Datum of 1983. Altitude of measuring point is land surface referenced to the National Geodetic Vertical Datum of 1929 (NGVD of 1929); NA, not available]

Local well identifier	USGS site identification number	Land net location	Latitude	Longitude	Altitude of measuring point	Total depth drilled (feet)	Depth of bottom of casing (feet)	End date of construc- tion
G-3671	254456080295301	SESE SEC11 T54S R38E	254456	802953	12	150	NA	8-7-98
G-3672	254822080290201	SENE SEC25 T53S R38E	254822	802902	20	45	18	8-8-98
G-3673	254822080290202	SENE SEC25 T53S R38E	254822	802902	20	160	18	8-10-98
G-3674	255529080251101	NWNW SEC14 T52S R39E	255529	802511	8	160	NA	8-16-98
G-3675	255723080261301	SESNE SEC27 T50S R39E	255723	802613	8	90	NA	8-21-98
G-3678	254050080295401	NW SEC1 T55S R38E	254050	802954	12	35	10	5-22-99
G-3679	254129080294301	SE SEC35 T54S R38E	254129	802943	10.5	40	10	5-23-99
G-3680	254252080294601	NW SEC25 T54S R38E	254252	802946	11	40	10	5-23-99
G-3681	254349080294901	NW SEC24 T54S R38E	254349	802949	9.5	45	10	5-23-99
G-3682	253937080295001	SWNW SEC12 T55S R38E	253937	802950	13.5	30	10	5-24-99
G-3683	253940080282601	SENE SEC7 T55S R39E	253940	802826	12	35	10	5-24-99
G-3684	253943080272201	SE SEC8 T55S R39E	253943	802722	11.5	35	10	5-24-99
G-3685	254543080305501	SE SEC3 T54S R38E	254543	803055	14	30	10	5-25-99
G-3686	254541080294301	SW SEC1 T54S R38E	254541	802943	11	30	10	5-25-99
G-3687	254542080284401	SW SEC6 T54S R39E	254542	802844	12.5	30	10	5-25-99
G-3688	254542080270001	SE SEC5 T54S R39E	254542	802700	9.5	30	10	5-26-99
G-3689	254542080259001	SE SEC3 T54S R39E	254542	802590	9	30	10	5-26-99
G-3690	254635080285801	SE SEC1 T54S R38E	254635	802858	11.5	30	10	5-26-99
G-3691	254542080315301	SE SEC4 T54S R38E	254542	803153	14	35	10	5-27-99
G-3692	254541080260001	SE SEC4 T54S R39E	254541	802600	9	30	NA	5-27-99
G-3693	254224080284701	SE SEC25 T54S R38E	254224	802847	11.5	35	NA	6-2-99
G-3694	254336080284401	NWNW SEC19 T54S R39E	254336	802844	11	35	10	6-2-99
G-3695	254339080272401	NW SEC20 T54S R39E	254339	802724	10.5	35	10	6-3-99
G-3696	254341080261101	NW SEC21 T54S R39E	254341	802611	11	35	10	6-3-99
G-3697	254429080265401	NENE SEC17 T54S R39E	254429	802654	9	30	NA	6-3-99
G-3710	254310080284801	SESE SEC24 T54S R38E	254310	802848	10	33	8	4-20-00
G-3711	254300080284701	SESE SEC24 T54S R38E	254300	802847	10	37	8	4-20-00
G-3712	254250080284601	SESE SEC24 T54S R38E	254250	802846	10	28	7	5-1-00
G-3713	254245080284501	SESE SEC24 T54S R38E	254245	802845	10	32.5	7	5-2-00
G-3714	253937080292901	SENW SEC12 T55S R38E	253937	802929	13	23	8	5-3-00
G-3715	253938080292301	SENW SEC12 T55S R38E	253938	802923	13	23	8	5-3-00
G-3716	253943080272301	SE SEC8 T55S R39E	253943	802723	9	28	8	5-4-00
G-3717	255039080290101	SESE SEC12 T53S R38E	255039	802901	9	43	7.75	5-8-00
G-3718	255220080290301	SESE SEC36 T52S R38E	255220	802903	9	30	6.3	5-9-00
G-3719	255355080284301	NENW SEC30 T52S R39E	255355	802843	9	30	6.5	5-10-00
G-3720	255530080271301	NWNW SEC16 T52S R39E	255530	802713	9	31	5	5-11-00
G-3721	255424080271201	NESE SEC20 T52S R39E	255424	802712	10	30	9	5-12-00
G-3722	255326080270901	NESE SEC29 T52S R39E	255326	802709	10	32	7.75	5-12-00
G-3723	255328080251201	NESE SEC27 T52S R39E	255328	802512	8	45	7	5-15-00
G-3724	254942080285801	NENE SEC24 T53S R38E	254942	802858	9	30	7	5-16-00
G-3725	254655080231201	NENE SEC1 T53S R39E	254655	802312	6	31.5	6.5	5-17-00
G-3726	254825080231201	NENE SEC25 T53S R39E	254825	802312	7	33	10	5-18-00

Table 1. List of all test coreholes drilled during this study (Continued)

[Well locations are shown in figure 2; all wells are located in Miami-Dade County, Florida; Wells G-3671 to G-3697 were drilled by Amdrill, Inc., using wireline-core drilling method and 3.5-inch solid polyvinyl chloride construction material, unless otherwise noted. Wells G-3710 to 3734 were drilled by U.S. Drilling, Inc., using conventional-core drilling method and 5.5-inch solid polyvinyl chloride construction material, unless otherwise noted. Latitudes and longitudes referenced to North American Datum of 1983. Altitude of measuring point is land surface referenced to the National Geodetic Vertical Datum of 1929 (NGVD of 1929); NA, not available]

Local well identifier	USGS site identification number	Land net location	Latitude	Longitude	Altitude of measuring point	Total depth drilled (feet)	Depth of bottom of casing (feet)	End date of construc-tion
G-3727	255033080231301	SWSW SEC7 T53S R40E	255033	802313	9	43	8.5	5-30-00
G-3728	255154080231301	NWNW SEC6 T53S R40E	255154	802313	8	38	6	5-31-00
G-3729	254843080261101	SWSESE SEC21 T53S R39E	254843	802611	6	36	6	6-1-00
G-3730	254842080250801	SESESE SEC22 T53S R39E	254842	802508	6	40	7	6-2-00
G-3731	255408080231801	NWSWSW SEC19 T52S R40E	255408	802318	11	43	7.5	6-5-00
G-3732	255724080235401	NENENW SEC01 T52S R39E	255724	802354	7	48	5	8-21-00
G-3733	255724080213401	NWNWNW SEC04 T52S R40E	255724	802134	5	43	7	9-8-00
G-3734	255540080222501	NWNENE SEC18 T52S R40E	255540	802225	8	33	7	9-8-00

Core samples were described using a 10-power hand lens and binocular microscope to determine vertical patterns of microfacies, sedimentary structures, and lithostratigraphic boundaries, to characterize porosity, and to estimate "relative" permeability. Limestones were classified by combining the schemes of Dunham (1962), Embry and Klovan (1971), and Lucia (1995). The rock color of dry core samples was recorded by comparison to a Munsell rock-color chart (Geological Society of America, 1991). Core-sample descriptions were classified as rock-fabric facies and are presented graphically in appendix I and on plates 1 to 5.

Horizontal and vertical permeability of 71 whole-core samples, horizontal permeability of 36 core-plug samples, and porosity and grain density of all 107 samples were measured at Core Laboratories, Inc. (app. II). At the time of this writing (2003), all continuous cores collected in this study were archived at the USGS office in Miami. Numerous (318) core-sample thin sections were examined using standard transmitted-light petrography to characterize and interpret rock properties and small-scale porosity.

Quantification of Vuggy Porosity from Borehole Images

Borehole images are digital photographs of the borehole wall recorded by a sonic-velocity or electrical-resistivity probe, or optical device (Lovell and others, 1999). The absence of borehole image logs requires that identification of vugs and fractures by geophysical logging is accomplished by combining and

interpreting several logs, including sonic, dipmeter, laterolog and induction, density, spontaneous potential, and natural gamma-ray spectrometry (Crary and others, 1987). Unfortunately, these logs commonly are not all collected in shallow environmental boreholes. In this study, it was found that visual interpretations of digital borehole images are the most reliable and practical method of identifying vuggy porosity in the limestone of the Biscayne aquifer. A BIPS borehole imaging tool was used to log continuous digital photographic images in 45 test coreholes. These images provide 100-percent circumferential coverage of the borehole wall and can yield critical information regarding the presence or absence of vuggy porosity, its spatial distribution, and vuggy pore shape and size. Results are presented as depth logs of vuggy porosity in appendix I and on plates 1 to 5. A detailed description of the method to quantify vuggy porosity using borehole images is provided by Cunningham and others (2004).

Molluscan and Benthic Foraminiferal Paleontology

Mollusks from 46 samples collected from 12 test coreholes (fig. 3) were prepared and identified at the USGS Paleontology Laboratory in Reston, Va. Most of the mollusks present in the strata were preserved as molds and casts. Core samples were initially examined under a binocular microscope to observe diagnostic characteristics of the molluscan remains and to make identifications based on their comparison with published species. Clay squeezes or latex casts were

made of the molluscan molds where appropriate to aid in identification. After initial identifications were made, samples were split open to expose fresh surfaces and the process repeated.

Identification of benthic foraminifera was made at the genus level, where possible, for 67 thin sections selected by lithology from five test coreholes (fig. 4). Six biofacies were recognized. One was distinguished by an absence of benthic foraminifera and the five others were based on data from Bock and others (1971), and on biofacies suggested by Poag (1981) adapted to thin section analysis. Poag's (1981) classification of biofacies is based on predominant benthic foraminifera genera in a sample. Poag (1981) suggests counting 200 to 300 free specimens to establish the presence of a particular biofacies; however, the number of recognizable genera in samples used here is much less, so the interpretation of the biofacies assignments are somewhat speculative.
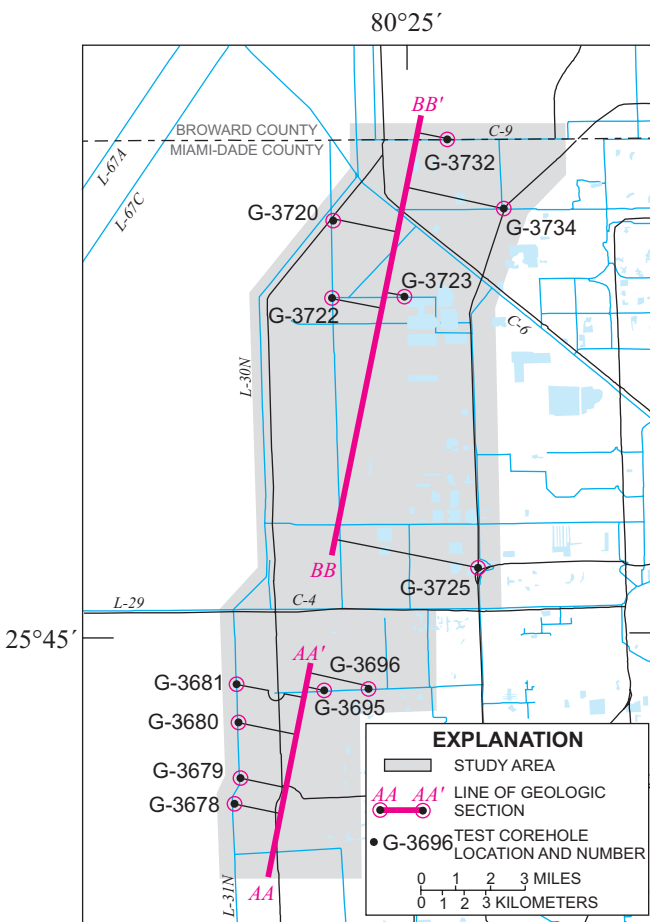
Figure 4. Location of test coreholes sampled for foraminiferal paleontology, and line of geologic section *CC-CC'* (fig. 12).

GEOLOGIC FRAMEWORK

Lithostratigraphy, rock-fabric facies, cyclostratigraphy, paleontology, and depositional facies were used to define a unique geologic framework for the rocks that make up the Biscayne aquifer in north-central Miami-Dade County. Lithostratigraphy is the description and systematic organization of rocks and sediments into distinctively named units based on the lithologic character of the rocks and sediments, and their stratigraphic relations (Jackson, 1997). "Rock-fabric facies" is a descriptive term intended to include lithologic character and pore-space properties. Vertical stacking of rock-fabric facies was related in terms of HFCs, pore-size distribution, and relative permeability. Cyclostratigraphy is defined here as the analysis of foot-scale depositional cycles, defined similarly as upward shallowing cycles (James, 1979), and deposited on ancient carbonate shelves or ramps. Molluscan and foraminiferal paleontology was useful in helping to establish paleoenvironments and depositional facies.

Lithostratigraphy

Lithostratigraphic units of interest in this study are contained within the Biscayne aquifer. They include the Tamiami Formation (Pinecrest Sand Member), Anastasia Formation, Key Largo Limestone, Anastasia Formation, Fort Thompson Formation, Miami Limestone, and Pamlico Sand (Fish and Stewart, 1991). Included in this report (present study) are the Lake Flirt Marl and peat of Holocene age within the Biscayne aquifer. These Quaternary units are present

Figure 3. Location of test coreholes sampled for molluscan paleontology and lines of geologic sections *AA-AA'* and *BB-BB'* (figs. 7 and 8).

locally in the study area (Parker and Cooke, 1944; Causaras, 1987); however, the focus of this study is on the upper part of the Fort Thompson Formation, Miami Limestone, Lake Flirt Marl, and Holocene peat (fig. 5). The lithology, limiting extent, and thickness of lithostratigraphic units were determined by examination of continuously drilled cores, borehole geophysical logs (especially digital optical borehole images), and GPR profiles. Graphical displays of lithologic core descriptions prepared for this study are presented in appendix I.

Molluscan Paleontology

Paleoenvironments and stratigraphic age of the Fort Thompson Formation were evaluated in the 46 core samples collected for molluscan paleontology from 12 test coreholes (fig. 3). Molluscan species diversity in the samples was low, and most of the species identified have a broad tolerance to change in salinity and water depth, so the samples have been classified within only three paleoenvironments based on the mollusks: shallow shelf to outer estuarine, inner estuarine, and freshwater (figs. 6-8 and app. III). Detailed information on the mollusks in specific samples is presented in appendix III.

Paleoenvironments

A paleoenvironmental analysis of the carbonate rocks that comprise the Biscayne aquifer is considered important for developing a hydrogeologic framework used to classify and categorize porosity types, and map distribution of permeability within the Biscayne aquifer. The porosity and permeability are related to the vertical arrangement of depositional environments, and thus, paleoenvironments within the Miami Limestone and Fort Thompson Formation.

Shallow Shelf to Outer Estuarine

Most core samples indicative of shallow-shelf to outer-estuarine environments are dominated by the mollusk *Chione cancellata* (figs. 7 and 8 and app. III). *Chione cancellata*, an abundant species within the Quaternary rock and sediment of southern Florida, is somewhat tolerant of salinity fluctuations, and has been known to survive hypersaline episodes. Core samples dominated by *Chione* may represent deposition in an estuarine environment with fluctuating salinity, although this mollusk can also thrive in shelf environments. This species is found in modern-day estuarine

and shelf environments in salinities typically ranging from 24,000 to 35,000 mg/L; however, *Chione cancellata* can tolerate 16,000 to 40,000+ mg/L. In Florida Bay, live specimens have been identified in eastern, central, western, Atlantic, and Gulf transition zones (fig. 9), but not in the northern transitional zone and areas subject to freshwater outflows.

Other molluscan fauna found in samples representative of the shallow-shelf to outer-estuarine environments include *Trachycardium, Anodontia, Lucina pensylvanica, Lucinisca nassula, Turbo castaneus, Turritella, Codakia, Dosinia, Lirophora, Modulus*, and *Cerithium* (figs. 7 and 8 and app. III). The majority of the species live in salinities from 25,000 to 40,000 mg/L, with some more tolerant of fluctuating salinities than others. Species less tolerant of salinity fluctuations (*Trachycardium, Anodontia, Codakia*, and *Dosinia*) presumably were deposited in a shallow-shelf to outer-estuarine environment in which salinity consistently ranged from 25,000 to 35,000 mg/L. A modern analogue is the western and Gulf transition zones of Florida Bay (fig. 9). *Codakia orbicularis* is typically considered a shelf species, but it has also been found alive in Florida Bay in the eastern, central and Gulf transition zones (fig. 9) in salinities ranging from 29,000 to 38,000 mg/L. *Modulus* and *Cerithium* are present in some of the samples and indicate that sub-aquatic vegetation, such as *Thalassia* or macrobenthic algae, was present at the time of deposition. Other molluscan fauna found in samples characterized as being shallow shelf to outer estuarine include *Carditimera floridana* and *Pleuromeris tridenta* (figs. 7 and 8 and app. III).

Inner Estuarine

Three core samples contained molluscan assemblages indicative of an inner-estuarine environment. One core sample obtained from a depth between 21.08 and 21.58 ft below land surface near the top of HFC3b (fig. 7) in the G-3695 test corehole is distinctive; the presence of *Brachidontes* and *Anomalocardia* sp. indicates deposition in an inner-estuarine environment (fig. 7 and app. III). These species are typical of the northern transition zone in present-day Florida Bay (fig. 9) and can tolerate wide extremes of salinity. The second core sample obtained from a 30.92- to 31.25-ft depth below land surface near the base of HFC3b (figs. 7 and 10) in the G-3696 test corehole contains a mixed assemblage. The mixed assemblage may represent the inner-estuarine environment based on the co-occurrence of *Planorbella,* a freshwater gastropod, and the estuarine

Figure 5. Relation of geologic and hydrogeologic units of the surficial aquifer system across central Miami-Dade County (modified from Reese and Cunningham, 2000).

to marine species *Turritella* and *Chione* (fig. 7 and app. III). This sample probably indicates an inner-estuarine environment. The third core sample collected from a depth of 39.3 ft below land surface in HFC1 in the G-3723 test corehole (figs. 8 and 10 and app. III) may indicate deposition in a specific inner-estuarine environment; namely, a shallow-water or estuarine mud-flat environment with fluctuating salinities that was located in close proximity to mangroves.

This could be analogous to modern mangrove islands or to the dwarf mangrove fringe seen at the northern transitional zone of present-day Florida Bay (fig. 9) and could represent deposition in close proximity to a mangrove island in an estuary, or on the fringe environment where the transition between terrestrial and estuarine habitat occurs. Characteristic molluscan fauna include *Pyrazisinus* (extinct), *Tagelus, Anomalocardia*, and *Melongena* (fig. 8 and app. III).

Rock-Fabric Facies

Peloid grainstone/packstone

Coral framestone

Peloid wackestone/packstone

Gastropod floatstone/rudstone

Conglomerate

Pedogenic limestone

Mudstone/wackestone

Root-mold limestone

Skeletal grainstone/packstone

Sandy skeletal grainstone/packstone

Laminated peloid grainstone/packstone

Pelecypod floatstone/rudstone

Sandy pelecypod floatstone/rudstone

Touching vug pelecypod floatstone/rudstone

Sandy touching vug pelecypod floatstone/rudstone

Vuggy wackestone packstone

Quartz sandstone

Skeletal sandstone

Miscellaneous

Fill

Peat

Marl

No recovery

Figure 6. Explanation of symbols in figures 7, 8, and 12.

Freshwater

Freshwater paleoenvironments represented in core samples are probably analogous to modern sawgrass marsh areas of the Everglades and freshwater ponds on tidal flats. Characteristic molluscan fauna of these freshwater areas are *Planorbella, Physa,* and *Pomacea paludosa* (figs. 7 and 8 and app. III). With one exception, samples containing these species were interpreted to represent deposition in a freshwater environment. The unusual sample, mentioned earlier from the G-3696 test corehole at a depth interval between 30.92 and 31.25 ft below land surface, contains *Planorbella*, *Turritella*, and *Chione* (fig. 7) and is indicative of an inner-estuarine environment.

Stratigraphic Age

The ages of most mollusks found in the cores range from Pliocene to Holocene throughout the entire stratigraphic intervals under study, so they are not diagnostic in terms of age or biostratigraphic position. Exceptions to the Pliocene-Holocene range in age include: (1) *Pyrazisinus scalatus* (G-3723 at 39.3 ft below land surface); and (2) *Modulus woodringi* [?=*M. bermontianus* Petuch] (G-3732 at 28.5 to 29.08 ft below land surface and G-3723 at 44 ft below land surface); both are extinct (fig. 8 and app. III), *Turritella apicalis*, *Codakia orbicularis*, *Anomalocardia concinna*, and *Anodontia* (app. III).

Foraminiferal Paleontology

Sixty-seven (67) thin sections obtained from Miami Limestone and Fort Thompson Formation core samples from five test coreholes were microscopically examined to identify significant benthic foraminifera and associated mollusks, ostracods, and echinoids (table 2). Each core sample was assigned to one of five biofacies (fig. 11) and the associated paleoenvironment based on: (1) biofacies suggested by Poag (1981) and Rose and Lidz (1977); (2) fossil and sedimentologic associations; (3) sample locations within the vertical organization of rock-fabric facies; and (4) the observation that the large imperforate foraminifera of biofacies 5 occur in wading depths in seagrass meadows, and also in water as much as about 130 ft deep (fig. 12 and table 3). Also presented in table 3 and figure 12 are the associated rock-fabric facies and HFCs in which the fossils were found.
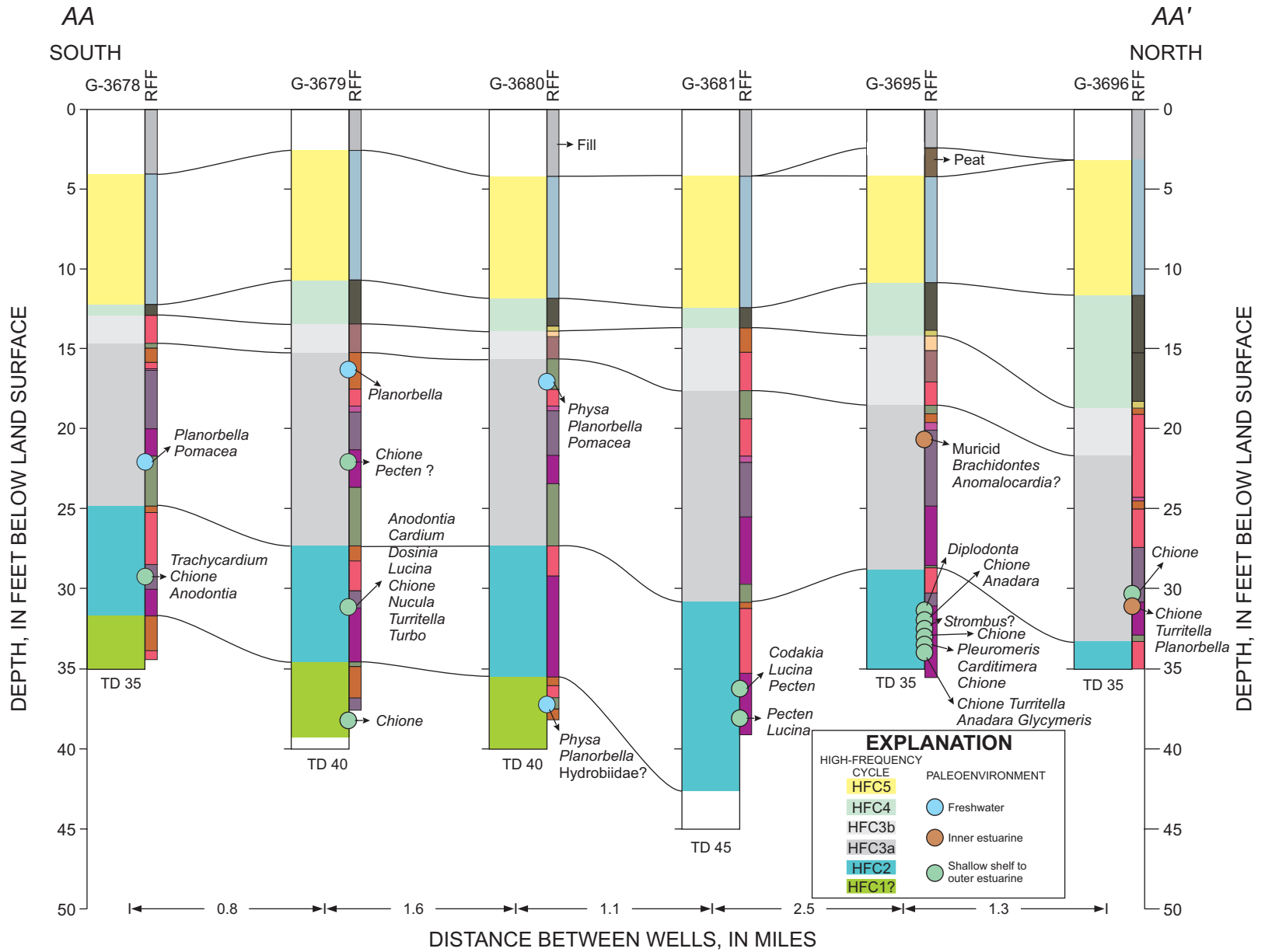
Figure 7. Geologic section *AA-AA'* showing molluscan taxonomy identified in test coreholes included in the study area. Line of section shown in figure 3. See figure 6 for rock-fabric facies (RFF) symbols.

Figure 8. Geologic section *BB-BB'* showing molluscan taxonomy identified in test coreholes included in the study area. Line of section shown in figure 3. See figure 6 for rock-fabric facies (RFF) symbols.
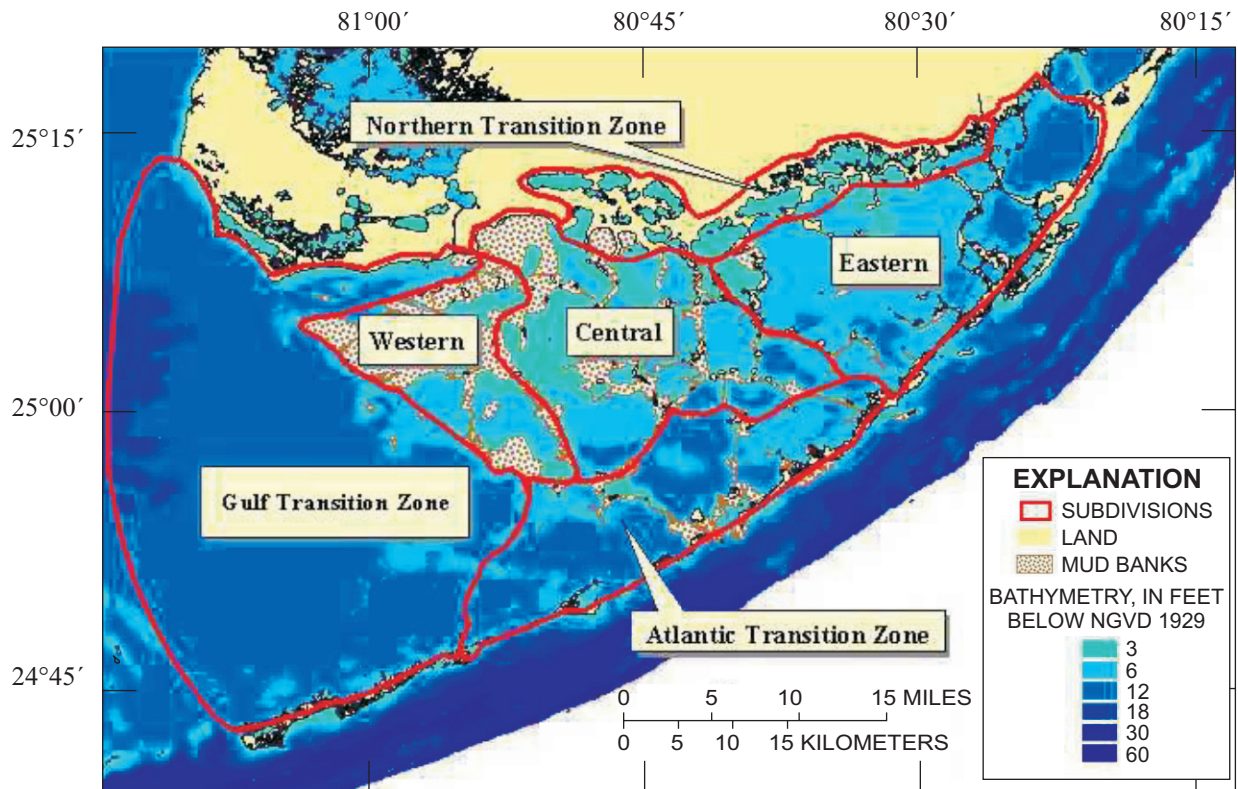
Figure 9. Present-day Florida Bay showing zonation based on differences in circulation and its connections, which play a role in salinity and habitat structure (modified from National Oceanic and Atmospheric Administration, 2002).

Series	Hydrogeologic Unit	Lithostrati-graphic Unit	Parasequences (Galli, 1991)	"Q Units" (Perkins, 1977)	HFC	Cycle Type	
HOLOCENE	SURFICIAL AQUIFER SYSTEM	PEAT OR MARL OR BOTH	NONE	NONE	NONE	NONE	
PLEISTOCENE		MIAMI LIMESTONE	NONE	Q5	HFC5	SUBTIDAL	Focus of This Study
			PARASEQUENCE "C"	Q4	HFC4		
		FORT THOMPSON FORMATION	1	Q3	HFC3 HFC3B / HFC3A	BFC	
	BISCAYNE AQUIFER		2				
			3,4, 5,6,7	Q2	HFC2*	MIXED BFC AND SUBTIDAL	Provisional
				Q1	HFC1?*		

- - - - - =Geologic contact, dashed where approximately located.
▬▬▬▬ =Surface of subaerial exposure.
BFC = upward-shallowing brackish- or freshwater-capped cycle.
HFC = high-frequency cycle

Figure 10. Shallow time-stratigraphic units, hydrogeology (Fish and Stewart, 1991), lithostratigraphy (Causarus, 1987), "Q units" of Perkins (1977), and high-frequency cycles (HFC) used in this report for southeastern Florida. Asterisk (*) indicates units can contain multiple high-frequency cycles and may be depositional sequences.

Table 2. Occurrence of stratigraphically important benthic foraminiferal taxa, mollusks, ostracods, and echinoids in test coreholes G-3671, G-3684, G-3687, G-3689, and G-3695

[Abbreviations: HFC, high frequency cycle; P, predominant foraminiferal taxa; Q, presence is questionable; RF, rotaliform foraminifera; X, present. Biofacies: biofacies 1, foraminifera absent (commonly contains smoothed-walled ostracods, commonly together with gastropods); biofacies 2, *Ammonia* predominant; biofacies 3, *Elphidium* predominant; biofacies 4, miliolids predominant; biofacies 5, archaiasinids, soritids, and peneroplids predominant]

Sample depth (below ground level, in feet)	HFC	Rock-fabric facies	Bio-facies	RF	Rotalia	Ammonia	Elphidium	Miliolids	Soritids	Sorites	Archaiasinids	Archaias	Androsina	Cyclorbiculina	Parasorites	Peneroplids	Peneroplis	Amphistegina	Mollusks	Gastropods	Pelecypods	Ostracods	Echinoids
										G-3671													
6.0	HFC5	Peloid grainstone and packstone	4					X												X			
9.0	HFC5	Peloid grainstone and packstone	4					X												X		X	
13.5	HFC3b	Mudstone and wackestone	2/3	X		Q														X		X	
14.5	HFC3b	Pedogenic limestone (root-mold limestone)	?													X							
18.5	HFC3b	Skeletal grainstone and packstone	5					X	X			Q	X			X					X	X	
19.5	HFC3a	Mudstone and wackestone	5	X			X													X			
20.8	HFC3a	Laminated peloid grainstone and packstone	5	X			X	X					X					X					
21.2	HFC3a	Pelecypod floatstone and rudstone	5	X				X					X								X		X
25.0	HFC3a	Touching-vug pelecypod floatstone and rudstone	3	X			P	X															
26.0	HFC3a	Touching-vug pelecypod floatstone and rudstone	1																	X	X	X	
27.2	HFC3a	Gastropod floatstone and rudstone	1																	X	X	X	
27.8	HFC3a	Gastropod floatstone and rudstone	1																				
29.5	HFC3a	Gastropod floatstone and rudstone	1																	X	X		
29.8	HFC3a	Gastropod floatstone and rudstone	1/2				X													X		X	
30.2	HFC2	Skeletal grainstone and packstone	2	X		P															X		
34.8	HFC2	Pelecypod floatstone and rudstone	?																		X		
38.0	HFC2	Skeletal grainstone and packstone	5	X				X	X			X	X				X		X				X
41.0	HFC2	Gastropod floatstone and rudstone	1																		X		
42.0	HFC2	Gastropod floatstone and rudstone	1																	X	X		
42.2	HFC2	Gastropod floatstone and rudstone	1																		X		
43.0	HFC2	Gastropod floatstone and rudstone	1																	X	X		
46.0	HFC1	Touching-vug pelecypod floatstone and rudstone	2/5	X		X		X	X														
49.5	HFC1	Touching-vug pelecypod floatstone and rudstone	4?					X															
50.8	HFC1	Sandy touching vug pelecypod floatstone and rudstone	?																				X
53.0	HFC1	Skeletal sandstone	?																				

Table 2. Occurrence of stratigraphically important benthic foraminiferal taxa, mollusks, ostracods, and echinoids in test coreholes G-3671, G-3684, G-3687, G-3689, and G-3695 (Continued)

[Abbreviations: HFC, high frequency cycle; P, predominant foraminiferal taxa; Q, presence is questionable; RF, rotaliform foraminifera; X, present. Biofacies: biofacies 1, foraminifera absent (commonly contains smoothed-walled ostracods, commonly together with gastropods); biofacies 2, *Ammonia* predominant; biofacies 3, *Elphidium* predominant; biofacies 4, miliolids predominant; biofacies 5, archaiasinids, soritids, and peneroplids predominant]

Sample depth (below ground level, in feet)	HFC	Rock-fabric facies	Bio-facies	RF	*Rotalia*	*Ammonia*	*Elphidium*	Miliolids	Soritids	*Sorites*	Archaiasinids	*Archaias*	*Androsina*	*Cyclorbiculina*	*Parasorites*	Peneroplids	*Peneroplis*	*Amphistegina*	Mollusks	Gastropods	Pelecypods	Ostracods	Echinoids
											G-3684												
16.0	HFC4	Peloid wackestone and packstone	?																				
16.4	HFC4	Peloid wackestone and packstone	5					X		X	X								X				
17.4	HFC3b	Mudstone and wackestone	2			P	X														X	X	
19.8	HFC3b	Skeletal grainstone and packstone	5								X					X	X					X	
22.0	HFC3a	Mudstone and wackestone	1?/2	X		P	X												X			X	
23.2	HFC3a	Pelecypod floatstone and rudstone	5	X		X	X						P		X	P	P						
27.2	HFC3a	Pelecypod floatstone and rudstone	5	X									X		X	X			X				
30.7	HFC3a	Touching-vug pelecypod floatstone and rudstone	4																X				X
31.5	HFC2	Skeletal grainstone and packstone	5	X	X		X	X	X		X								X			X	X
											G-3687												
14.0	HFC3a	Mudstone and wackestone	3			Q	X												X			X	
15.0	HFC3a	Skeletal grainstone and packstone	4/5	X		X		X						X		X			X			X	
16.2	HFC3a	Skeletal grainstone and packstone	4/5	X			X	X			X								X			X	
17.7	HFC3a	Skeletal grainstone and packstone	4/5					X			X			Q		X			X				
20.0	HFC3a	Gastropod floatstone and rudstone	1																	X		X	
21.6	HFC2	Skeletal grainstone and packstone	4/5	X							X		X						X			X	
24.7	HFC2	Skeletal grainstone and packstone	2	X		X												X	X			X	X
26.2	HFC2	Touching-vug pelecypod floatstone and rudstone	5					X	X			X			Q				X	X			X
27.5	HFC2	Touching-vug pelecypod floatstone and rudstone	5?			X			X						X								
											G-3689												
8.9	HFC4	Peloid grainstone and packstone	?																	X	X		
10.4	HFC4	Peloid grainstone and packstone	5								X										X		
12.5	HFC4	Peloid wackestone and packstone	5							X	X										X		
13.4	HFC4	Gastropod floatstone and rudstone	1																X	X	X		
13.9	HFC4	Conglomerate	5							X	X							X					
14.8	HFC3b	Mudstone and wackestone	3	X		X	P				X								X	X	X		

Table 2. Occurrence of stratigraphically important benthic foraminiferal taxa, mollusks, ostracods, and echinoids in test coreholes G-3671, G-3684, G-3687, G-3689, and G-3695 (Continued)

[Abbreviations: HFC, high frequency cycle; P, predominant foraminiferal taxa; Q, presence is questionable; RF, rotaliform foraminifera; X, present. Biofacies: biofacies 1, foraminifera absent (commonly contains smoothed-walled ostracods, commonly together with gastropods); biofacies 2, *Ammonia* predominant; biofacies 3, *Elphidium* predominant; biofacies 4, miliolids predominant; biofacies 5, archaiasinids, soritids, and peneroplids predominant]

Sample depth (below ground level, in feet)	HFC	Rock-fabric facies	Bio-facies	RF	*Rotalia*	*Ammonia*	*Elphidium*	Miliolids	Soritids	*Sorites*	Archaiasinids	*Archaias*	*Androsina*	*Cyclorbiculina*	*Parasorites*	Peneroplids	*Peneroplis*	*Amphistegina*	Mollusks	Gastropods	Pelecypods	Ostracods	Echinoids
17.0	HFC3b	Pedogenic limestone (root-mold limestone)	5	X		X	X			X		X				X			X				
20.7	HFC3a	Skeletal grainstone and packstone	5	X				X		X		X					X		X				
22.1	HFC3a	Skeletal grainstone and packstone	2			X													X				
23.2	HFC3a	Skeletal grainstone and packstone	5				X	X				X					P			X	X	X	
26.6	HFC3a	Gastropod floatstone and rudstone	1																	X		X	
27.3	HFC3a	Gastropod floatstone and rudstone	1																			X	
28.6	HFC3a	Gastropod floatstone and rudstone	1																				

G-3695

Sample depth (below ground level, in feet)	HFC	Rock-fabric facies	Bio-facies	RF	*Rotalia*	*Ammonia*	*Elphidium*	Miliolids	Soritids	*Sorites*	Archaiasinids	*Archaias*	*Androsina*	*Cyclorbiculina*	*Parasorites*	Peneroplids	*Peneroplis*	*Amphistegina*	Mollusks	Gastropods	Pelecypods	Ostracods	Echinoids
8.2	HFC5	Peloid grainstone and packstone	4					X												X	X		
11.4	HFC4	Peloid wackestone and packstone	5								X			X									
12.6	HFC4	Peloid wackestone and packstone	4/5					X				X										X	
15.4	HFC3b	Pedogenic limestone (root-mold limestone)	2	X		X	X																
18.4	HFC3b	Skeletal grainstone and packstone	5					X		X							X						
20.1	HFC3a	Mudstone and wackestone	1																	X	X		
21.0	HFC3a	Pelecypod floatstone and rudstone	5											X						X			
30.1	HFC2	Skeletal grainstone and packstone	5	X		X	X							Q				X		X	X	X	X
31.1	HFC2	Pelecypod floatstone and rudstone	4?					X													X		X
33.1	HFC2	Touching-vug pelecypod floatstone and rudstone	?																		X		X
34.3	HFC2	Touching-vug pelecypod floatstone and rudstone	5					X				X			X			X			X		X
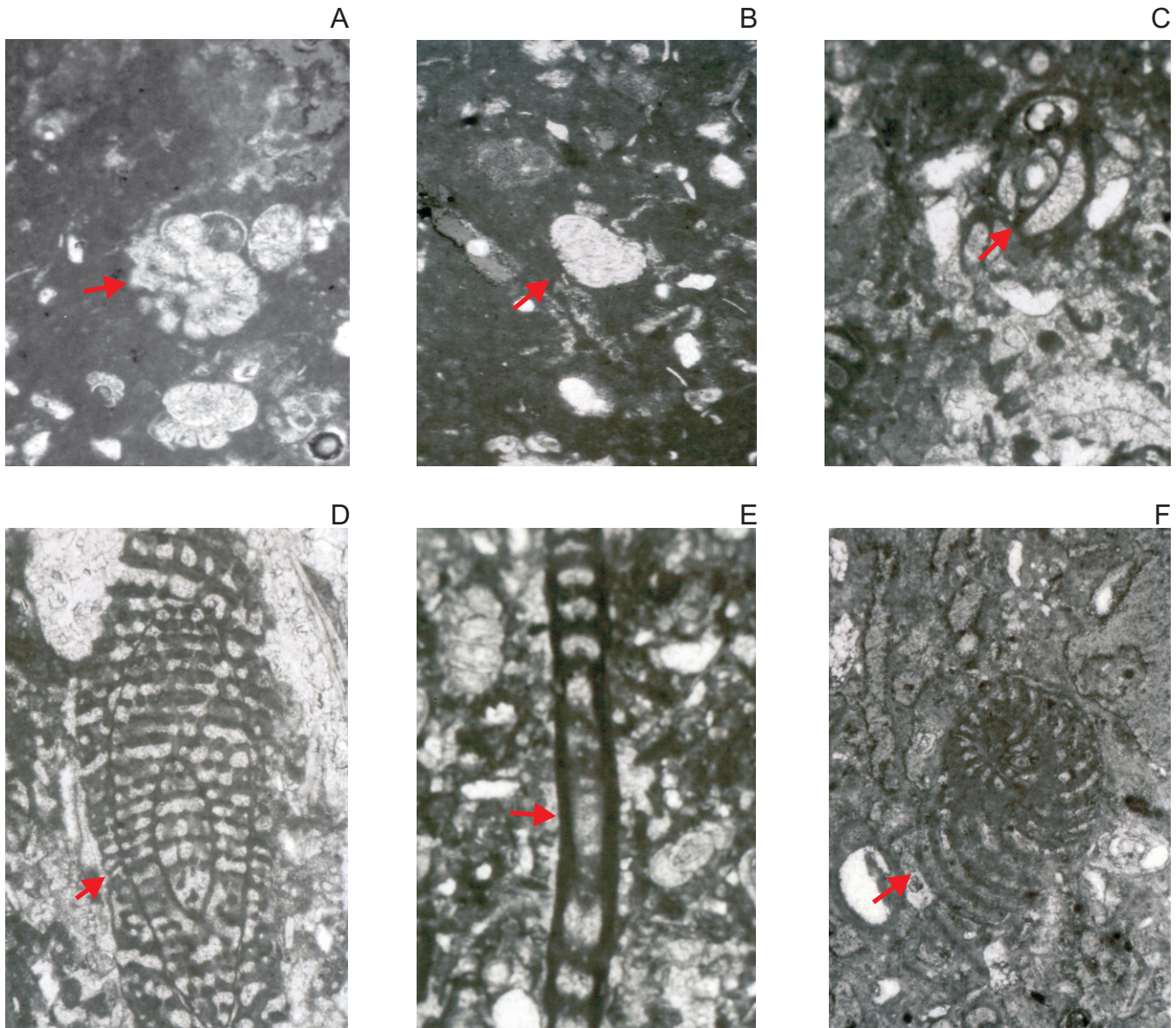
Figure 11. Photomicrographs of foraminifera that are characteristic of foraminiferal biofacies 2, 3, 4, and 5. (A) *Ammonia* sp. of biofacies 2, (B) *Elphidium* sp. of biofacies 3, (C) miliolid of biofacies 4, (D) *Archaias* sp. of biofacies 5, (E) soritid of biofacies 5, and (F) *Peneroplis* sp. of biofacies 5. Refer to table 3 for explanation of biofacies relation to foraminiferal taxonomy.

Cyclostratigraphy

In platform carbonate successions, high-frequency, about 1- to 30-ft thick, subtidal and upward-shallowing brackish- or freshwater-capped cycles (James, 1979; Chen and others, 2001) or HFCs can be delineated by the vertical organization of rock-fabric facies and depositional facies, character of bounding surfaces, and depositional facies relations across boundaries. Using a modified definition by Kerans and Tinker (1997) and Lucia (1999), the HFC is a chrono-stratigraphic unit composed of an unconformity-bounded succession of genetically related textures contained in beds or bedsets. The HFCs are the smallest set of genetically related lithofacies deposited during a single relative rise and fall of sea level. The upper and lower bounding surfaces of the HFC are at or near the switch from a relative sea-level fall to a relative sea-level rise. Correlation of HFCs to hydrogeologic and lithostratigraphic units of the study area is shown in figure 10. HFCs can be organized into longer term relative sea-level signals referred to as depositional sequences (DSs), however, this work is in progress.
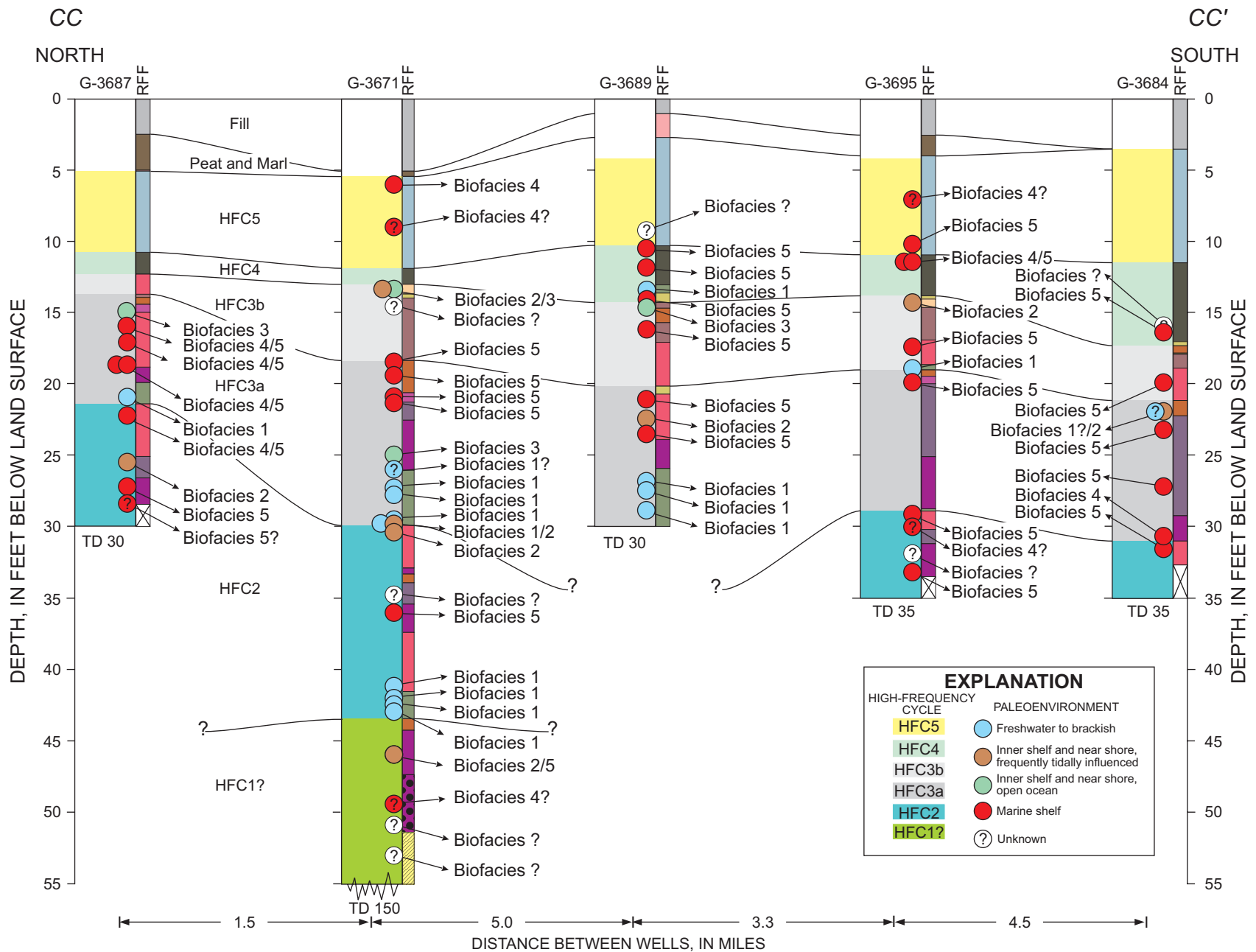
Figure 12. Geologic section *CC-CC'* showing foraminiferal taxonomy identified in test coreholes included in the study area. Line of section shown in figure 4. See figure 6 for rock-fabric facies (RFF) symbols. Refer to table 3 for explanation of biofacies relation to foraminiferal taxonomy.

Table 3. Foraminiferal biofacies and associated interpretive paleoenvironments

Biofacies	Predominant foraminiferal genera	Paleoenvironments
1	Foraminifera[1] absent	Freshwater
2	*Ammonia*	Inner shelf and nearshore in coastal bays, lagoons, and lower reaches of estuaries having variable salinity values, frequently tidally influenced.
3	*Elphidium*	Inner shelf and nearshore in coastal bays, lagoons, and lower reaches of estuaries having variable salinity values, but more normal salinity, open ocean.
4	Miliolids	Continental shelf environments of normal to mildly hypersalinity, typically with grassy meadows and associated with areas of significant biogenic carbonate production. Depths can vary from about 3 feet to more than 130 feet.
5	Archaiasinids, soritids, and peneroplids	Continental shelf environments of normal to mildly hypersalinity, typically with grassy meadows and associated with areas of significant biogenic carbonate production. Depths can vary from about 3 feet to more than 130 feet.

[1]Commonly contains smooth-walled ostracods and *Planorbella* gastropods.

Organization of all HFCs of the Fort Thompson Formation into DSs has not been attempted due to limited data from the lower part of the Fort Thompson Formation. Figures 13 and 14 present characteristics of idealized subtidal and brackish- or freshwater-capped HFCs from the Miami Limestone and upper part of the Fort Thompson Formation. Marine flooding surfaces occur at or near the lower boundary of each idealized HFC. A marine flooding surface is defined for this study as a surface separating younger from older strata and is marked by deeper water, marine strata resting on shallower water, freshwater or marine strata. The stratal section directly below the surface typically has evidence for subaerial exposure (compare to Posamentier and Allen, 1999). Table 4 shows the depths, relative to land surface, of the tops of HFCs defined for all test coreholes drilled for this study.

Rock-Fabric and Depositional Facies

Sixteen rock-fabric facies types were identified in the Miami Limestone and upper part of the Fort Thompson Formation: (1) peloid grainstone and packstone, (2) coral framestone, (3) peloid wackestone and packstone, (4) gastropod floatstone and rudstone, (5) conglomerate, (6) pedogenic limestone (laminated calcrete, massive calcrete, and root-mold limestone), (7) mudstone and wackestone, (8) skeletal grainstone and packstone, (9) sandy skeletal grainstone and packstone, (10) laminated peloid grainstone and packstone, (11) pelecypod floatstone and rudstone, (12) sandy pelecypod floatstone and rudstone, (13) touching-vug pelecypod floatstone and rudstone, (14) sandy touching-vug pelecypod floatstone and rudstone, (15) vuggy wackestone and packstone, and (16) quartz sandstone and skeletal sandstone (app. IV and table 5). These 16 rock-fabric facies were organized into three principal depositional facies: (1) shallow shelf (Enos, 1977), (2) brackish, and (3) freshwater (table 5). The shallow-shelf facies are the most common depositional facies found in the both the Miami Limestone and the Fort Thompson Formation (figs. 13 and 14). The brackish and freshwater facies are characteristic of the upper part of HFCs in the upper part of the Fort Thompson Formation. Where present, the freshwater facies commonly occurs at the top of HFCs, but less commonly is present as a transgressive unit at the base (pls. 1-5), as in the idealized Holocene sequence for Florida Bay (Enos, 1989).

Shallow-Shelf Depositional Facies

For the Miami Limestone, the shallow-shelf depositional facies typically include the peloid grainstone and packstone, peloid wackestone and packstone, coral framestone, and pedogenic limestone rock-fabric facies (table 5). Peloid grainstone and packstone are the principal rock-fabric facies of HFC5 (fig. 13) and uncommonly are the main rock-fabric facies of HFC4. Peloid wackestone and packstone are the primary rock-fabric facies of HFC4 (fig. 13). The cheilostome bryozoan *Schizoporella floridana* Osburn (Hoffmeister and others, 1967) is common to both the peloid grainstone and packstone, and peloid wackestone and packstone facies, but is rarely the principal component of the rock.
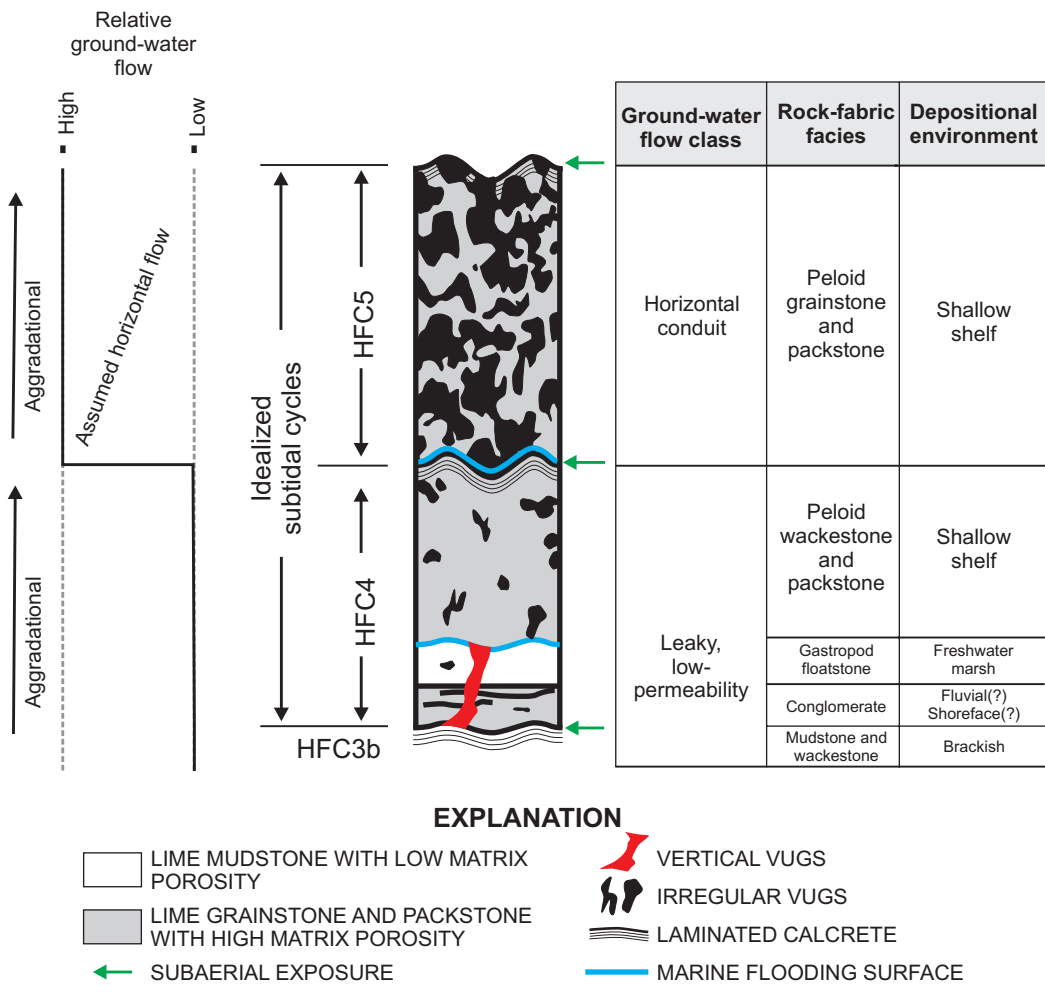
Figure 13. Idealized subtidal high-frequency cycles (HFC) of the Miami Limestone. Ground-water flow classes are related to rock-fabric facies and depositional environments.

The peloid wackestone and packstone are similar to the peloid grainstone and packstone of HFC5, but the intergranular matrix is mostly micrite. Commonly, the peloids of both the peloid grainstone and packstone and peloid wackestone and packstone rock-fabric facies have been dissolved and are identifiable only by their molds. A notable presence of archaiasinid and soritid benthic foraminifers in the peloid wackestone and packstone rock-fabric facies of HFC4 (table 2) can be useful in distinguishing this cycle from HFC5. Small coral heads that form the coral framestone rock-fabric facies can occur locally, encrusting the upper surface of the Fort Thompson Formation.

Pedogenic limestone forms the cap of HFC4 (fig. 13), with the most common type a wavy, laminated calcrete similar to those described by Multer and Hoffmeister (1968). The pedogenic cap of HFC4 is typically very thin, with a range of thickness from almost absent to 1.2 in. Karstic erosion of HFC4 locally can be so complete as to have almost or completely removed it (Cunningham, 2004). The upper part of HFC5 may locally lack the calcrete that typically caps HFC4. It is not uncommon for the upper part of HFC5 to be altered to reddish and brownish colors. Dissolution depressions and wide pipes can also be found along the upper surface of HFC5. These depressions
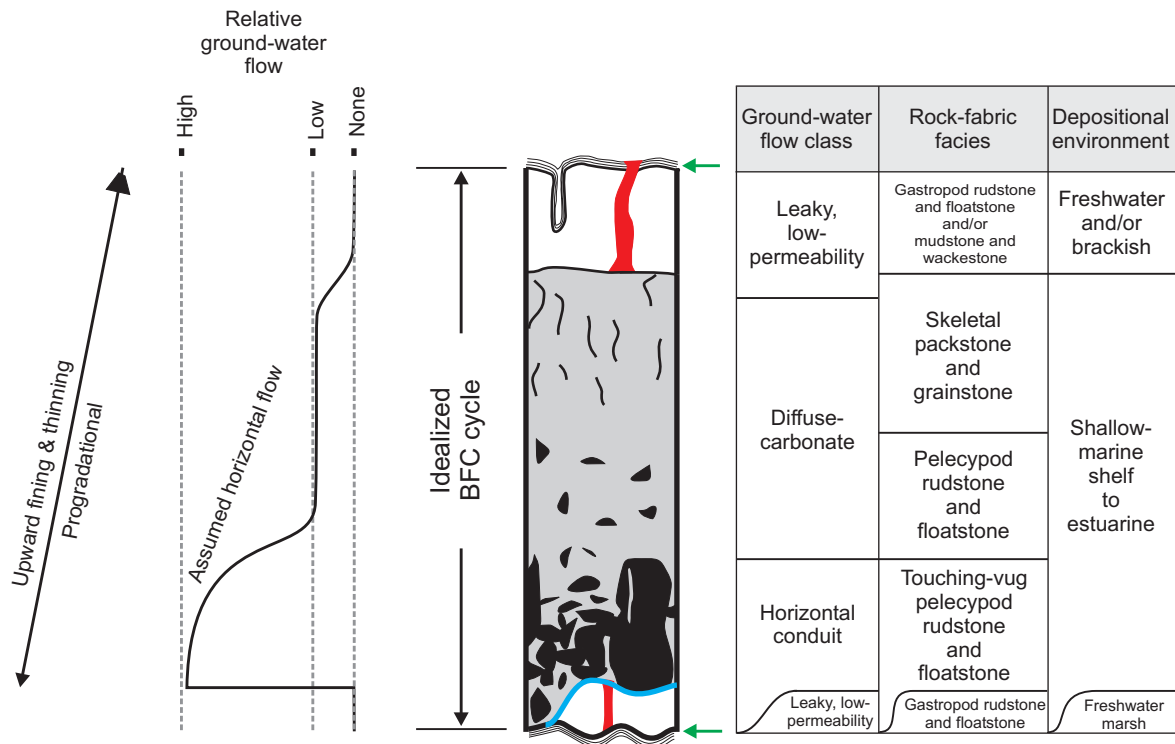
Figure 14. Idealized upward-shallowing brackish- or freshwater-capped high-frequency cycle of the Fort Thompson Formation. Ground-water flow classes are related to rock-fabric facies and depositional environments.

and pipes, as well as small-scale solution-enlarged burrows, can be filled with peat or marl or both, thereby reducing permeability.

For the upper part of the Fort Thompson Formation, the shallow-shelf depositional facies commonly includes the following rock-fabric facies: touching-vug pelecypod floatstone and rudstone, pelecypod floatstone and rudstone, skeletal grainstone and packstone, laminated peloid packstone and grainstone, sandy skeletal grainstone and packstone, sandy pelecypod floatstone and rudstone, sandy touching-vug pelecypod floatstone and rudstone, quartz sandstone and skeletal sandstone, and pedogenic limestone (table 5). Touching-vug pelecypod floatstone and rudstone or pelecypod

floatstone and rudstone most commonly occur in the lower part, but commonly above flooding surfaces at or near the base of HFCs (fig. 14). Laminated peloid grainstone and packstone are located in the middle part of HFC3a and can be correlated widely throughout the study area (pls.1-5). It is interpreted to represent a thin, but broad accumulation of stromatolites. Skeletal grainstone and packstone comprise the middle, upper, or both parts of the HFCs (fig. 14). Pelecypod-rich rock-fabric facies interpreted to represent the shallow-shelf environments mostly fall in the middle or lower part of the HFCs in the upper part of the Fort Thompson Formation (figs. 7 and 8). The sandy skeletal grainstone and packstone, sandy pelecypod floatstone and

Table 4. Tops of geologic units in test coreholes drilled for this study

[Well locations shown in figure 2. All units shown in feet. Altitude of measuring point is land surface referenced to National Geodetic Vertical Datum of 1929 (NGVD of 1929). Depths are from land surface. DNP, did not penetrate; HFC, high frequency cycle]

Local well identifier	Altitude of measuring point	Fill	Depth to top of peat	Depth to top of HFC5	Depth to top of HFC4	Depth to top of HFC3b	Depth to top of HFC3a	Depth to top of HFC2	Depth to top of HFC1	Depth to top of Tamiami
G-3671	12.0	0.0	5.0	5.3	11.8	12.9	18.3	29.8	41.4	55.0
G-3672	20.0	0.0	15.0	16.0	19.3	21.2	22.8	35.0	DNP	DNP
G-3673	20.0	0.0	15.0	16.0	19.3	21.2	22.8	35.0	52.0	60.0
G-3674	8.0	0.0	Not present	3.0	8.6	9.0	15.7	23.1	29.0	70.5
G-3675	8.0	0.0	Not present	4.0	5.4	7.3	11.2	20.3	42.0	75.0?
G-3678	12.0	0.0	Not present	4.0	12.0	12.9	14.4	24.8	32.0	DNP
G-3679	10.5	0.0	Not present	2.5	10.7	13.3	15.1	27.1	34.8	DNP
G-3680	11.0	0.0	Not present	2.0	11.5	13.9	15.4	26.9	35.5	DNP
G-3681	11.0	0.0	Not present	3.0	12.1	13.7	17.4	31.3	42.8	DNP
G-3682	13.0	0.0	Not present	3.5	11.0	14.2	16.7	25.3	DNP	DNP
G-3683	12.0	0.0	Not present	2.0	10.9	14.8	17.6	28.9	DNP	DNP
G-3684	11.5	0.0	Not present	3.5	11.5	17.3	21.1	30.9	DNP	DNP
G-3685	14.0	0.0	6.5	7.0	11.9	14.3	17.9	28.3	DNP	DNP
G-3686	11.0	0.0	2.5	6.4	10.6	12.1	14.9	25.9	DNP	DNP
G-3687	12.5	0.0	2.5	5.1	10.8	12.3	13.7	21.4	DNP	DNP
G-3688	9.5	0.0	1.5	4.5	9.4	12.0	16.2	25.9	DNP	DNP
G-3689	9.0	0.0	Not present	2.7	10.4	14.3	20.1	DNP	DNP	DNP
G-3690	11.5	0.0	5.0	7.0	10.5	11.3	12.6	25.1	DNP	DNP
G-3691	14.0	0.0	4.0	6.7	12.4	13.1	14.2	24.5	31.5	DNP
G-3692	9.0	0.0	1.0	1.9	9.7	11.3	16.7	26.7	DNP	DNP
G-3693	11.5	0.0	5.0	5.2	12.3	16.0	18.2	31.5	DNP	DNP
G-3694	11.0	0.0	4.0	6.1	15.0	16.2	20.0	30.3	DNP	DNP
G-3695	10.5	0.0	2.5	4.0	10.9	14.0	18.5	28.6	DNP	DNP
G-3696	11.0	0.0	Not present	3.0	11.8	18.4	21.8	33.5	DNP	DNP
G-3697	9.5	0.0	1.0	2.8	10.0	13.4	16.4	26.5	DNP	DNP
G-3710	10.0	0.0	Not present	2.2	9.2	11.8	16.6	28.5	DNP	DNP
G-3711	10.0	0.0	Not present	3.0	12.1	13.7	16.7	29.7	DNP	DNP
G-3712	10.0	0.0	Not present	1.5	14.5	15.2	17.2	26.9	DNP	DNP
G-3713	10.0	0.0	Not present	2.0	10.2	13.3	16.8	30.6	DNP	DNP
G-3714	13.0	0.0	Not present	3.0	14.3	15.5	17.1	DNP	DNP	DNP
G-3715	13.0	0.0	Not present	3.0	12.8	15.5	17.5	DNP	DNP	DNP
G-3716	9.0	0.0	Not present	3.0	11.4	17.3	21.1	DNP	DNP	DNP
G-3717	9.0	0.0	4.0	7.0	10.5	13.0	15.6	24.5	38.0	DNP
G-3718	9.0	0.0	1.8	5.0	6.2	9.5	14.3	24.0	DNP	DNP
G-3719	9.0	0.0	1.8	4.1	8.5	9.5	10.0	18.3	DNP	DNP
G-3720	9.0	0.0	2.1	4.3	6.6	7.7	13.2	21.3	DNP	DNP
G-3721	10.0	0.0	6.5	8.5	10.2	11.9	13.0	23.0	DNP	DNP
G-3722	10.0	0.0	6.5	7.5	7.8	10.4	12.2	21.7	DNP	DNP
G-3723	8.0	0.0	3.1	5.8	9.6	12.8	15.0	22.4	31.6	DNP
G-3724	9.0	0.0	1.0	6.6	8.7	10.0	13.3	24.0	DNP	DNP
G-3725	6.0	0.0	Not present	0.5	9.5	13.6	17.2	25.2	DNP	DNP
G-3726	7.0	Poor data	Poor data	4.9	Poor data	5.5	Poor data	8.4	DNP	DNP
G-3727	9.0	0.0	3.0	7.5	12.9	13.5	15.5	24.3	34.9	DNP

Table 4. Tops of geologic units in test coreholes drilled for this study (Continued)

[Well locations shown in figure 2. All units shown in feet. Altitude of measuring point is land surface referenced to National Geodetic Vertical Datum of 1929 (NGVD of 1929). Depths are from land surface. DNP, did not penetrate; HFC, high frequency cycle]

Local well identifier	Altitude of measuring point	Fill	Depth to top of peat	Depth to top of HFC5	Depth to top of HFC4	Depth to top of HFC3b	Depth to top of HFC3a	Depth to top of HFC2	Depth to top of HFC1	Depth to top of Tamiami
G-3728	8.0	0.0	Not present	4.0	8.7	9.8	12.8	19.6	31.2	DNP
G-3729	6.0	0.0	Not present	5.0	9.4	10.0	11.7	24.0	DNP	DNP
G-3730	6.0	0.0	Not present	4.0	9.5	12.5	14.8	24.8	34.0	DNP
G-3731	11.0	0.0	Not present	6.0	9.4	10.6	13.7	20.8	35.2	DNP
G-3732	7.0	0.0	Not present	3.0	6.2	8.3	12.0	19.1	36.2	DNP
G-3733	5.0	0.0	1.0	2.0	Absent	10.3	14.5	24.5	33.3	DNP
G-3734	8.0	0.0	3.0	4.0	Absent	8.9	12.7	23.7	DNP	DNP

rudstone, sandy touching-vug pelecypod floatstone and rudstone, and skeletal sandstone principally occur in HFC1 of the lower part of the Fort Thompson Formation. The skeletal grainstone and packstone can be host to pedogenic-altered limestone at the top of HFC2. At the top of HFC2, gray- to light-brown gastropod floatstone and rudstone (freshwater deposits) from overlying units fill the cracks and root molds (mainly mangrove) that intersect skeletal grainstone and packstone.

Brackish Depositional Facies

The brackish depositional facies typically include the following rock-fabric facies: mudstone and wackestone, gastropod floatstone and rudstone, and pedogenic limestone (fig. 14 and table 5). The mudstone and wackestone locally contain tubes that are typically irregular and semi-horizontal. The tubular structures represent root molds, including molds of mangrove roots (Galli, 1991), or cavities created by thin worms(?). Dissolution depressions and pipes, and cracks and veins are fairly common. The depressions, pipes, and cracks may be filled with subtidal deposits from the overlying cycle. Wavy laminated calcrete commonly caps upward-shallowing brackish- or freshwater-capped cycles. The brackish environment is suggested by the presence of a faunal assemblage composed of mostly only two benthic foraminifers (*Ammonia* and *Elphidium*), small gastropods, and smooth-shelled ostracods (Rose and Lidz, 1977).

Pedogenic altered limestone commonly forms the top of HFCs of the Fort Thompson Formation with host substrates most typically of brackish or freshwater depositional facies. Pedogenic processes have produced common features that include dissolution cracks and fills, root molds and fills, terra-rossa type soils(?),

wavy laminated crusts, and rare pisoliths. Some cracks and root molds (mangrove) extend as deep as about 4 ft downward from the erosion surface and typically taper toward the base.

Freshwater Depositional Facies

The freshwater depositional facies typically include the gastropod floatstone and rudstone, mudstone and wackestone, and pedogenic limestone rock-fabric facies (figs. 13 and 14 and table 5). Mudstone and wackestone depositional textures mostly form the matrix of the floatstone-rudstone rock-fabric facies. The gastropod floatstone-rudstone typically contains the gastropods *Planorbella duryi-disstoni*, *Planorbella scalaris*, *Physa* sp.(?), *Pomacea paludosa* Say, and less commonly Hydrobiidae(?). In a study of five cores from the study area, Wassum (2000) determined that *Planorbella* is the most commonly occurring gastropod and comprises as much as 55 percent of the total fauna found in the freshwater facies of the Fort Thompson Formation. Wassum (2000) also found that peloids are common, constituting up to 60 percent of the total grains observed in thin sections. Smooth-walled ostracods and charophytes, a freshwater algae, also are common grain types.

A wavy laminated calcrete type pedogenic limestone locally caps the freshwater limestone of this depositional facies at the tops of HFC3b, HFC3a, and HFC2 (pls. 1 and 5) similar to those described by Multer and Hoffmeister (1968). It is typically very thin, with a range of thickness from almost absent to 1.4 in. Karstic erosion of the limestone of this depositional facies can form *in situ* breccia. Dessication cracks are relatively common.

Table 5. Summary of rock-fabric facies of the Miami Limestone and Fort Thompson Formation in north-central Miami-Dade County

Rock-fabric facies	Color	Depositional texture	Sedimentary structures/ textures	Carbonate and accessory grains	Porosity (percent)	Hydraulic conductivity	Paleoe-nviron-ment
Peloid grainstone and packstone	Very pale orange 10YR 8/2, grayish orange 10YR 7/4 and pale yellowish orange 10YR 8/6 matrix	Burrow-mottled pelmold and peloid grainstone and packstone	Highly burrowed, including minor *Calli-anassa* shrimp burrows, very thickly bedded	Mainly pelmolds and peloids; minor pelecypods, gastropods, oomolds, and *Schizoporella* bryozoans, miliolids, quartz grains, intraclasts	25-45 percent pelmol-dic, 5-15 percent solu-tion-enlarged burrow porosity, trace root-mold porosity	High to very high	Shallow shelf
Coral framestone	Very pale orange 10YR 8/2, grayish orange 10YR 7/4, dark yellowish orange 10YR 6/6, moderate yellowish brown 10YR 5/4, pale yel-lowish brown 10YR 6/2	Coral framestone	Massive with borings and vugs	Mainly *Monastrea*(?) head coral, minor medium to large pebble-sized *Schizoporella*; trace to 5 per-cent quartz grains with peloids in boring and vug fill	15 percent intragrain porosity, 5-10 percent separate vug porosity, 5 percent root-mold porosity	Moderate	Shallow shelf
Peloid wackestone and packstone	Very pale orange 10YR 8/2, dark yellowish orange 10YR 6/6, moderate yellowish brown 10YR 5/4, pale yellowish brown 10YR 6/2, and light brown 5YR 5/6 matrix	Mainly mud-dominated fabric characterized by pelecypod, benthic foram lime floatstone with a peloid lime wackestone to mud-dominated lime pack-stone matrix, but minor grain-dominated fabric characterized by peloid lime grainstone or skeletal grain-dominated lime packstone matrix; minor solution-enlarged burrows filled with peloid grain-stone or packstone	Highly burrowed, including minor *Calli-anassa* shrimp burrows, common ~0.5-1 mm diameter rhizoliths and less common up to 5-cm wide subvertical root molds, medium to very thickly bedded	Mainly peloids, pelecypods (including *Chione*) and benthic foraminifers (including archaias-inids, *Sorites*, miliolids, *Cyclorbi-culina*), ostracods, and minor *Schizoporella* bryozoans, quartz grains, and intraclasts	5-20 percent pelmol-dic and skeletal moldic porosity, 5-40 percent separate- and touch-ing-vug porosity, trace to 10 percent root-mold porosity, 1 percent intraparticle porosity	Matrix of float-stone low, burrow fill moderate, vuggy porosity low to very high	Shallow shelf
Gastropod floatstone and rudstone	Pale yellowish brown 10YR 6/2, very pale orange 10YR 8/2, light gray N7 to medium dark gray N4	Moldic gastropod float-stone and rudstone with skeletal wackestone and packstone matrix; local lime wackestone	~0.5-1 mm diameter rhizoliths, local desic-cation cracks, very thinly to very thickly bedded	Mainly gastropods molds includ-ing *Planorbella, Pomacea, Physa, Hydrobiidae*?, smooth-walled ostracods, and skeletal fragments; minor quartz sand, pelecypods, freshwater-algae *Charophyta*	15 percent skeletal-moldic separate vugs, solution-enlarged semivertical root molds, minor vertical or irregular vugs and local root-mold porosity	Matrix low, vertical vuggy hydraulic con-ductivity low to high, horizontal vuggy hydraulic conductivity low to medium	Fresh-water marsh, freshwater pond, or brackish

28

Characterization of Aquifer Heterogeneity Using Cyclostratigraphy and Geophysical Methods in the Upper Part of the Karstic Biscayne Aquifer, Southeastern Florida

Table 5. Summary of rock-fabric facies of the Miami Limestone and Fort Thompson Formation in north-central Miami-Dade County (Continued)

Rock-fabric facies	Color	Depositional texture	Sedimentary structures/ textures	Carbonate and accessory grains	Porosity (percent)	Hydraulic conductivity	Paleoe-nviron-ment
Conglomerate	Very pale orange 10YR 8/2 and pale yellowish brown 10YR 6/2 matrix, and very pale orange 10YR 8/2, dark yellowish orange 10YR 6/6, moderate yellowish brown 10YR 5/4, pale yellowish brown 10YR 6/2, moderate brown 5YR 4/4, light brown 5YR 6/4, grayish orange pink 5YR 7/2 and dark gray N3 to light gray N7 intraclasts	Intraclast lime rudstone with quartz sandstone matrix or quartz sand-rich lime grainstone or mud-dominated lime packstone matrix	Common ~0.5-1-mm diameter rhizoliths, thinly to medium bedded	Mainly intraclasts and quartz grains; local minor peloids, pelecypods	5-15 percent intergrain porosity, 5-15 percent separate- and touch-ing-vug porosity, local 5-10 percent root-mold porosity	Matrix low, vuggy porosity low to high	Fluvial(?), shore-face(?)
Pedogenic limestone	(A) very pale orange 10YR 8/2, dark yellowish orange 10YR 6/6, moderate yellowish brown 10YR 5/4, pale yellowish brown 10YR 6/2 and grayish orange 10YR 7/4; (B) very pale orange 10YR 8/2 and grayish orange 10YR 7/4; (C) dark yellowish orange 10YR 6/6, grayish orange 10YR 7/4, pale yellowish brown 10YR 6/2, moderate yellowish brown 10YR 5/4 and very pale orange 10YR 8/2	3 principal types: (A) lami-nated calcrete, (B) massive calcrete, (C) root-mold limestone	(A) Thinly to very thickly bedded and drapes over micro-topography; (B) very finely laminated; (C) thinly to very thickly bedded or poorly bedded, desiccation cracks	(A) minor quartz grains; (B) minor intraclasts, pelecypods, skeletal fragments, quartz grains, rotali-form benthic foraminifera includ-ing *Ammonia* and *Elphidium*; (C) skeletal fragments and local miliolids, minor quartz sand	(A) Minor microporosity; (B) 20-30 percent root-mold porosity, 5-10 percent vuggy poros-ity, 5 percent pelmol-dic and skeletal moldic porosity; (C) 2-5 percent skele-tal moldic porosity, 2-5 percent desicca-tion crack porosity	(A) Low, (B) moderate to high, (C) matrix very low to low	Subaerial exposure
Mudstone and wackestone	Very pale orange 10YR 8/2, grayish orange pink 5YR 7/2, pale yellowish brown 10YR 6/2, grayish orange 10YR 7/4	Lime mudstone and wackestone	Common subvertical cracks, ~0.5-1 mm diameter rhizoliths, semivertical solution-enlarge vugs, thinly to thickly bedded	(A) Brackish: mainly ostracods, skeletal fragments, gastropods (including *Planorbella* in the G-3679 test corehole), benthic foraminifers (including *Ammonia*, *Elphidium*, miliolids, soritids, *Archaias*, peneroplids, *Androsina*; minor pelecypods quartz sand; (B) mud mound: peloids, pelecy-pods, benthic foraminifers (includ-ing miliolids), quartz sand, intraclasts, ostracods	5-20 percent skeletal mold porosity, 5 per-cent root-mold poros-ity, 5 percent separate vug porosity, none to 30 percent semiverti-cal touching vug porosity, none to 15 percent desicca-tion-crack porosity	Matrix very low to low; moderate to high vertical vuggy hydraulic conductivity; very Low to low horizontal vuggy hydraulic con-ductivity	Two prin-cipal envi-ronments (A) brack-ish and (B) mud mound(?)

Table 5. Summary of rock-fabric facies of the Miami Limestone and Fort Thompson Formation in north-central Miami-Dade County (Continued)

Rock-fabric facies	Color	Depositional texture	Sedimentary structures/ textures	Carbonate and accessory grains	Porosity (percent)	Hydraulic conductivity	Paleoe-nviron-ment
Skeletal grainstone and packstone	Very pale orange 10YR 8/2, pale yellowish brown 10YR 6.2, grayish orange 10YR 7/4; light gray N7 to very light gray N8	Skeletal grainstone and packstone	Principally massive and highly burrowed, thickly to very thickly bedded	Mainly skeletal fragments, benthic foraminifers (including archaias-inids, soritids, miliolids, pener-oplids, *Elphidium*, *Ammonia*, *Androsina*, *Amphistegina*, rotaliforms), peloids, pelecypods (including *Trachycardium*, *Anodontia*), ostracods, gastro-pods, echinoids; minor quartz grains; trace red algae	15-30 percent skeletal moldic porosity, 5-15 percent intergrain porosity, trace to 10 percent pelmoldic porosity, 5-15 percent root-mold porosity, 1 percent intraparticle	Matrix moderate	Shallow shelf
Sandy skeletal grainstone and packstone	Very pale orange 10YR 8/2, very light gray N8	Sandy skeletal grainstone and packstone	Thickly to very thickly bedded	Mainly peloids, quartz sand, mollusks (including *Chione*, *Modulus*, *Turritella*, *Codakia*, *Lucina*, *Lirophora*, *Pyrazisinus*, *Tagelus*, *Anomalocardia*, *Melongena*, *Lucinisca*, *Carditimera*, *Codakia*, *Cerithium*), skeletal fragments	2-10 percent skeletal molds, separate and touching vugs	Matrix medium, vugs medium to very high	Shallow shelf
Laminated peloid grain-stone and packstone	Very pale orange 10YR 8/2	Peloid grainstone and packstone	Thinly laminated to very thinly bedded	Mainly peloids; minor quartz grains, skeletal fragments, and benthic foraminifers (including miliolids, *Elphidium*, *Androsina*, rotaliforms), mollusk fragments	10-15 percent moldic porosity, 10-20 per-cent intergrain poros-ity, bedding plane vug porosity 5-20 percent	Matrix moder-ate, bedding plane vugs high to very high	Intertidal
Pelecypod floatstone and rudstone	Very pale orange 10YR 8/2, very light gray N8	Pelecypod floatstone and rudstone with skeletal wackestone, packstone or grainstone matrix	Thickly to very thickly bedded	Mainly mollusks (*Chione*, *Turritella*, *Trachycardium*, *Bellucina*, *Diodora*, *Muricid*, *Brachidontes*, *Anomalocardia*?) benthic foraminifers (including archaiasinids, peneroplids, miliolids, *Parasorites*, soritids, *Amphistegina*, *Ammonia*, *Elphidium*, *Androsina*, rotali-forms), peloids, ostracods; minor quartz grains; trace echinoids	10-25 percent moldic, 5-15 percent inter-grain, irregular separate and touching vugs	Matrix moder-ate, irregular vugs low to very high	Shallow shelf

Table 5. Summary of rock-fabric facies of the Miami Limestone and Fort Thompson Formation in north-central Miami-Dade County (Continued)

Rock-fabric facies	Color	Depositional texture	Sedimentary structures/ textures	Carbonate and accessory grains	Porosity (percent)	Hydraulic conductivity	Paleoe-nviron-ment
Sandy pelecypod floatstone and rudstone	Very pale orange 10YR 8/2, very light gray N8	Pelecypod floatstone and rudstone with sandy wackestone or packstone matrix	Thickly to very thickly bedded	Mainly peloids, quartz sand, pelecypods, skeletal fragments, benthic foraminifers	5-20 percent skeletal molds,	Matrix medium	Shallow shelf
Touching-vug pelecypod floatstone and rudstone	Very pale orange 10YR 8/2, very light gray N8	Pelecypod floatstone and rudstone with peloid and skeletal fragment wackestone and packstone matrix	Medium to very thickly bedded	Mainly peloids, mollusks (including *Chione, Modulus, Turritella, Codakia, Lucina, Pecten, Diplodonta, Strombus?, Pleuromeris, Carditimera, Anadara, Glycymeris, Anodonita, Cardium, Dosinia, Nucula, Turbo, Glycymeris, Pecten*?), skeletal fragments, benthic foraminifers (including soritids, archaiasinids, miliolids, *Ammonia, Parasorites, Amphistegina, Elphidium*, peneroplids, rotaliforms, *Androsina*), ostracods, echinoids; trace *Porites*? coral	2-25 percent skeletal moldic porosity, 5-100 percent separate and touching vugs	Matrix medium, vugs medium to very high	Shallow shelf
Sandy touching-vug pelecypod floatstone and rudstone		Pelecypod floatstone and rudstone with	Thickly to very thickly bedded	Mainly peloids, quartz sand, mollusks (including *Chione, Cerithium, Trachycardium, Modulus, Turritella, Lucinisca*), skeletal fragments	5-20 percent skeletal molds,	Matrix medium	Shallow shelf
Vuggy wackestone and packstone	Very pale orange 10YR 8/2	Peloid wackestone and packstone	Thickly to very thickly bedded	Mainly peloids, benthic foramini-fers (including miliolids), gastro-pods; minor to abundant quartz grains	5-25 percent irregular separate and touching vugs	Matrix low, vugs moderate to very high	Shallow shelf (mud bank)
Quartz sandstone and skeletal sandstone	Very pale orange 10YR 8/2, very light gray N8	Skeletal sandstone	Thickly to very thickly bedded	Mainly quartz sand, peloids, pelecypods, skeletal fragments, gastropods	2-10 percent skeletal molds	Matrix medium	Shallow shelf

The common micrite-rich mudstone and wacke-stone rock-fabric facies comprising these depositional facies result in relatively low permeability. The dessication cracks and root molds may be enlarged by meteoric dissolution, enhancing the vertical permeability of the limestone of these depositional facies, and providing small conduits for vertical passage of ground water through the limestone of these depositional facies. However, touching vugs that are oriented with a preferred horizontal orientation are not common, so the overall horizontal permeability of the limestone of these freshwater facies is relatively low.

High-Frequency Cycles

Two types of HFCs are present in the upper part of the Biscayne aquifer in the study area (fig. 10). One is an upward-shallowing brackish- or freshwater-capped cycle, composed of a succession of textures that mostly decrease upward in grain size, mainly shallows upward in terms of water depth, and is capped by a brackish or freshwater depositional facies (fig. 14). Upward shallowing brackish- or freshwater-capped cycles are exclusive to the Fort Thompson Formation. Comprising the Miami Limestone, the second type of HFC, a subtidal cycle, is formed by vertical aggradation of shallow-shelf, peloidal, highly burrowed, marine sediments (fig. 13). Depositional environments of the Miami Limestone are discussed in more detail by Hoffmeister and others (1967), Perkins (1977), and Evans (1984). A type of subtidal cycle is under investigation in the lower part of the Fort Thompson Formation. Cycle boundaries are abrupt, and generally upper boundaries have a pedogenic-limestone cap. A marine flooding surface occurs at or near the base of the HFCs (figs. 13 and 14). Cycle thicknesses may range up to about 20 ft in the lower part of the Fort Thompson Formation. Cycle durations are of about 10,000 to 120,000 years based on sediment ages (Broeker and Thurber, 1965; Osmond and others, 1965; Mitterer, 1975, Multer and others, 2002). The HFCs of the upper part of the Fort Thompson Formation and Miami Limestone may correspond to the fourth- and fifth-order Milankovitch cycles as defined by Goldhammer and others (1987).

Upward-Shallowing Brackish- or Freshwater-Capped Cycles

The upward-shallowing brackish- or freshwater-capped cycles in the upper part of the Fort Thompson Formation are similar to the idealized stratigraphic sequence that Enos (1989) described for the Holocene sediments of Florida Bay. In ascending order, the conceptual upward-shallowing brackish- or freshwater-capped cycle of the upper part of the Fort Thompson Formation consists of: (1) molluscan-rich rudstones and floatstones that can have abundant touching skeletal molds and irregular vugs (the lower boundary of these facies forms a marine flooding surface that overlies the freshwater marsh or pond deposit); (2) skeletal grainstone and packstone with abundant moldic porosity; (3) low-permeability brackish lime mudstone and wackestone that can contain the benthic foraminifera *Ammonia* and *Elphidium* (Rose and Lidz, 1977), ostracods, and gastropods; (4) a freshwater marsh or pond deposit containing smooth-walled ostracods and pulmonate gastropods, a low-permeability matrix, and mostly "nontouching" fossil molds; and (5) a calcrete unit that forms the upper bounding surface of the cycle (fig. 14).

The upward-shallowing brackish- or freshwater-capped cycles are typically characterized by shallow-shelf depositional environments in the lower part and grade upward to brackish or freshwater facies. All accommodation was filled during deposition of the shallowing-upward brackish- or freshwater-capped cycles, which are considered regressive. The presence of a pedogenic limestone cycle cap is indicative of subaerial exposure and a relative fall in sea level, punctuating the end of cycle development.

Three shallowing-upward brackish- or freshwater-capped HFCs are recognized in the upper part of the Fort Thompson Formation (fig. 10): HFC3b, HFC3a, and the upper part of HFC2. Correlation of these HFCs to the marine units of Perkins (1977) is based on similarities of lithologies he described, and his mapping of the paleotopography of the lower bounding surface of the marine units. Perkins (1977) delineated three marine units or "Q units" separated by regional discontinuity surfaces within the Fort Thompson in southern Florida (fig. 10). Only four test coreholes drilled during the course of this study fully penetrated the Q1 unit of Perkins (fig. 2; G-3671, G-3673, G-3674, and G-3675).

In a study throughout Miami-Dade County, Galli (1991) defined the Fort Thompson Formation as a single depositional sequence bounded below and above by inconformities that correspond to the contacts between the Tamiami and Fort Thompson Formations and between the Fort Thompson Formation and Miami Limestone, respectively. Galli (1991, fig. 6) dissected this depositional sequence into seven parasequences (fig. 10) that thicken toward the northern boundary of Miami-Dade County and thin to the south. To the south, Galli (1991) shows that there is onlap of the oldest parasequences onto an unconformity at the top of the Tamiami Formation with the top of the Tamiami Formation increasing in elevation to the west and south.

Subtidal Cycles

The Miami Limestone is composed of two subtidal cycles, which typically are composed of shallow-shelf depositional facies that have an abrupt subaerial erosion surface at the top capped by a pedogenic limestone (fig. 13). In general, the subtidal cycles are characterized by a relatively homogeneous succession of shallow-shelf deposits. The sediments contained in the two Miami Limestone subtidal cycles correspond to the bryozoan facies of the Miami Limestone as designated by Hoffmeister and others (1967). They described the sediments of this facies as composed of pellets, ooids, skeletal sands, and bryozoans, and interpreted the environment for its deposition as a marine shelf lagoon. Later, both Perkins (1977) and Evans (1984) stated that the bryozoan facies was deposited on an open-marine platform. Herein, HFC4 of the Miami Limestone mostly corresponds to foraminiferal biofacies 5 and HFC5 mostly to foraminiferal biofacies 4, which are both interpreted to represent shallow-shelf depositional environments of normal to mildly hypersaline conditions (figs. 11 and 12 and tables 2 and 3). The base of HFC4 can consist of a freshwater limestone, also recognized by Halley and Evans (1983), that represents development of a freshwater marsh during initial transgression of the underlying exposure surface at the top of HFC3b.

The subtidal cycles are only partially developed because accommodation was not completely filled prior to subaerial erosion. Their occurrence suggests that the increase in accommodation outpaced sediment aggradation because of the absence of any peritidal depositional facies. Deposition of the cycles was followed by a prolonged period of subaerial exposure, based on the intensity of subaerial erosion of the upper boundary between HFC4 and HFC5, and the ages of the sediments in HFC4 and HFC5 (Broeker and Thurber, 1965; Osmond and others, 1965; Mitterer, 1975; Cunningham, 2004). Subtidal cycles also are present in the lower part of the Fort Thompson Formation; however, characterizing these cycles is beyond the scope of this study.

The lower subtidal cycle (HFC4) and the upper subtidal cycle (HFC5) of the Miami Limestone are respectively equivalent to the Q4 and Q5 units of Perkins (1977) (fig. 10). HFC4 and HFC5 both contain the miliolid, bryozoan, pellet packstone and grainstone lithologic facies of Perkins (1977). The five marine units or "Q units" of Perkins (1977) were the first recognized unconformity-bound, time-stratigraphic units within the Miami Limestone and Fort Thompson Formation of southernmost peninsular Florida. Figure 10 shows the relation of the Q units to the HFCs of this study.

CHARACTERIZATION OF CYCLOSTRATI-GRAPHY, POROSITY, AND PERMEABILITY USING GROUND-PENETRATING RADAR

Interpreted GPR profiles were integrated with test corehole data to construct maps showing the top of HFC4 (figs. 15-17). The upper surface of the HFC4 cycle is considered important because it is the approximate top of the semiconfining unit that extends across the base of the Miami Limestone and the top of the Fort Thompson Formation. A GPR profile for a single site along Krome Avenue (fig. 2) is used herein to illustrate how GPR was used to characterize the upper part of the Biscayne aquifer. The Krome Avenue GPR site is located about 8 mi south of the C-4 Canal and along a flat unpaved road that is parallel to and about 30 ft west of Krome Avenue (fig. 2). Additional information on the GPR investigation of the Krome Avenue site, as well as results of a study of a GPR site in ENP that investigates the characterization of porosity and permeability within the limestone of the Biscayne aquifer, can be found in Cunningham (2004).
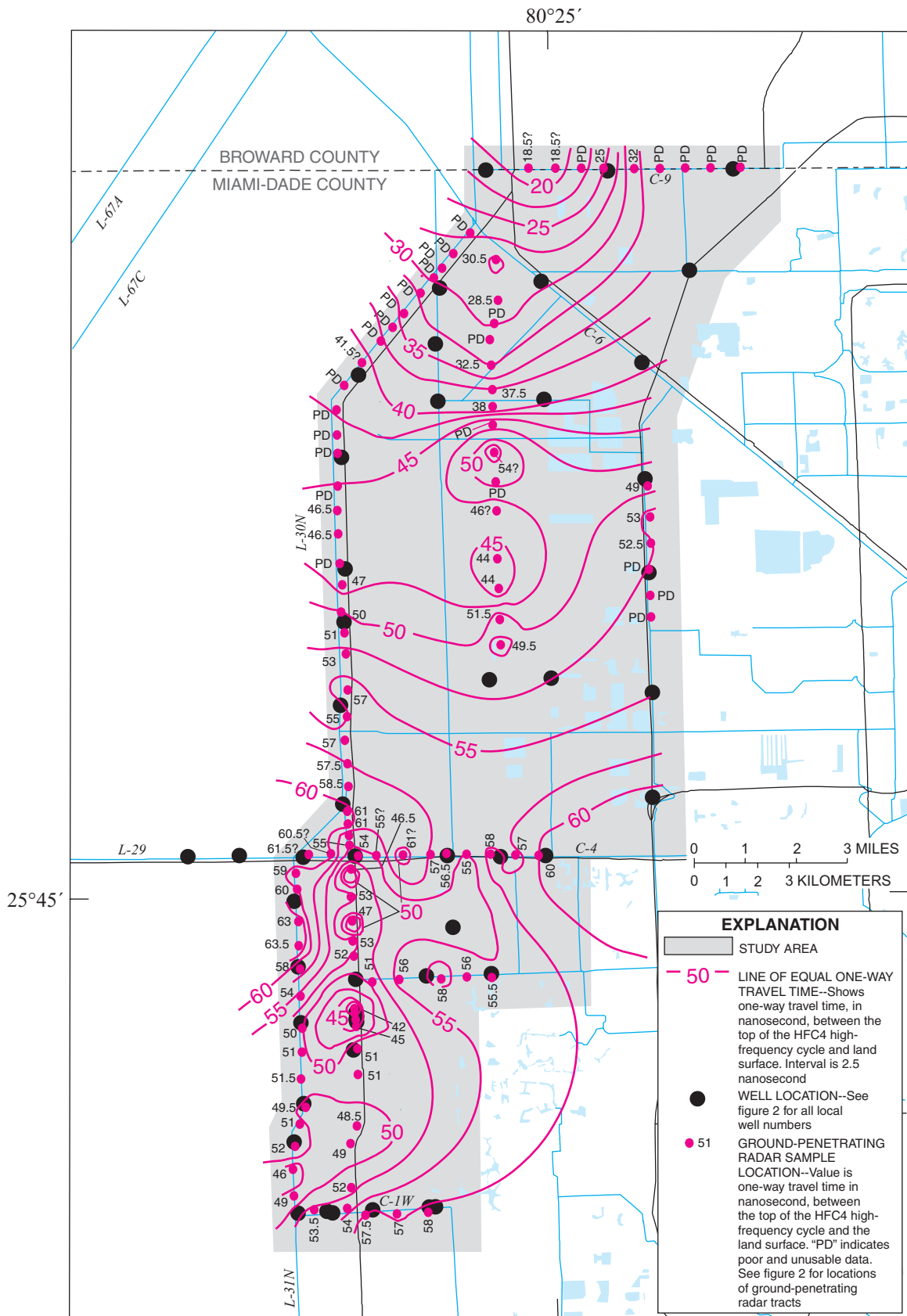
Figure 15. One-way travel time to top of HFC4.

Figure16. Electromagnetic-wave velocity between land surface and top of HFC4.

Characterization of Aquifer Heterogeneity Using Cyclostratigraphy and Geophysical Methods in the Upper Part of the Karstic Biscayne Aquifer, Southeastern Florida

Figure 17. Altitude of the top of HFC4.

Upper Surface of HFC4

The upper surface of HFC4 was mapped throughout the study area by combining GPR and test corehole data. First, a contour map (fig. 15) was constructed for one-way travel time from land surface to the top of HFC4. Second, a velocity contour map (fig. 16) was constructed using: (1) correlation of profile reflections with core sample lithologies and digital borehole images, and (2) CMP surveys (for example, Cunningham, 2004, fig. 9). Both methods have been previously described. The interval velocity between land surface and the upper surface of HFC4 is typically about 0.197 ft/ns as determined by six CMP analyses in the study area (fig. 16). This velocity is similar to a velocity (~0.164 ft/ns) calculated by Kruse and others (2000) for the limestone of the upper part of the Biscayne aquifer in an area of ENP. Third, a contour map (fig. 17) was constructed to show the altitude of the top of HFC4. This map integrates the altitude of the top of HFC4 determined from borehole data and from GPR profiles. The altitudes of HFC4 in figure 17 were established as the product of the inverse of the one-way travel time between the land surface and the GPR reflection corresponding to the top of HFC4 (fig. 15) multiplied by radar propagation velocities (fig. 16). Much of the GPR data north of the C-4 Canal (fig. 2) was of poor quality, and therefore, of limited use in construction of the map shown in figure 17. The altitude of the top of HFC4 is about 6 ft higher on the northern and southern sides of the study area relative to a structural closure that crosses the middle of the Pennsuco Canal (fig. 17).

Krome Avenue Site

Two high-frequency carbonate cycles (HFC4 and HFC5) of the Miami Limestone and the uppermost high-frequency cycle (HFC3b) of the Fort Thompson Formation were successfully imaged on GPR profile 242, which was collected at the Krome Avenue site (fig. 2). Pedogenic limestone at the tops of each HFC provides evidence that a surface of subaerial exposure, related to a relative fall in sea level, caps each HFC (fig. 12). A prominent karstic exposure surface that shows evidence for substantial dissolution along the surface separates HFC5 and HFC4 as shown in figure 18. This buried karstic surface has about 3 ft of paleorelief, and karstic dissolution has locally almost entirely removed HFC4 (fig. 18). Digital optical borehole images and continuously drilled cores confirm the presence of relatively thick to very thin vertical sections of HFC4 (fig. 19). Verification of the interpretation of GPR profile 242 would not have been possible with cores only because of incomplete recovery and the accompanying error in the drilled core depth. The digital optical borehole image data (fig. 19) made it possible to develop an unambiguous interpretation (fig. 18).
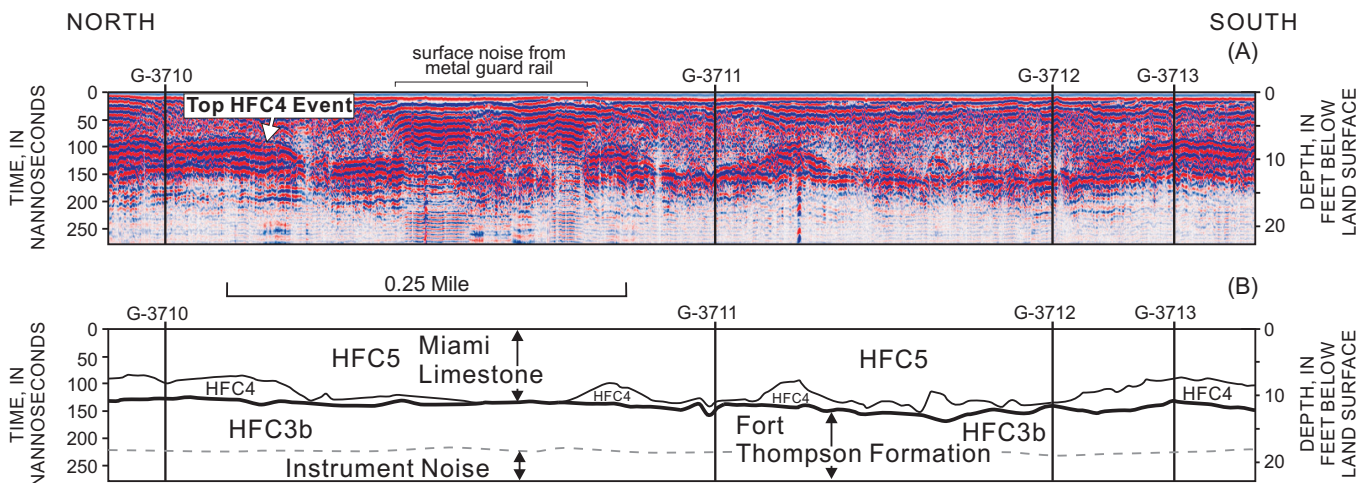

Figure 18. Ground-penetrating radar (GPR) line 242 at the Krome Avenue site (fig. 2). (A) 100-MHz GPR profile, and (B) line drawing of GPR profile. HFC5, HFC4, and HFC3b correspond to the high-frequency cyclostratigraphy shown in figure 10.
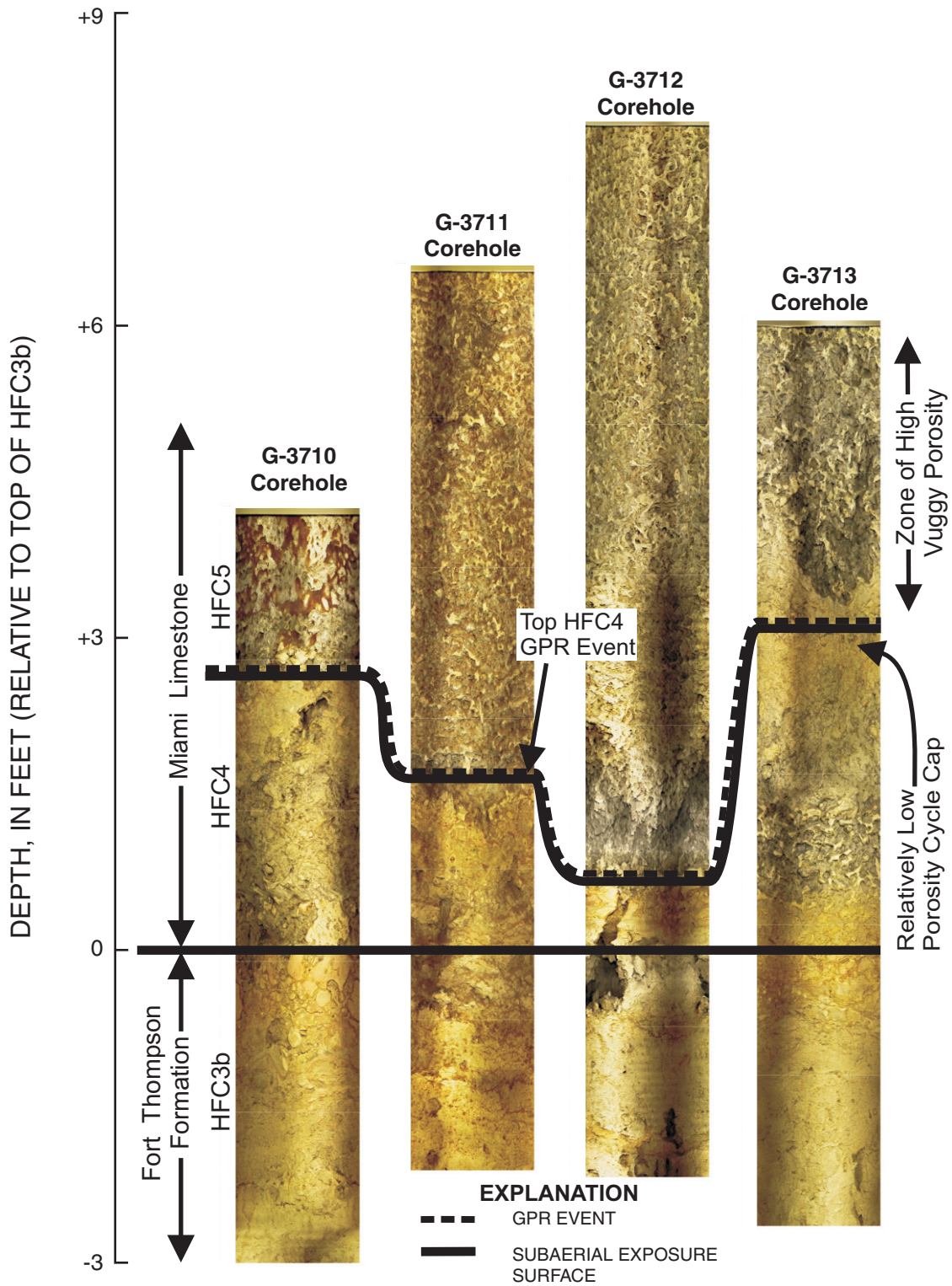
Figure 19. Correlation of four digital optical image logs from test coreholes G-3710, G-3711, G-3712, and G-3713 used to verify ground-penetrating radar (GPR) at the Krome Avenue site (figs. 2 and 18).

At the Krome Avenue site, radar reflections from subtidal HFC5 typically have poor horizontal continuity or hummocky configurations (fig. 18). These reflection patterns image highly bioturbated massive beds (without well-defined bedding planes) composed of pelmoldic grainstone and packstone that have very high vuggy porosities (figs. 18 and 19). The reflections of HFC5 generally are lower in amplitude than compared to the reflections in the underlying uppermost limestone of HFC4 (fig. 18). The amplitude analysis shown in figure 20 demonstrates that reflection amplitudes are significantly lower for the base of HFC5 than for the top layers of HFC4 (fig. 18). Figure 18 shows that the GPR reflections of HFC5 are dimmer than reflections of HFC4 and the upper part of HFC3b. Average reflection amplitudes are about 7dB lower at base of HFC5 than at the top of HFC4 (fig. 20). The median of this difference is significant at about the 95-percent confidence level (fig. 20). The relatively low amplitudes of the HFC5 reflections probably are related to its very high pelmoldic matrix porosity and solution-enlarged burrow porosity. In contrast, the higher amplitudes of HFC4 probably result from its relatively lower matrix porosity associated with more micrite-rich peloidal facies (fig. 21). Additionally, the relatively low

amplitudes of the HFC5 reflections represent rocks with relatively high permeability when compared to the high amplitude HFC4 reflections and correspondingly lower permeability of HFC4 (fig. 22). The relation between the GPR reflection amplitude, porosity, and permeability of HFC5 and those of HFC4 are present almost everywhere throughout the study area.

The lower amplitudes of the reflections in HFC5 relative to higher reflection amplitudes in the upper layers of HFC4 probably are influenced by larger freshwater content due to higher porosities in HFC5. Formation conductivity of HFC5 is higher than the formation conductivity of the rock layers of HFC4 (fig. 23). The attenuation of electromagnetic waves increases as the electrical conductivity of a medium increases (Lane and others, 2000). Therefore, there is an empirical relation between formation porosity, permeability, formation conductivity, and reflection amplitudes—as porosity and permeability increase, formation conductivity increases and reflection amplitude decreases. This relation is observed throughout the entire vertical and lateral section of the Biscayne aquifer represented in figure 18. Cunningham (2004) determined that near the base of the uppermost upward-shallowing brackish- or freshwater-capped cycle of the Fort Thompson
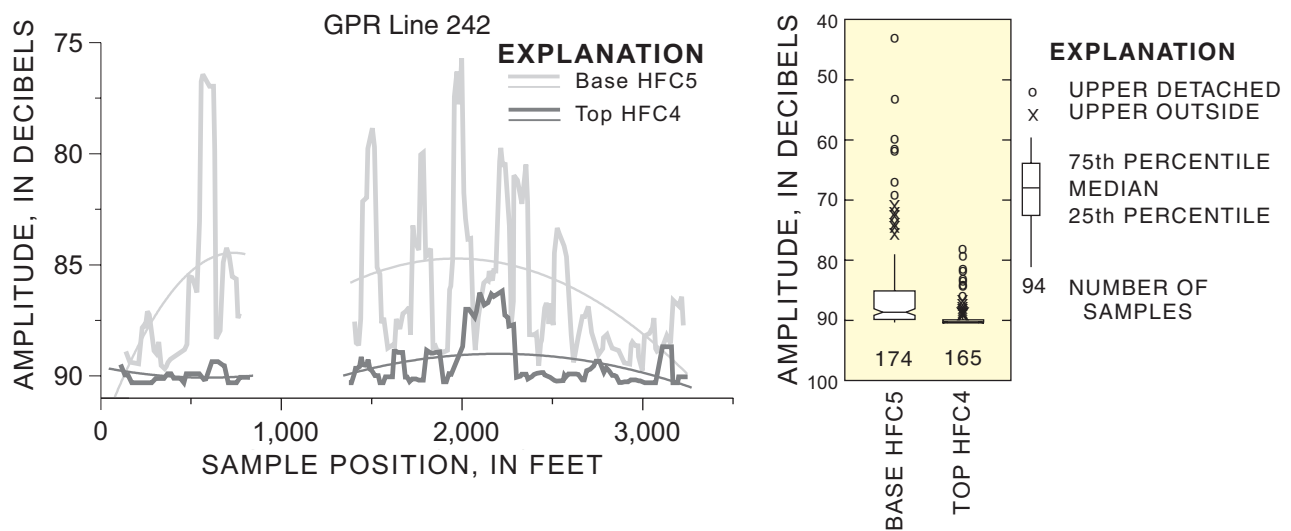

Figure 20. Changes in ground-penetrating radar (GPR) reflection amplitudes along GPR survey line 242, and corresponding box-whisker plots showing reflection amplitude sample populations for GPR reflection events at the bases and tops of high-frequency cycles (HFC). In the box plot, the upper and lower quartiles of the data are portrayed by the top and bottom of the polygon and the horizontal line segment within the polygon represents the median. When comparing the notches on two boxes, if the notches do not overlap, this indicates a difference in the median of porosity populations at about a 95-percent confidence level. Where there is an overlap of notches, there is not a significant difference in the medians. Roughly 99 percent of the data is contained between the limits of the whiskers, and the remaining 1 percent of the data are plotted as individual points. GPR line 242 was collected at the Krome Avenue GPR site (fig. 2).
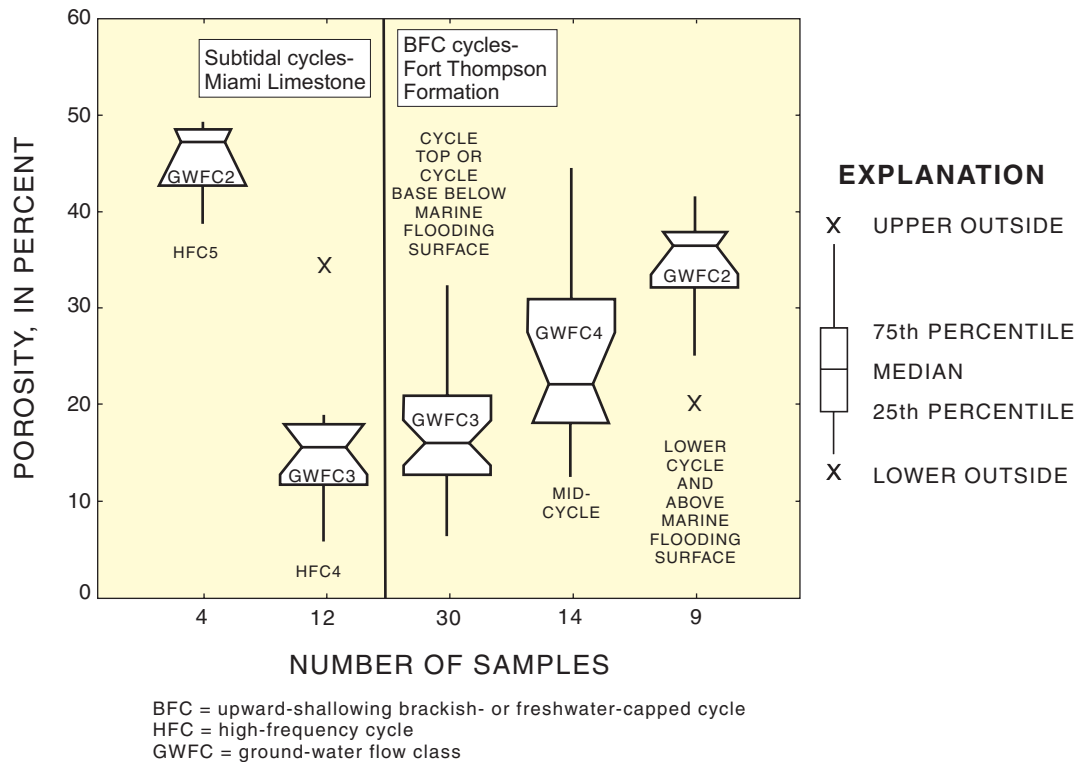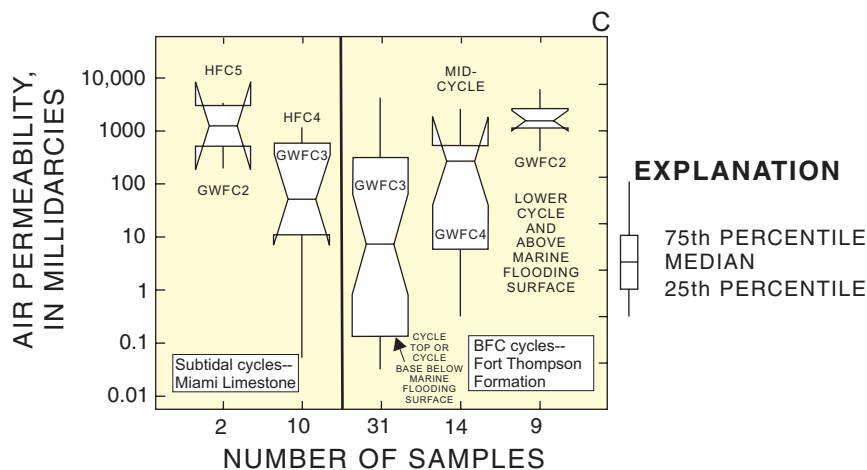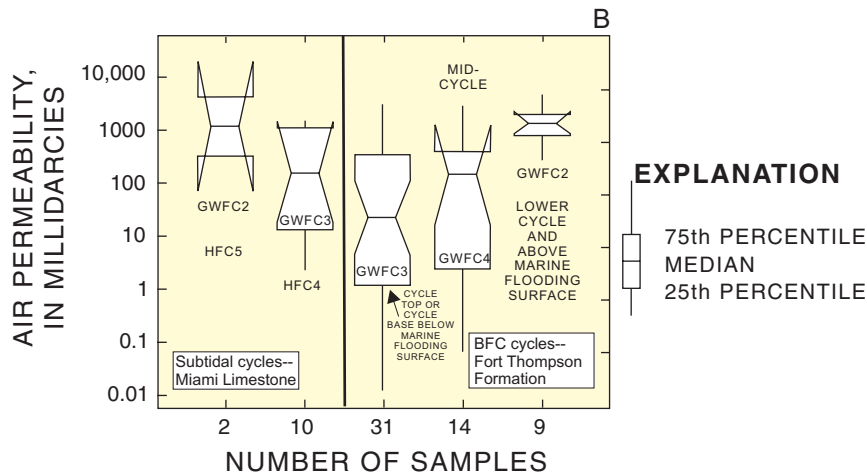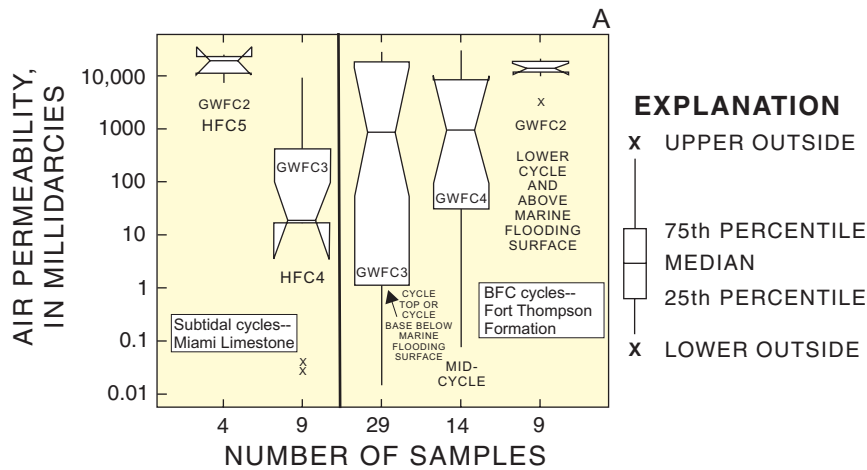
Figure 21. Box-whisker plots of laboratory-measured porosity of whole-core samples (modified from Cunningham, 2004). See figure 20 for an explanation of box-whisker plots. Box-whisker plots are for samples from the following ground-water flow classes: horizontal conduit ground-water flow class (GWFC2); leaky, low-permeability ground-water flow class (GWFC3); and diffuse-carbonate ground-water flow class (GWFC4); and arranged according to sampling from subtidal cycles (HFC4 and HFC5) of the Miami Limestone and vertical position within upward-shallowing brackish- or freshwater-capped cycles of the upper part of the Fort Thompson Formation.

Formation (HFC3), radar-reflection amplitudes are lower than the middle and upper parts of the cycle. These lower amplitudes also correspond to relatively higher porosity, permeability, and formation conductivity that occur at the base of HFC3.

A time-varying gain was employed during collection of GPR profile 242 at the Krome Avenue GPR site (fig. 18). Because this gain altered the amplitude of the received electromagnetic waves, the above observations may be skewed by amplitude values affected by gain. However, the abrupt shift in amplitude of the lowest reflection in HFC5 and the highest reflection of HFC4 is probably due to an abrupt shift in electrical and hydrologic properties, and not an artifact of gain. The time-varying gain would not produce such an abrupt shift at so many different depths across GPR profile 242 (fig. 18).

HYDROGEOLOGIC FRAMEWORK

Geologic units of varying permeability underlie southeastern Florida from land surface to depths between 150 and 400 ft. These units, known as the surficial aquifer system, form an unconfined aquifer system, which is the source of much of the potable water used in the area (Fish and Stewart, 1991). In Miami-Dade County, a highly permeable part of the aquifer system has been named the Biscayne aquifer (Parker, 1951; Parker and others, 1955). This study focuses on the upper part of the Biscayne aquifer underlying the study area shown in figure 2. Discussion will concentrate on previous concepts of the hydrogeology of the Biscayne aquifer and introduce a high-resolution hydrogeologic framework for the upper part of the Biscayne aquifer.

Figure 22. Box-whisker plots of air permeabilities of most of the same whole-core samples displayed in figure 21. See figure 20 for an explanation of box-whisker plots. Box-whisker plots are for samples from the following ground-water flow classes: horizontal conduit ground-water flow class (GWFC2); leaky, low-permeability ground-water flow class (GWFC3); and diffuse-carbonate ground-water flow class (GWFC4); and arranged according to sampling from subtidal cycles (HFC4 and HFC5) of the Miami Limestone and vertical position within upward-shallowing brackish- or freshwater-capped cycles of the Fort Thompson Formation. (A) Vertical permeability, (B) maximum horizontal permeability, and (C) horizontal permeability measured 90° to maximum flow.
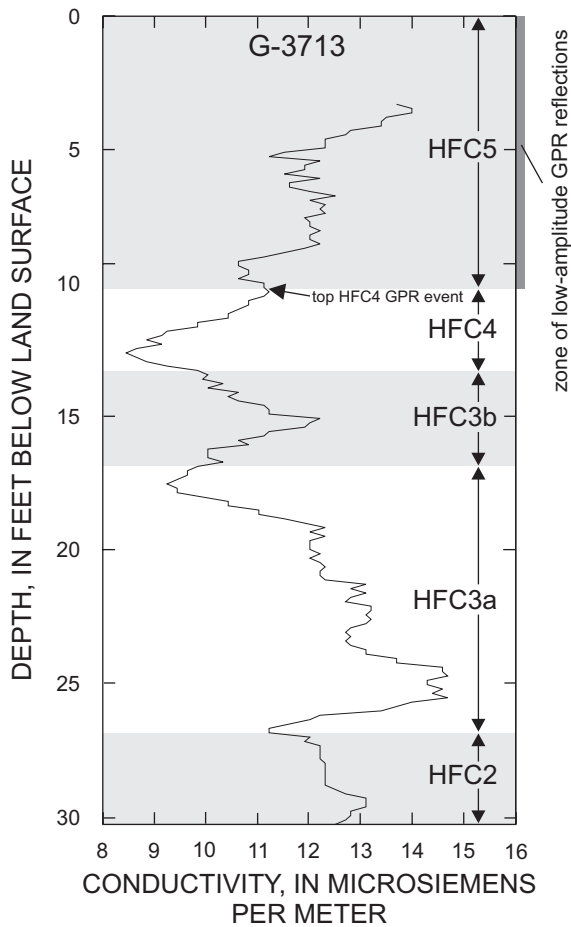
BFC = upward-shallowing brackish- or freshwater-capped cycle
HFC = high-frequency cycle
GWFC = ground-water flow class

Figure 23. Formation conductivity measured by an induction-resistivity borehole geophysical tool for the G-3713 test corehole shown in figure 18. The zone of relative high conductivity within HFC5 corresponds to a vertical and lateral zone of relatively low-amplitude reflections assigned to HFC5 shown on the ground-penetrating radar profile in figure 18.

Previous Interpretations

In Miami-Dade County, the surficial aquifer system includes all rock and sediment from land surface downward to the top of the intermediate confining unit (fig. 5). The rock and sediment are mostly composed of limestone, sandstone, sand, shell, and clayey sand and ranges in age from Holocene to Pliocene (Causaras, 1987). The top of the system is land surface, and the base is defined by a substantial decrease in permeability. The permeability of the rock and sediment of the surficial aquifer system is variable, allowing the system to be divided locally into one or more aquifers separated by less-permeable or semiconfining units. The uppermost

part of these water-bearing units is the Biscayne aquifer and the lowermost water-bearing unit is the gray lime-stone aquifer (Fish and Stewart, 1991).

The Biscayne aquifer is the primary aquifer in southeastern Florida and has been declared a sole-source aquifer (Federal Register Notice, 1979). Parker (1951) named and defined the Biscayne aquifer as a hydrologic unit of water-bearing rocks that carries unconfined ground water in southeastern Florida. Later, Fish (1988), defined the Biscayne aquifer more completely as:

> *That part of the surficial aquifer system in southeastern Florida composed of (from land surface downward) the Pamlico Sand, Miami Oolite [Limestone], Anastasia Formation, Key Largo Limestone, and Fort Thompson Formation (all of Pleistocene age) and contiguous, highly permeable beds of the Tamiami Formation of Pliocene and late Miocene age where at least 10 ft of section is very highly permeable (a horizontal hydraulic conductivity of about 1,000 ft/d or more).*

Fish (1988) provided further definition of the base of the Biscayne aquifer:

> *If there are contiguous, highly permeable (having hydraulic conductivities of about 100 ft/d or more) limestone or calcareous sandstone beds of the Tamiami Formation, the lower boundary is the transition from these beds to subjacent sands or clayey sands. Where the contiguous beds of the Tamiami Formation do not have sufficiently high permeability, the base of highly permeable lime-stones or sandstones in the Fort Thompson Formation, Anastasia Formation, or Key Largo Limestone is the base of the Biscayne aquifer.*

This study focuses on the part of the Biscayne aquifer that is composed of the Fort Thompson Formation and Miami Limestone (fig. 5). Most test coreholes drilled as part of this study did not fully penetrate the Fort Thompson Formation—four test coreholes (G-3671, G-3673, G-3674, and G-3675) reached the base of the Fort Thompson Formation (fig. 2). Discussion of the portion of test coreholes that penetrated rock and sediment below the Fort Thompson Formation is beyond the scope of this report.

High-Resolution Hydrogeologic Framework

A new high-resolution hydrogeologic framework has been delineated within the upper part of the Biscayne aquifer (fig. 24). This new framework divides the upper part of the Biscayne aquifer into four categories of ground-water flow classes: (1) a low-permeability peat, muck, and marl ground-water flow class (GWFC1); (2) a horizontal conduit ground-water flow class (GWFC2); (3) a leaky, low-permeability ground-water flow class (GWFC3); and (4) a diffuse-carbonate ground-water flow class (GWFC4). Classification into these four ground-water flow classes is based on visual examination of digital optical borehole logs, borehole caliper logs, ground-penetrating radar profiles, established hydraulic analyses of the Biscayne aquifer (for example, Fish and Stewart, 1991), and flowmeter results from the G-3710 test corehole. Ground-water flow for the horizontal conduit flow class is visualized as ground water flowing from vug to vug in a pore system characterized by touching vugs (Lucia, 1999, p. 26 and 31). Ground-water flow associated with this ground-water flow class is not through pipes or underground streams, but along a passage (typically with a sheet-like geometry) formed by touching vugs that act as a major route for ground-water flow. The pore system of the diffuse-carbonate ground-water flow class is characterized by both intergrain porosity and separate vug porosity (Lucia, 1999, p. 26). Movement of ground water for the diffuse-carbonate ground-water flow class is visualized as ground water flowing from matrix to vug to matrix (Lucia, 1999, p. 31). Some discrete field-scale hydraulic testing of the low-permeability peat, muck, and marl unit was carried out by Parker and others (1955), but reporting of discrete testing of GWFC2, GWFC3, and GWFC4 is not known. Discrete testing of all four ground-water flow classes should be considered in the future to quantify the hydraulic nature of the flow zones. Hydrogeologic sections (pls. 1-5) show the distribution of these ground-water flow classes in the upper part of the Biscayne aquifer throughout the study area.

Low-Permeability Peat, Muck, and Marl Ground-Water Flow Class (GWFC1)

Numerous (119) soft-sediment push core samples (app. V) were collected throughout the study area to define the thickness and areal extent of peat, muck, and marl that delineate the top of the Biscayne aquifer 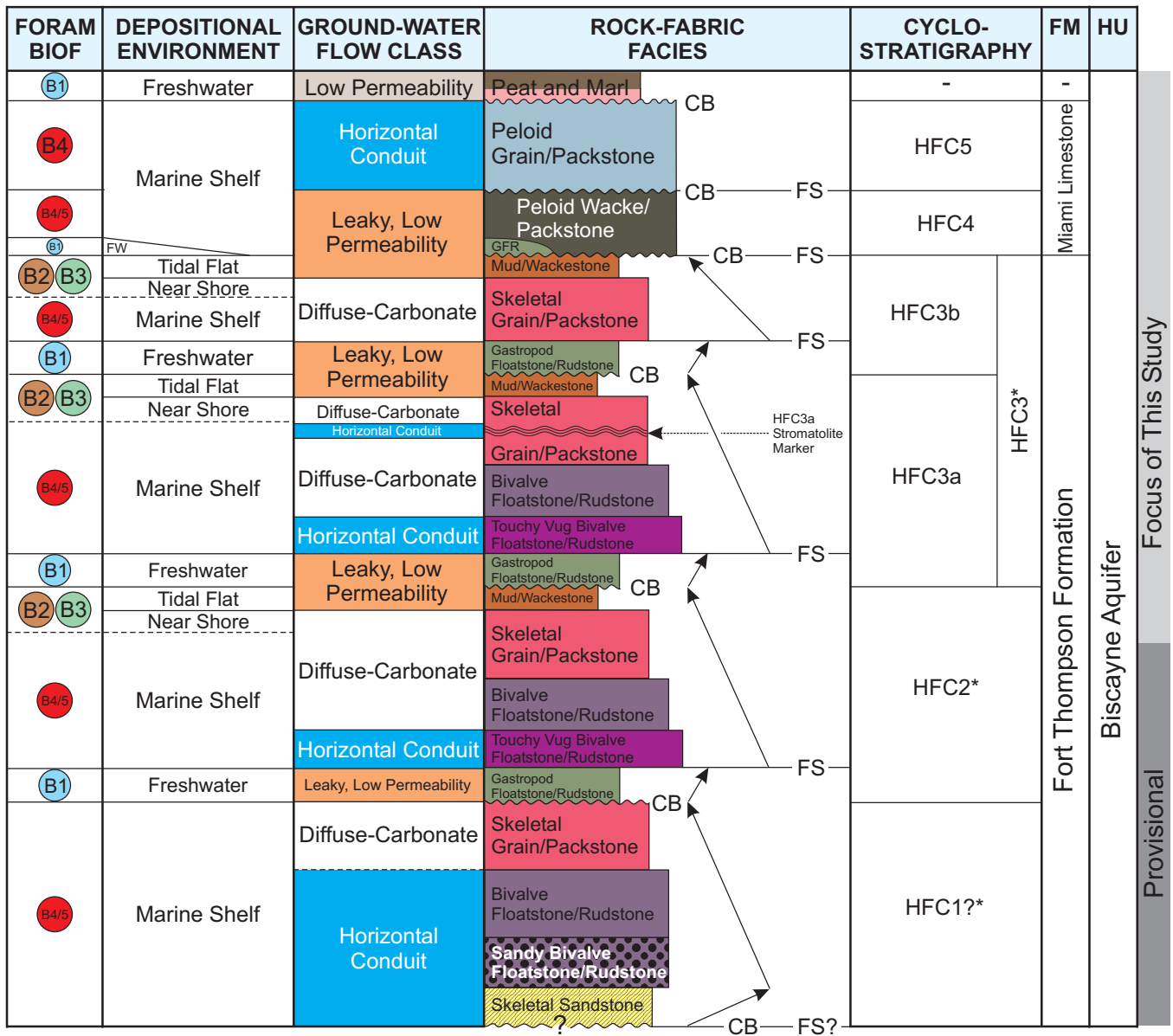throughout most of the study area. At several core sites, some or all of these sediments have been removed and replaced by road or levee fill. The composite thickness of the peat, muck, and marl ranges from less than 1 ft to slightly more than 3.5 ft in the study area (fig. 25). Parker and others (1955) referred to the marl as the Lake Flirt marl. The marl is intercalated with the peat and muck, and its composite thickness ranges from being entirely absent to slightly more than 1 ft at selected core sites (fig. 26). Parker and others (1955) indicated that the marl is relatively impermeable and "where present in thicknesses of a foot or more, it is an important aid in controlling water levels, especially above the highly permeable parts of the Fort Thompson Formation and the Miami Oolite [Limestone]". Parker and others (1955) also assigned a relatively low permeability to the organic soils of the Everglades, or the peat and muck of the study area. They stated:

> Water moves through them very slowly under the low gradients existing there. In a test pit 5 ft square by 3 ft deep, with the water table standing about 1 ft below land surface, the ground water seeped in so slowly that the pit could be emptied by slow bailing with a pint can.

In the area of Levee 30 (fig. 2), Sonenshein (2001) assigned a lateral hydraulic conductivity value of 50 ft/d to the peat, muck, and marl, which was then used in calibrated flow models. The peat, muck, and marl form the ground-water flow class designated GWFC1 (fig. 24 and pls. 1-5).

Horizontal Conduit Ground-Water Flow Class (GWFC2)

Both the Miami Limestone and Fort Thompson Formation contain flow zones characterized by the horizontal conduit ground-water flow class. The Miami Limestone forms the bedrock throughout the study area. Fish and Stewart (1991, pls. A-K) assigned a very high lateral hydraulic conductivity (>1,000 ft/d) to the limestone of the Miami Limestone. However, they stated "the Miami Oolite [Limestone] does not appear to have as well developed a network of open cavities as the Fort Thompson Formation." Nemeth and others (2000) estimated that the hydraulic conductivity of the Miami Limestone ranges from 1,000 to 5,000 ft/d throughout an area that includes part of Levee 31N in the study area (fig. 2). Sonenshein (2001) assigned a lateral hydraulic conductivity value of 1,000 ft/d to the Miami Limestone in an area near Levee 30 (fig. 2) for purposes of simulating ground-water flow.

Figure 24. Idealized foraminiferal biofacies, depositional environments, ground-water flow classes (GWFCs), rock-fabric facies, cyclostratigraphy, and stratigraphic units of Pleistocene to Holocene age in north-central Miami-Dade County. Refer to table 3 for explanation of biofacies relation to foraminiferal taxomony. Asterisk (*) indicates units can contain multiple high-frequency cycles and may be depositional sequences.

Figure 25. Composite thickness of Holocene peat, muck, and marl.

Figure 26. Composite thickness of Holocene marl.

The rock-fabric facies that comprise the horizontal conduit ground-water flow class of the Miami Limestone (GWFC2, fig. 24) are peloid grainstone and packstone (app. IV). Results of this study indicate that the hydraulic conductivity values assigned to the Miami Limestone by Fish and Ste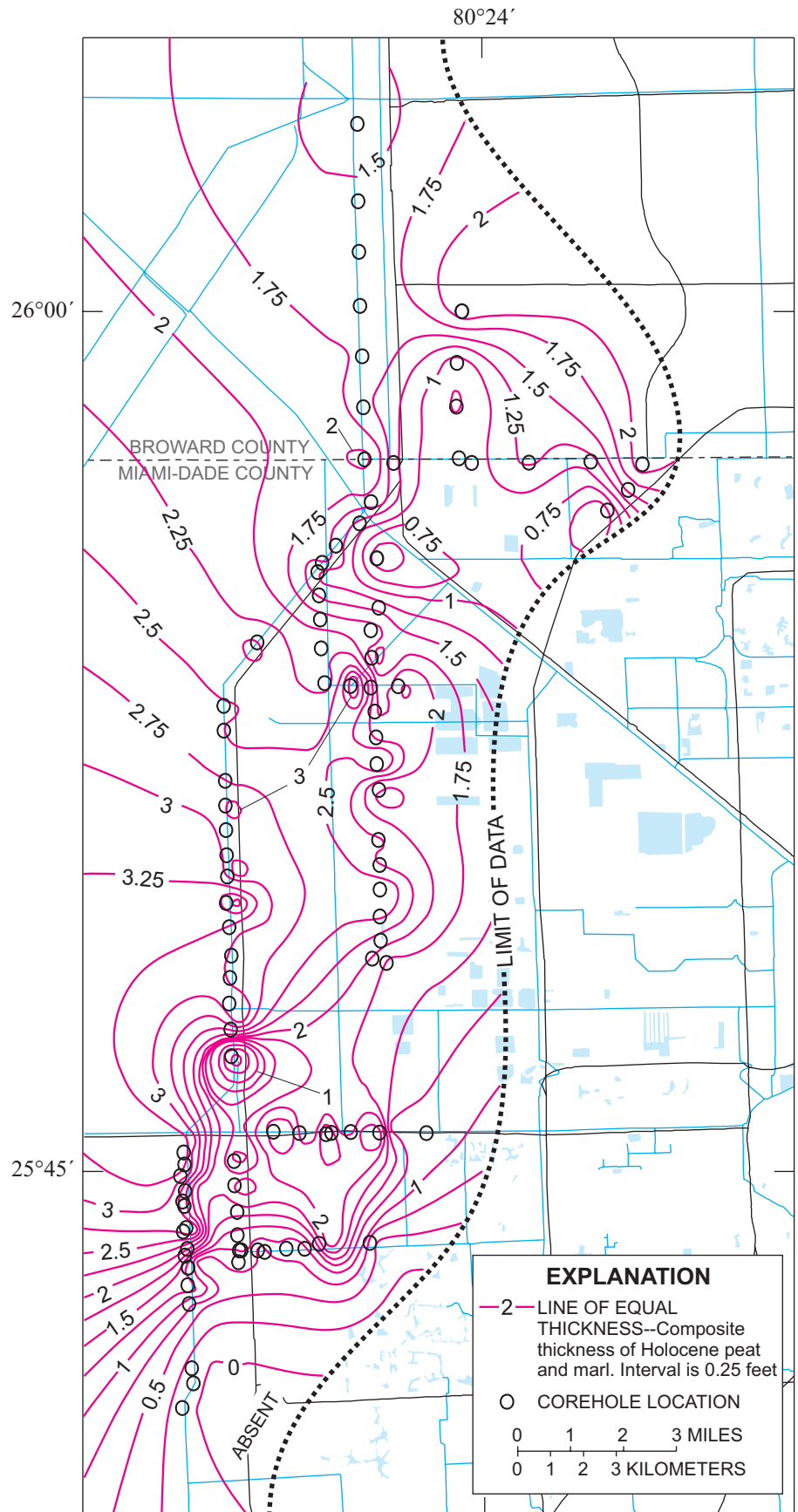wart (1991), Nemeth and others (2000), and Sonenshein (2001) are appropriate for all of HFC5, but only locally apply to part or possibly all of HFC4. The rock-fabric facies that comprise much of HFC4 tend to have lower core-scale permeability than the rock-fabric facies of HFC5 (fig. 22). Much or all of HFC4 has been included in the semiconfining unit that spans the base of the Miami Limestone and the top of the Fort Thompson Formation (pls. 1-5). Both vertical and horizontal median permeability values of the whole core samples from HFC5 (fig. 22) show that there is a significant difference between these two permeability populations, suggesting different field-scale lateral and vertical permeabilities of about one order of magnitude. This is probably due to preferred dissolution in a vertical direction during paleo-vadose events (for example, fig. A1a and A1b). Results of heat-pulse flowmeter data from the G-3710 test corehole indicates that HFC5 has a relatively high transmissivity compared to much of the underlying HFC4 (fig. 27). The two-dimensional distribution of the high-permeability flow class represented by HFC5 and part of HFC4 is shown on plates 1 to 5.

Three principal hydrologic zones, which are characterized by the horizontal conduit ground-water flow class, are contained in HFC3a and HFC2 in the upper part of the Fort Thompson Formation (fig. 24). The GWFC2 type flow zone near the top of HFC3a is characterized by bedding plane vugs that can be correlated throughout much of the study area (fig. 28 and pls. 1-5). It is associated with the laminated peloid grainstone-packstone rock-fabric facies. This flow zone coincides with the stromatolite marker shown on plates 1 to 5. Two other candidate GWFC2 type flow zones are characterized by moldic porosity and irregular vugs that form a touching-vug network of secondary porosity. Touching-vug porosity typically occurs near or at the base of HFC3a and another within HFC2 (figs. 28 and 29). A map showing the altitude of the upper surface of the GWFC2 type flow zone located near or at the base of HFC3a is shown in figure 30. The distribution and thickness of this zone is shown in figure 31. The median values of both vertical and horizontal whole-core air permeability is similar to that of HFC5,

and significantly higher than median whole-core air permeability values for the three other types of flow classes (fig. 22). At the whole-core scale, there is a significant difference of about one order of magnitude in the median vertical and horizontal permeability values of samples collected near or at the bases of HFC3a and HFC2 (fig. 22). No measurements of permeability were made on core samples containing the bedding plane vugs. The three GWFC2 type flow zones of the upper part of the Fort Thompson Formation are conceptualized as having a thin, sheet-like geometry throughout much of the study area. It is suggested that at the field scale, the horizontal permeability would be very high due to a widespread, well-connected distribution of each flow zone.

In summary, four principal GWFC2 flow zones have been delineated in the upper part of the Biscayne aquifer (fig. 24 and pls. 1-5). A GWFC2 flow zone corresponds mainly to HFC5 and has a thick blanket-like geometry. A GWFC2 flow zone is found within the upper part of HFC3a and contains thin bedding plane vugs that are regionally widespread. A GWFC2 flow zone occurs near or at the base of HFC3a and another within HFC2. Both zones include irregular and moldic touching vugs, and the HFC3a zone has been correlated over much of the study area (figs. 30 and 31 and pls. 1-5). Median whole-core permeability values suggest that the candidate conduit flow zones have significantly higher porosity and horizontal permeability than the diffuse-carbonate ground-water flow zones and leaky, low-permeability flow zones (figs. 21 and 22). Intervals containing large touching vugs are present in HFC1; however, only six test coreholes either partly or fully penetrated this HFC. Future hydrostratigraphic research in the study area is required to further delineate and better characterize the potential flow pathways within HFC1.

Leaky, Low-Permeability Ground-Water Flow Class (GWFC3)

A leaky, low-permeability ground-water flow class (GWFC3) typically spans the boundary between HFC4 and HFC3a, as well as the uppermost and lowermost parts of upward-shallowing brackish- or fresh-water-capped cycles occurring within the upper part of the Fort Thompson Formation (pls. 1-5). Rock-fabric facies that comprise the GWFC3 zones (fig. 24) include: (1) coral framestone, (2) peloid wackestone

Figure 28. Example of vuggy porosity distribution in the upward-shallowing brackish- or freshwater-capped cycle HFC3a of the Fort Thompson Formation.

and packstone, (3) conglomerate, (4) pedogenic-limestone, (5) gastropod floatstone and rudstone, and (6) mudstone and wackestone (app. IV). Lower permeability has been verified by whole-core air-permeability measurements (app. II). Solution-enlarged, semivertical root molds penetrate the low-permeability unit that spans the basal Miami Limestone and uppermost part of the Fort Thompson Formation

(figs. 32 and 33 and pls. 1-5), suggesting high vertical permeability relative to the horizontal permeability. At the field scale, this unit is anisotropic with relatively higher vertical permeability than horizontal permeability. The top and base of the semiconfining or low-permeability unit, in general, are inclined toward the east (figs. 34 and 35). In the study area, the thickness of the unit is as much as 5.35 ft, but absent locally (fig. 36).
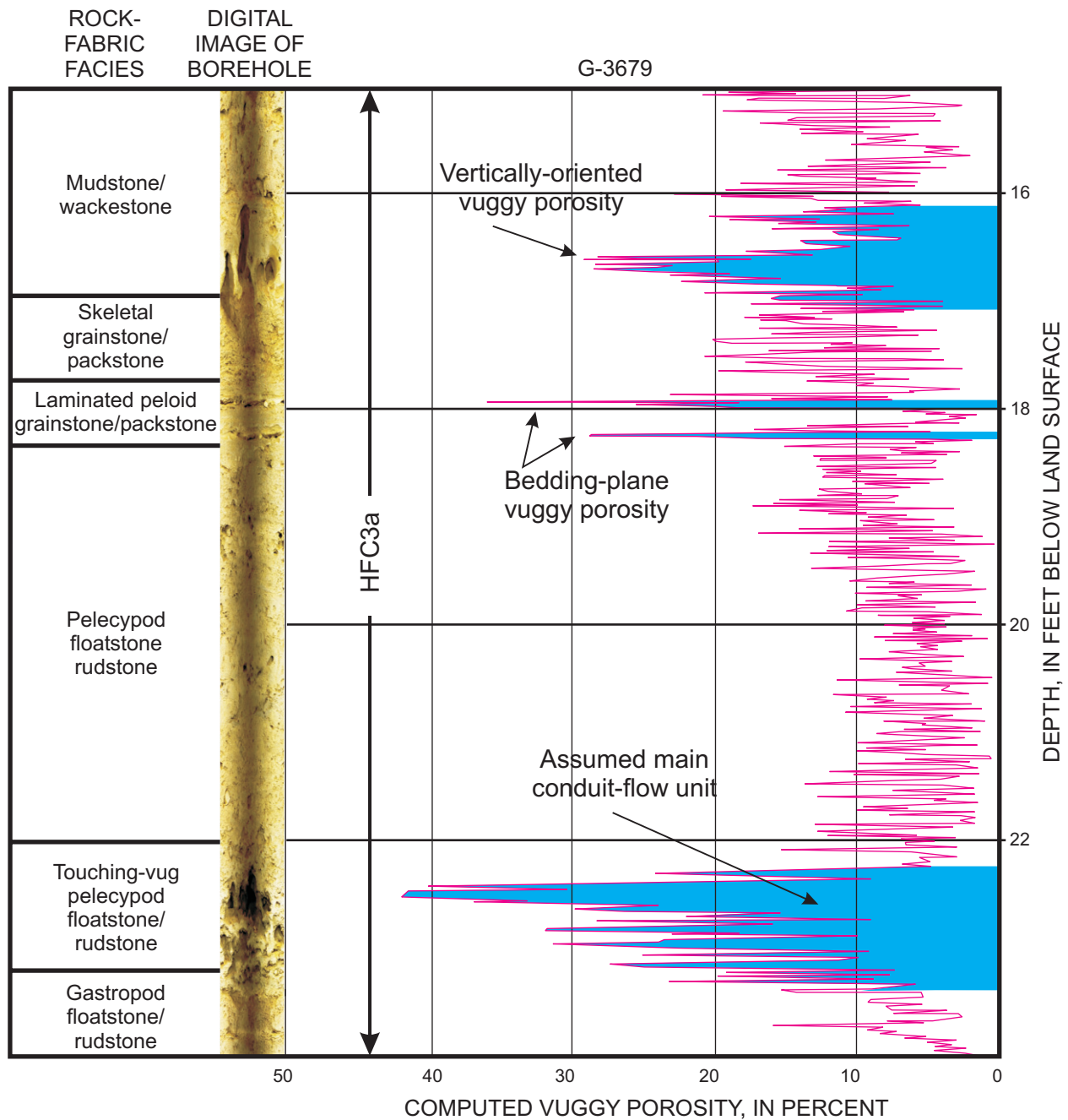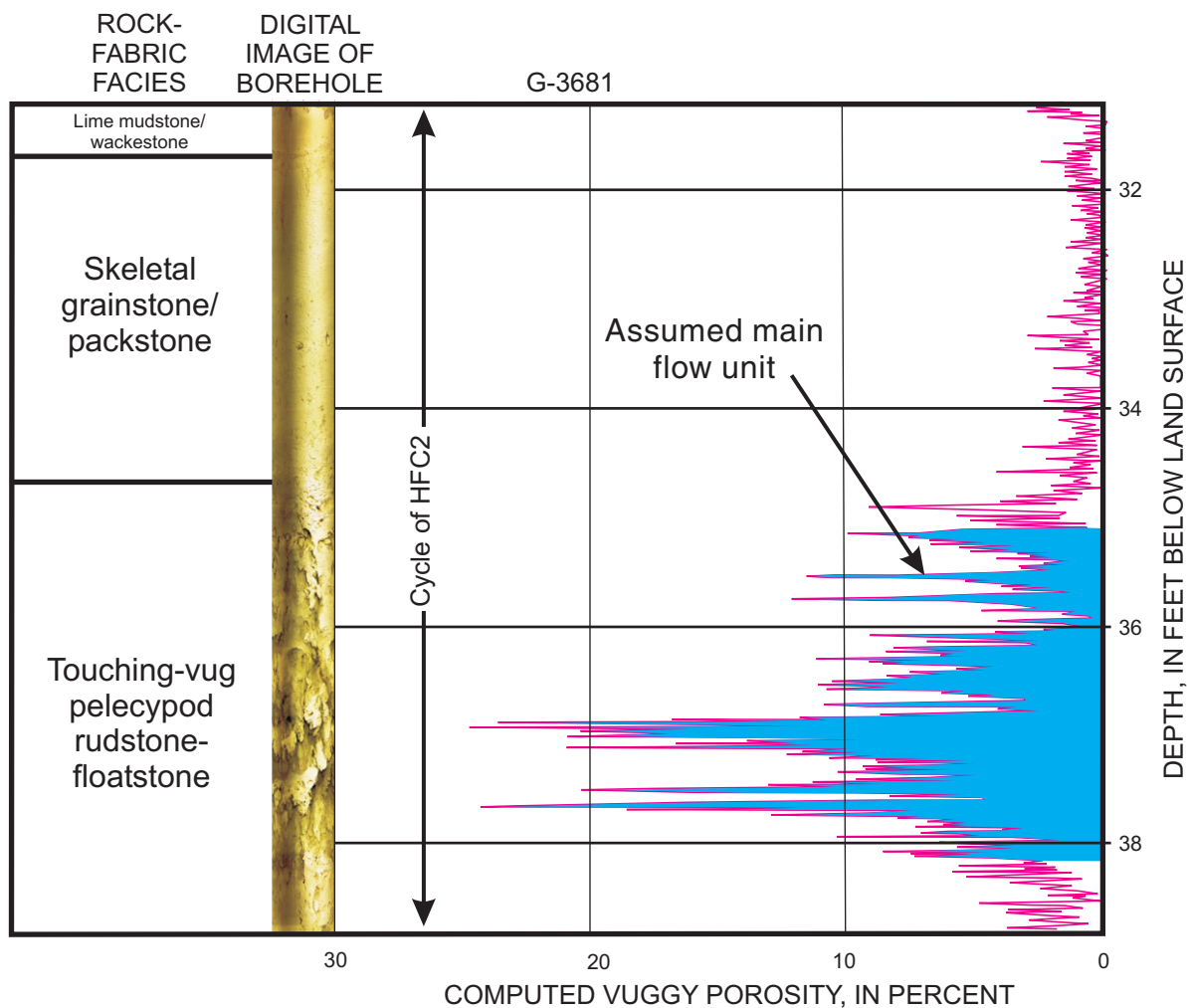
Figure 29. Example of vuggy porosity distribution in an upward-shallowing brackish- or freshwater-capped cycle of HFC2 of the Fort Thompson Formation.

Diffuse-Carbonate Ground-Water Flow Class (GWFC4)

Much of the porosity that makes up the diffuse-carbonate ground-water flow class (GWFC4) is characterized by small-scale moldic, interparticle, and intraparticle porosity that is mostly separate-vug porosity with vug-to-matrix-to-vug connections (Lucia, 1999, p. 31). The rock-fabric facies that comprise the GWFC4 diffuse flow zones include: (1) skeletal grainstone and packstone, (2) pelecypod floatstone and rudstone, (3) sandy skeletal grainstone and packstone, (4) sandy pelecypod floatstone and rudstone, and (5) quartz sandstone and skeletal sandstone (fig. 24 and app. IV). Diffuse flow porosity within these zones

contains much of the ground-water storage capacity of the limestone of the Fort Thompson Formation. Candidate diffuse flow zones typically occur in the middle part of upward-shallowing brackish- or freshwater-capped cycles of the upper Fort Thompson Formation. The range in median whole-core porosity values of GWFC4 is significantly different from that of the other three flow classes (fig. 21). However, median values of vertical whole-core permeability are not different between GWFC4 and GWFC3, but values are significantly different between GWFC4 and GWFC2 (fig. 22). The median values in horizontal whole-core permeability are not significantly different than other flow classes, except for GWFC2 (fig. 22). The median values of whole-core scale horizontal and vertical permeabilities
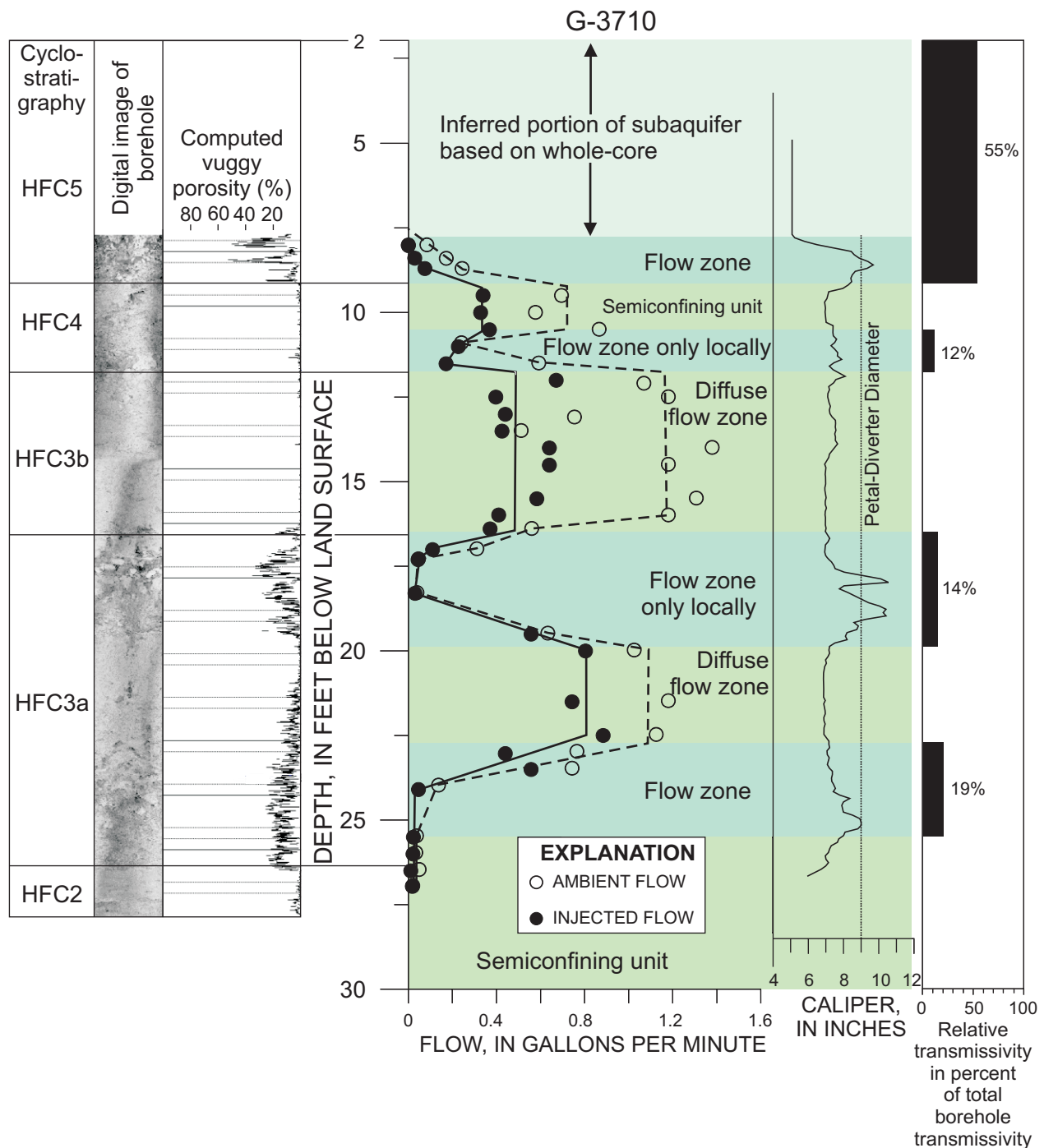
Figure 27. Heat-pulse flowmeter measurement of relative borehole transmissivity, indicating that limestone of the upper part of the Biscayne aquifer can be subdivided into several flow and diffuse zones and a semiconfining unit. Initial results show: (1) HFC5 is interpreted as one single flow zone, (2) the basal part of HFC4 is interpreted to form a local flow zone, (3) the basal part of HFC3a forms a flow zone, and (4) the top of HFC3a has potential to act as a local flow zone.
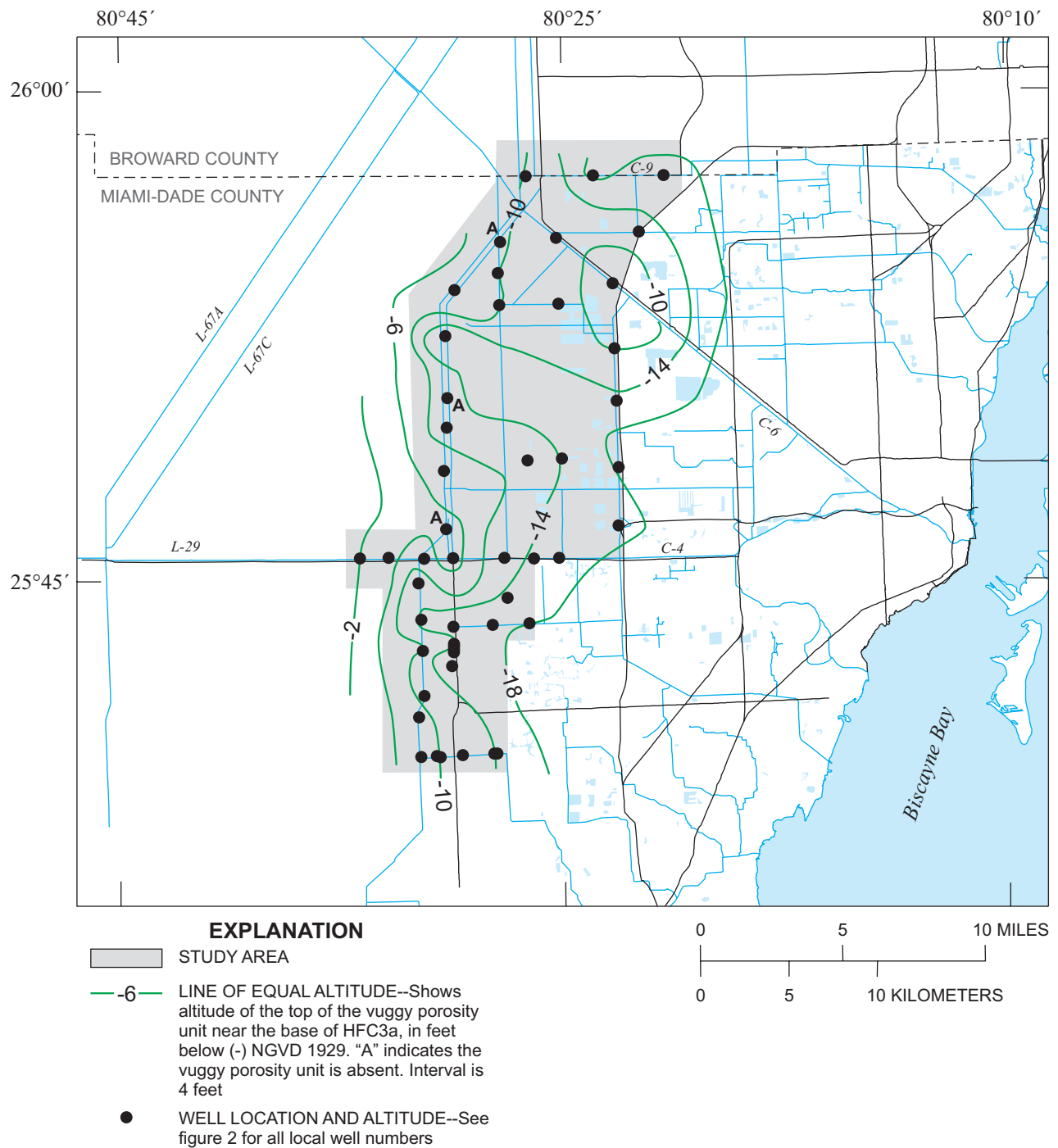
Figure 30. Altitude of the top of the vuggy porosity near the base of HFC3a of the Fort Thompson Formation.
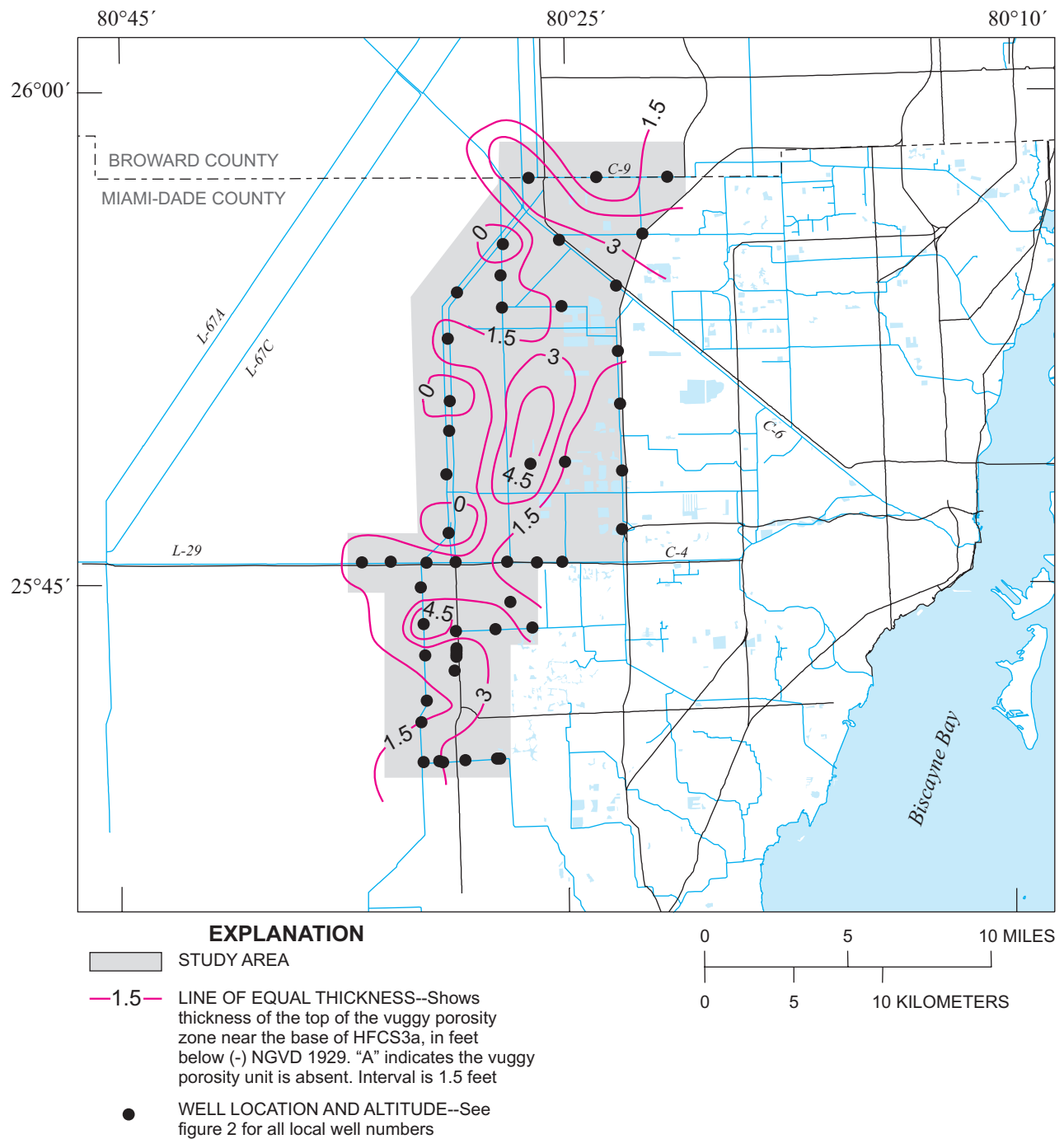
Figure 31. Thickness of the vuggy porosity near the base of HFC3a of the Fort Thompson Formation.

52

Characterization of Aquifer Heterogeneity Using Cyclostratigraphy and Geophysical Methods in the Upper Part of the Karstic Biscayne Aquifer, Southeastern Florida
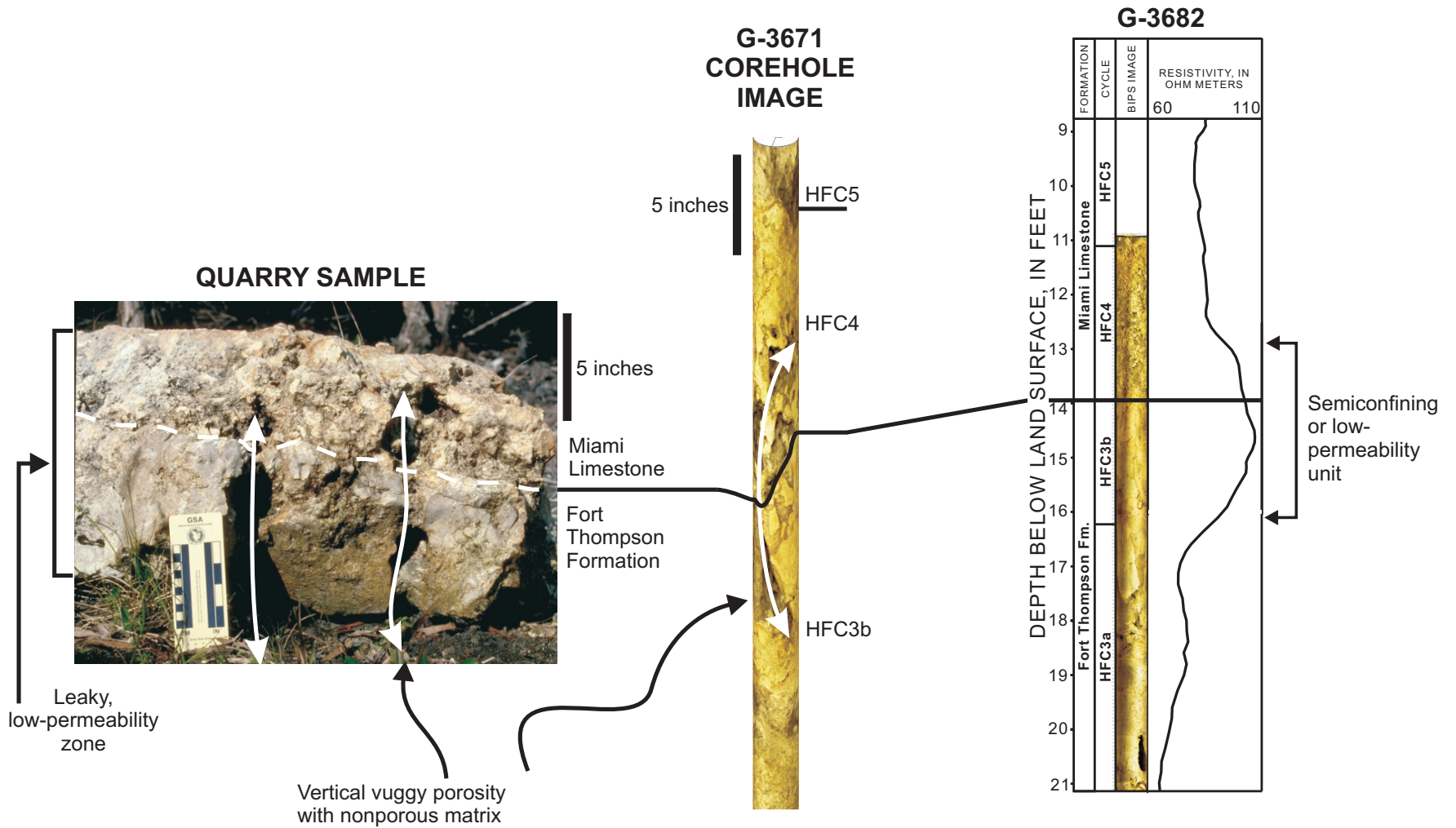
Figure 32. Comparison of quarry sample, digital optical image, and resistivity log of the low-permeability limestone or semiconfining unit that spans the base of the Miami Limestone and top of the Fort Thompson Formation. Note that the unit can be perforated with semi-vertical vugs and has a relatively high-resistivity log signature.
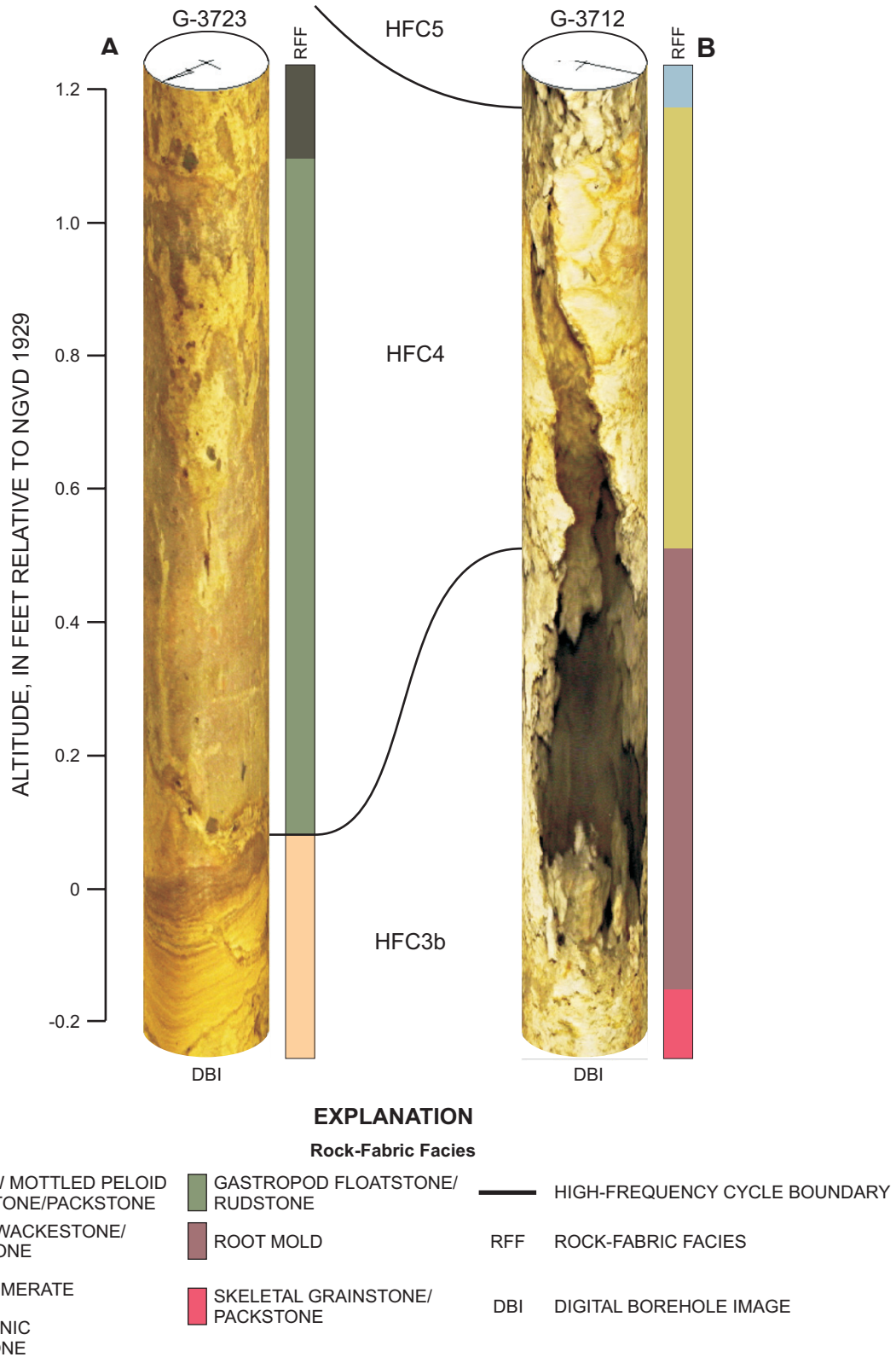
Figure 33. Correlation between rock-fabric facies that span the base of the Miami Limestone and top of the Fort Thompson Formation. The limestone at the base of the Miami Limestone and top of the Fort Thompson Formation in the G-3723 test corehole (A) has high potential to retard vertical seepage, whereas a semi-vertical solution pipe in the G-3712 test corehole (B) allows local vertical conduit flow. This interval of limestone, in approximately two-thirds of the coreholes drilled in the study area, functions as a semiconfining unit.
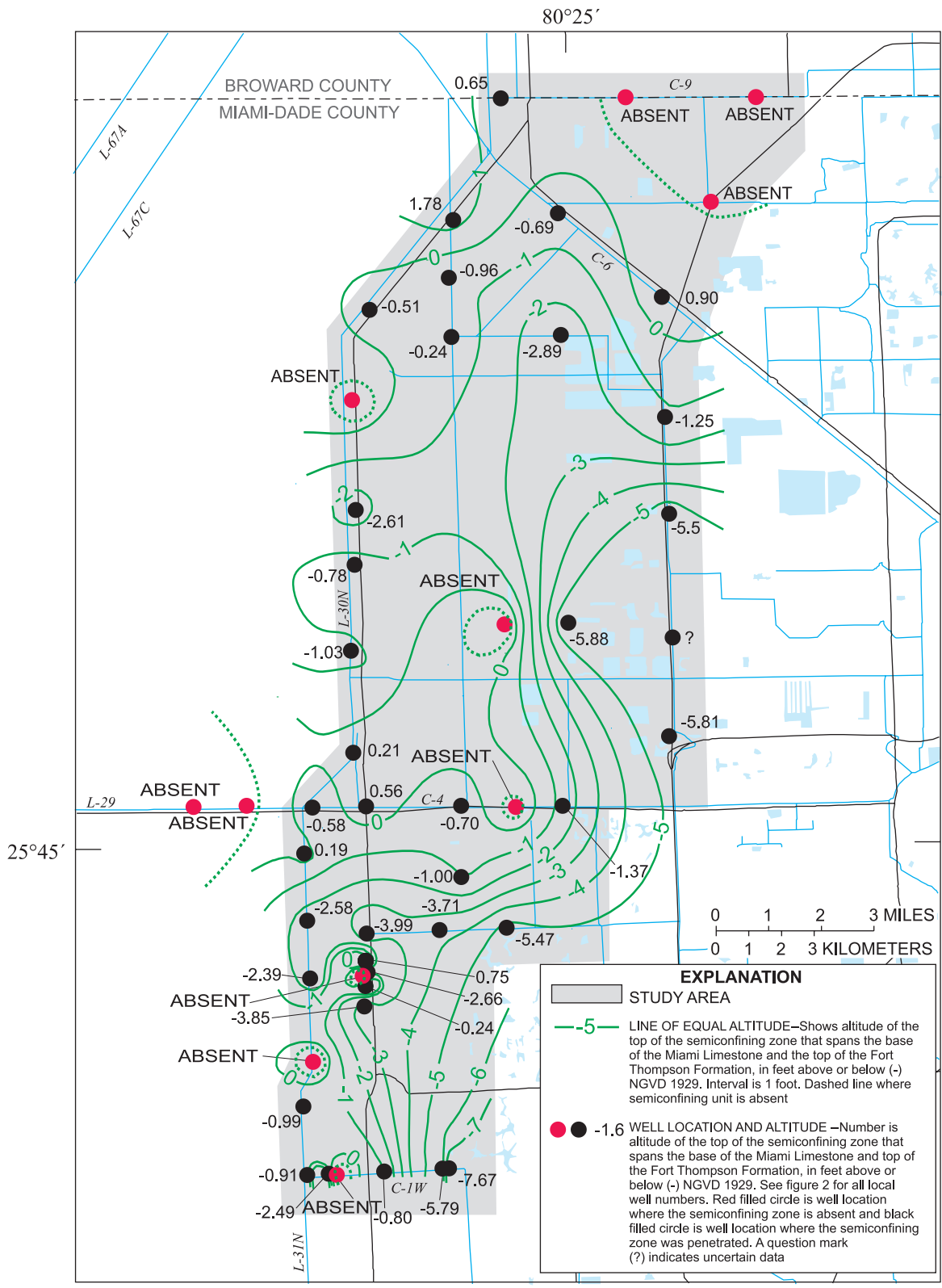
Figure 34. Altitude of the top of the semiconfining unit that spans the base of the Miami Limestone and the top of the Fort Thompson Formation within the upper part of the Biscayne aquifer.

Figure 35. Altitude of the base of the semiconfining unit that spans the base of the Miami Limestone and the top of the Fort Thompson Formation within the upper part of the Biscayne aquifer.

Figure 36. Thickness of the semiconfining unit that spans the base of the Miami Limestone and the top of the Fort Thompson Formation within the upper part of the Biscayne aquifer.

of the diffuse flow class (GWFC4) are not significantly different, suggesting that permeability is heterogeneous but isotropic at the core 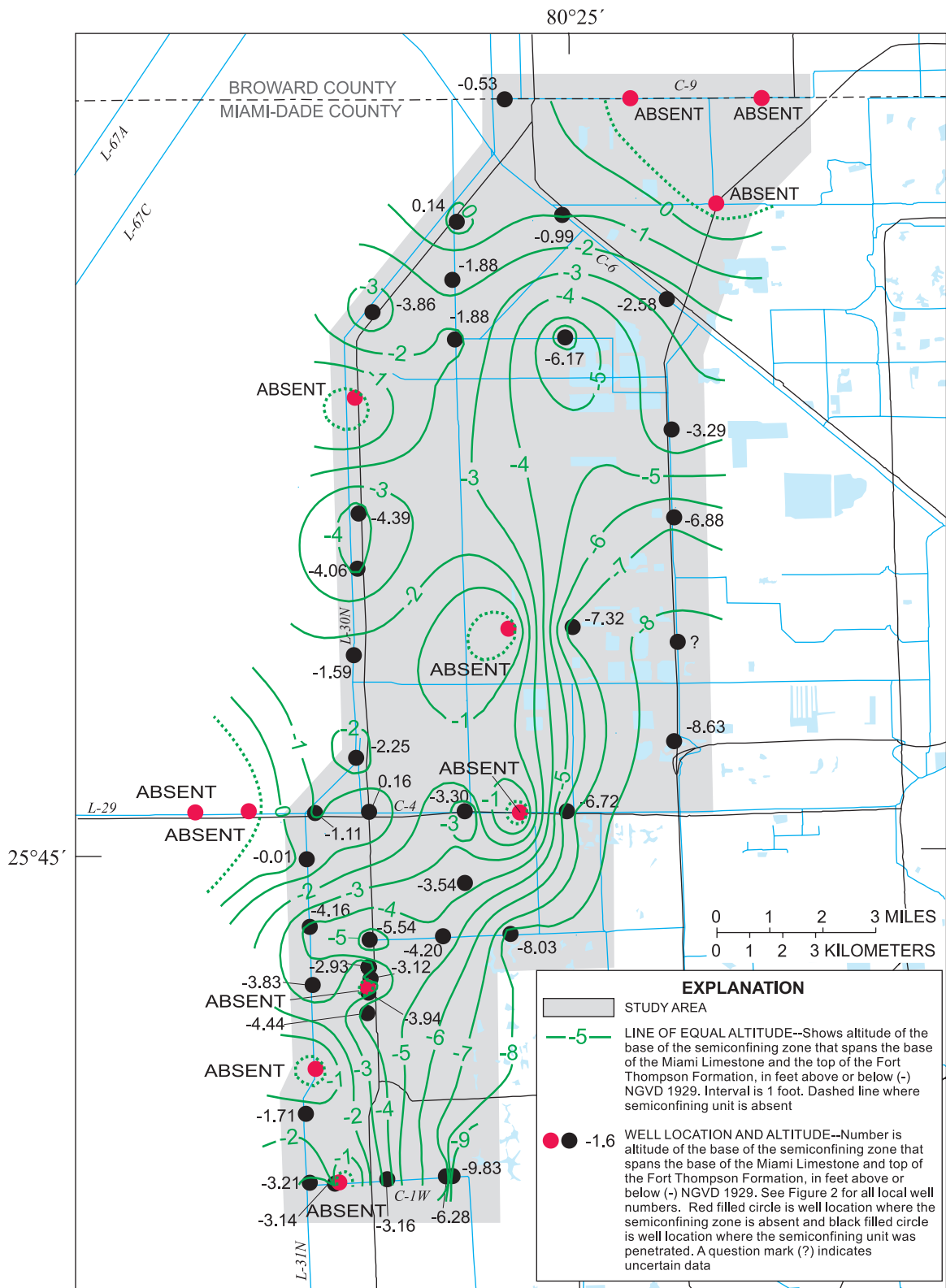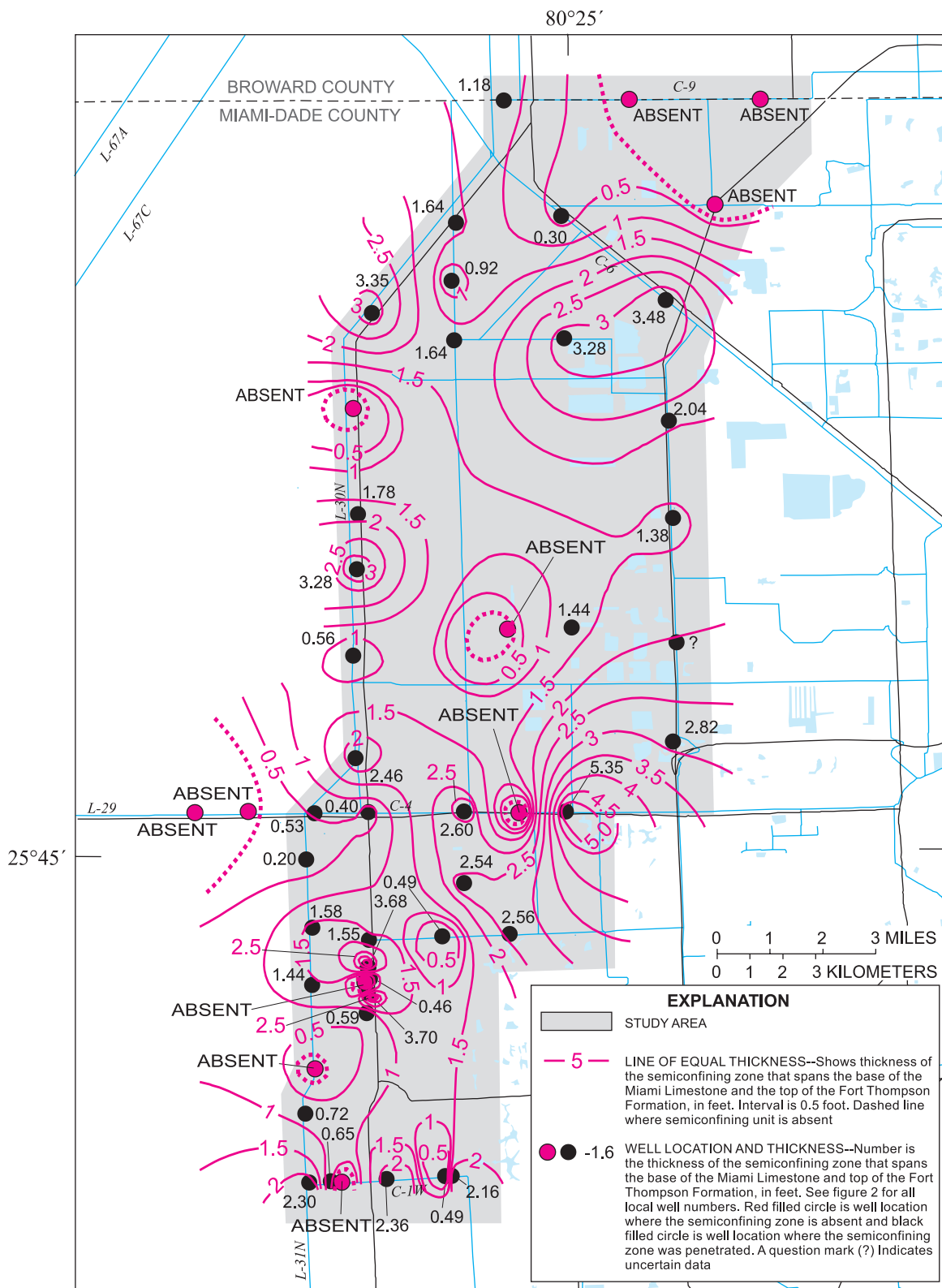scale. The hydraulic properties of diffuse flow zones have been tested only with flowmeter measurements at the G-3710 test corehole (fig. 27), and the relation between whole-core and aquifer-test permeability measurements, and hydraulic properties has not been evaluated.

High-Resolution Hydrogeologic Framework Along Selected Canals

The high-resolution hydrogeologic framework developed in this study has been projected from one-dimensional data at test coreholes onto selected study area canal walls and displayed as two-dimensional cross sections (figs. 37 and 38). These cross sections are intended to assist in any future seepage studies of the canals and evaluation of migration of surface-water microorganisms into the karst limestone of the Biscayne aquifer (Bruno and others, 2003). Most of the test coreholes for this study were drilled on right-of-ways beside canals, so the projection of the hydrogeology developed at each well onto canal walls is only across a distance of several tens of feet. The lateral conduit flow zone of HFC5 is exposed fully on the walls of most of the canals shown in figures 37 and 38. HFC3a is, at least, partly exposed in the canal walls of most canals except the C-4 and Bird Road Canals (figs. 37 and 38). The lateral conduit flow zone of HFC2 is only exposed in the canal walls of the Snapper Creek Extension Canal (fig. 37). Because the Snapper Creek Extension Canal is the deepest canal shown in figure 37, and has the greatest number of flow zones exposed along its walls, it is likely the most vulnerable to migration of microorganisms, including pathogenic varieties, into and through the network of conduit flow zones that are present in the deeper limestone of the Biscayne aquifer.

Biscayne Aquifer Pore System and Evolution

The Biscayne aquifer is an eogenetic karst aquifer. The term eogenetic karst is applied to the land surface and the pore system of young limestone (generally not older than Quaternary) undergoing shallow, meteoric diagenesis (Vacher and Mylroie, 2002) that results in a dual-porosity system consisting of matrix and conduit porosity. This differs from older karst systems contained in consolidated carbonate rock in which the rock matrix contributes little to the porosity system, and ground-water flow is dominated by conduit and fracture porosity (Vacher and Mylroie, 2002). The movement of ground-water in the karstic Biscayne aquifer is both conduit and diffuse-carbonate ground-water flow. Conduit and diffuse-carbonate ground-water flow have been documented in the Floridan aquifer system (USA), the Yucatan aquifer (Mexico), and the North Coast limestone aquifer (Puerto Rico). These three aquifers are composed largely of Tertiary rocks (Thrailkill, 1976, p. 759; Renken and others, 2002; Ward and others, 2003). Cressler (1993) described large-scale karst features of the limestone of the Biscayne aquifer, such as caves and sink holes.

Analysis of the pore system at the core scale and interpolated connection at the interwell scale indicates that ground-water flow in the Biscayne aquifer is heterogeneous, anisotropic, and mostly constrained to secondary permeability caused by solution enlargement of depositional textures, bedding planes, cracks, and root molds. All of these dissolution features are classified as touching vugs and contribute to conduit flow. The size, shape, and spatial distribution of much of the touching vugs in the Pleistocene carbonate rocks of the Biscayne aquifer are related to rock-fabric facies that are best described by a stratigraphic framework composed of HFCs. Small-scale intergrain and separate-vug porosity (Lucia, 1999, p. 26) contributes to diffuse-carbonate ground-water flow through the limestone of the Biscayne aquifer. This small-scale porosity also is related to rock-fabric facies, and its relatively high volume suggests that it contains much of the ground-water storage for the Biscayne aquifer. Figure 39 shows a three-dimensional hydrogeologic model of the arrangement of three ground-water flow classes (GWFC2, GWFC3, and GWFC4) in much of the upper part of the Biscayne aquifer. Also, shown is the relation between the three ground-water flow classes and HFCs.

Presence of small-scale, semivertical conduits within the large-scale, horizontal conduit flow zones of the Biscayne aquifer suggests enlargement of pores by dissolution during downward flow of meteoric water through the flow paths in a vadose environment at times of low stands in relative sea level. It is possible that dissolution of carbonate grains and depositional textures was especially active during flow of meteoric water along the tops of low-permeability units bounded at their tops by flooding surfaces, creating lateral flow zones near or at the base of cycles. Numerous vadose events occurred during the deposition of the limestone
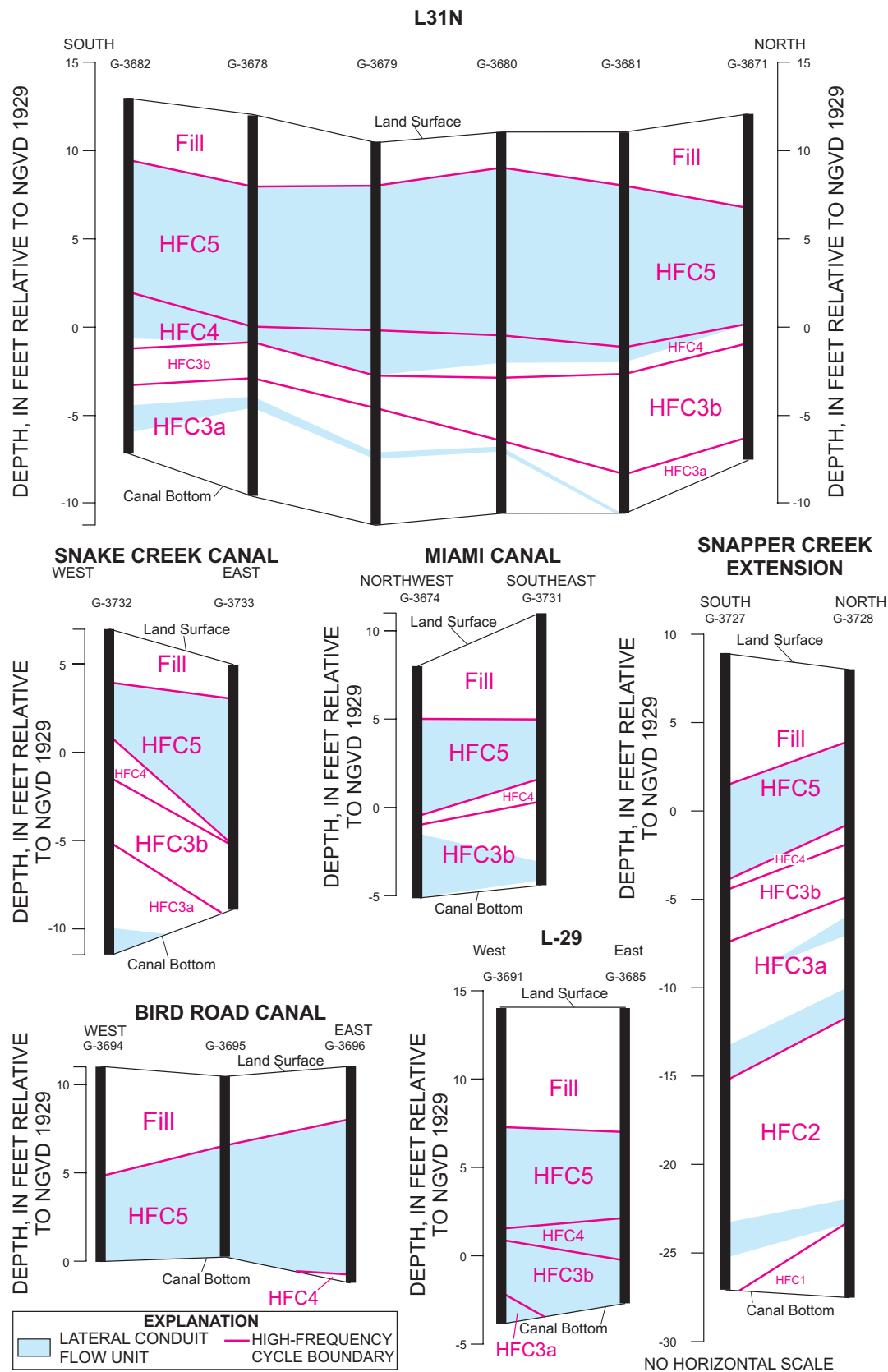
Figure 37. Cross sections of the hydrogeology of selected canal walls (L-31N, Snake Creek Canal, Miami Canal, Bird Road Canal, L-29, and Snapper Creek Extension). NGVD of 1929 is National Geodetic Vertical Datum of 1929. See figure 2 for location of canals.
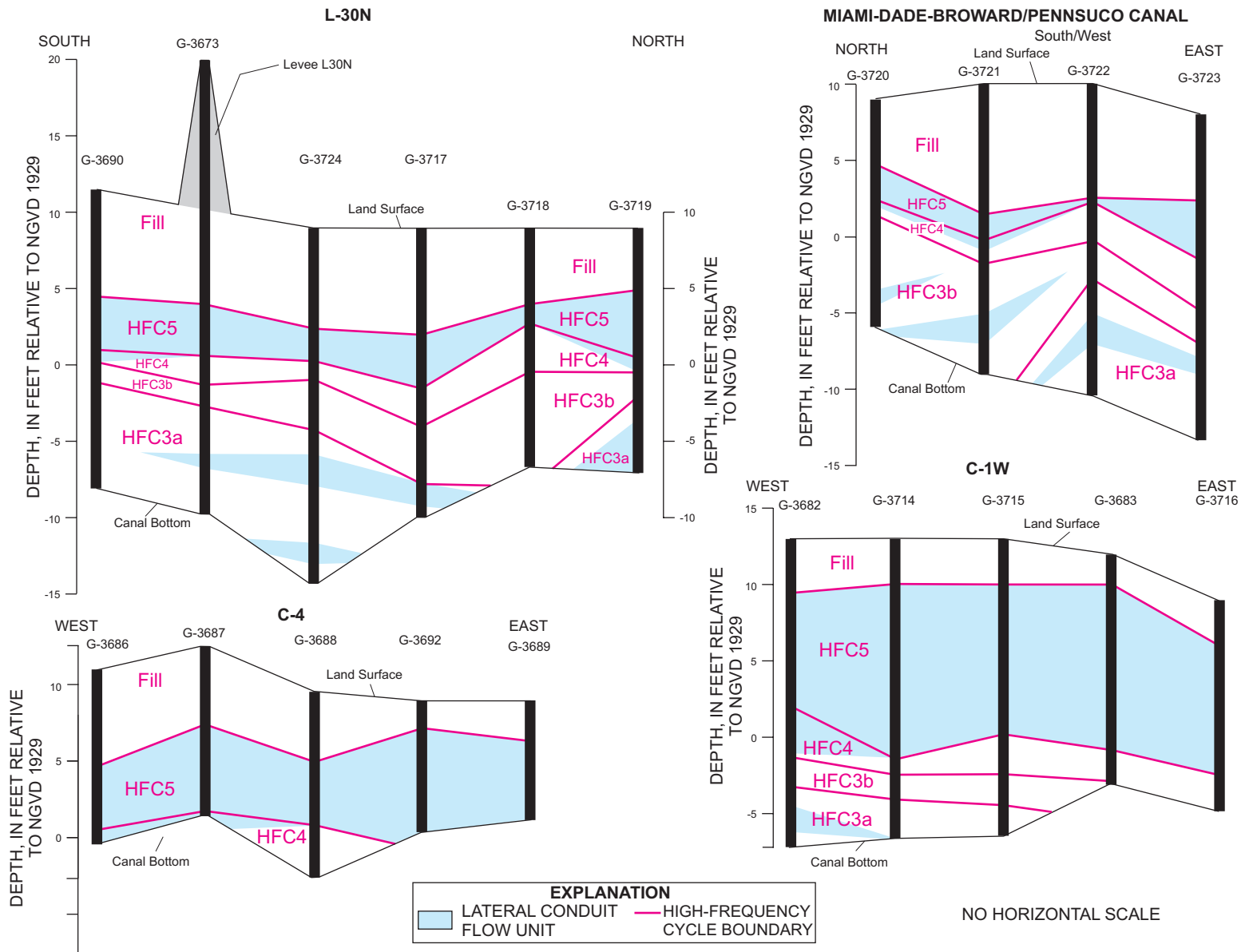
Figure 38. Cross sections of the hydrogeology of selected canal walls (L-30N, Miami-Dade-Broward/Pennsuco Canal, C-4, and C1W). NGVD of 1929 is National Geodetic Vertical Datum of 1929. See figure 2 for location of canals.
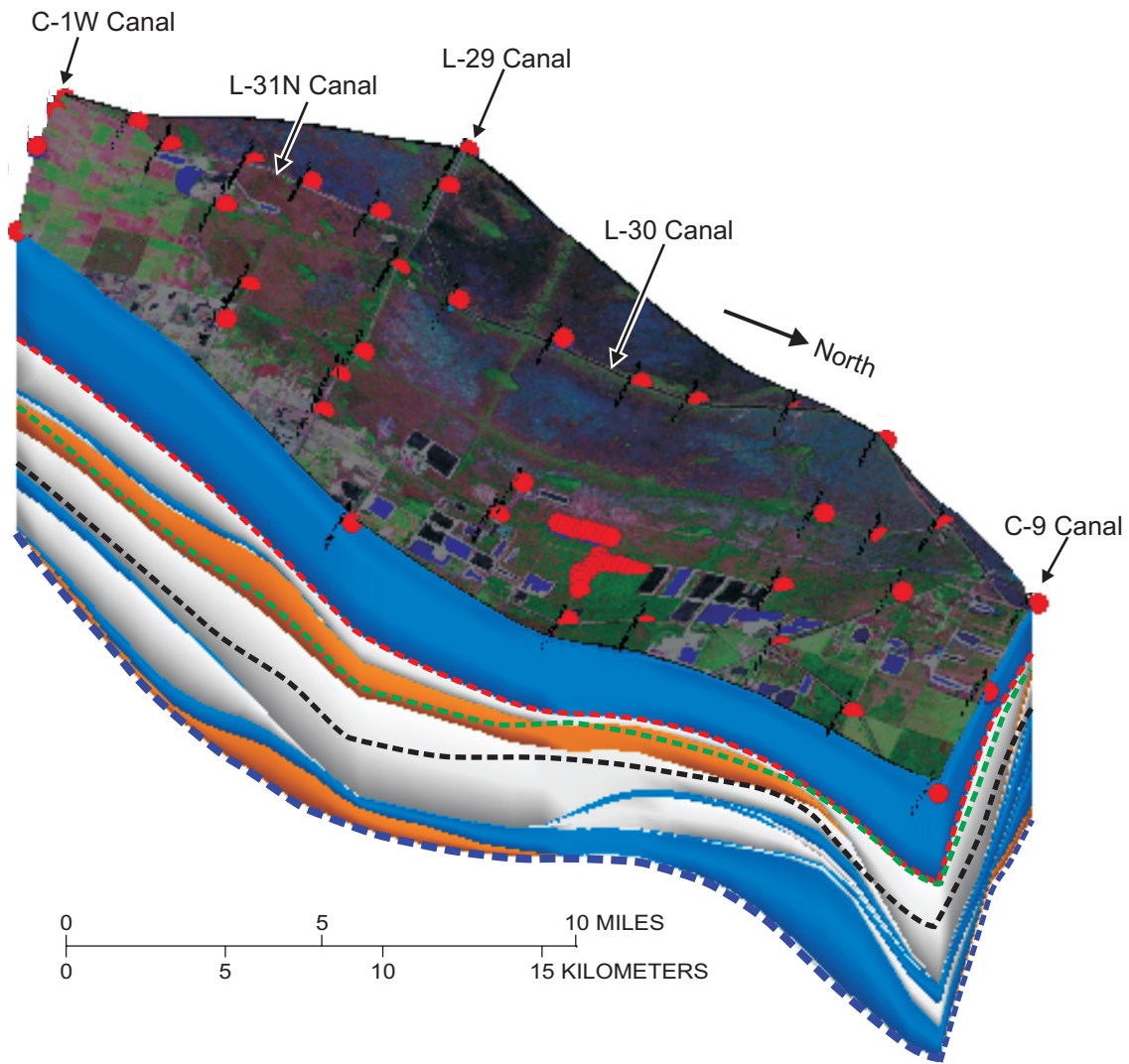
EXPLANATION

GROUND-WATER FLOW CLASS

LEAKY, LOW-PERMEABILITY GROUND-WATER FLOW CLASS

DIFFUSE-CARBONATE GROUND-WATER FLOW CLASS

HORIZONTAL CONDUIT GROUND-WATER FLOW CLASS

HIGH-FREQUENCY CYCLE

- - - - - APPROXIMATE TOP OF HFC4

- - - - - APPROXIMATE TOP OF HFC3b

- - - - - APPROXIMATE TOP OF HFC3a

- - - - - APPROXIMATE TOP OF HFC2

Figure 39. Three-dimensional hydrogeologic model of the upper part of the Biscayne aquifer for the study area in north-central Miami-Dade County. See figure 2 for location of canals.

that comprises the Biscayne aquifer, each event related to distinct relative Quaternary sea-level falls (Perkins, 1977). Cumulative dissolution along flow paths was greatest in the lower high-frequency cycles (HFC1 and HFC2) of the Fort Thompson Formation, thus, contributing to high permeability. Determining the precise ages of most of the cycles of the Miami Limestone and Fort Thompson Formation could permit calculation of the dissolution rates required to produce a network of touching vugs, and thus, a karst aquifer. The paleontology data collected during this study did not produce precise ages.

SUMMARY AND CONCLUSIONS

In southeastern Florida, ground-water supply is augmented by surface storage of water in large-scale WCA's and ENP. Surface water seeps into the Biscayne aquifer from the wetlands, then moves as ground water beneath a system of levees and canals on the eastern perimeter of the wetlands, and continues to flow toward agricultural, urban, and coastal areas to the east. Sustainable ground-water levels east of the wetlands are critical for maintaining water levels at water-supply wells and preventing saltwater intrusion at the coast. Managing the water levels in the WCA's and ENP is critical for establishing rates and volumes of water seeping from these areas to the Biscayne aquifer. A realistic, conceptual hydrogeologic model of the Biscayne aquifer, especially its karst limestone, is critical input to accurately model the movement of ground water for determining a water budget to meet natural, agricultural, and urban needs.

In 1998, the USGS, in cooperation with the SFWMD, initiated a study to provide a regional-scale hydrogeologic framework and characterization of two of the semiconfining units within the Biscayne aquifer. During the earliest stages of this study, the primary goal was to characterize and map a low-permeability unit in the upper part of the Biscayne aquifer that spans the base of the Miami Limestone and the top of the Fort Thompson Formation. Mapping of this unit was to serve as input into the SFWMD Lake Belt ground-water model. During the early phase of this investigation, collected data suggested additional hydraulic compartmentalization of the Biscayne aquifer. This led to the need to characterize and delineate all candidate flow zones and relatively low-permeability units within the upper part of the Biscayne aquifer. That is, it was realized that the historical view of the Biscayne did not adequately describe the porosity system and pathways of ground-water flow within the aquifer.

About 60 mi of GPR profiles were used to calculate depths to shallow geologic contacts and hydrogeologic units, image karst features, and produce qualitative views of the porosity distribution. Descriptions of the lithology, rock fabrics, and cyclostratigraphy, and interpretation of depositional environments of 50 test coreholes were linked to the geophysical interpretations to provide an accurate hydrogeologic framework. Molluscan and benthic foraminiferal paleontologic constraints guided interpretation of depositional environments represented by rock-fabric facies. Digital borehole images were used to help quantify large-scale vuggy porosity. Preliminary heat-pulse flowmeter data were coupled with the digital borehole image data to identify candidate ground-water flow zones.

Combined results of surface and borehole geophysics, and continuously drilled cores show that vuggy porosity, matrix porosity and hydraulic conductivity of the karst limestone of the upper part of the Biscayne aquifer have a distribution that is highly heterogeneous and anisotropic. This distribution is mostly related to a relatively predictable vertical arrangement of depositional environments and depositional textures within a carbonate architecture of HFCs. This high-resolution study of the shallow, karst Biscayne aquifer serves as a guide for developing improved and more accurate karst-aquifer models.

In general, the results of this study suggest that:

- The young (Tertiary) eogenetic karst limestone of the Biscayne aquifer has a dual-porosity system consisting of diffuse-carbonate and conduit flow zones.

- Porosity and permeability in the limestone of the Biscayne aquifer is heterogeneous and anisotropic.

- Rock-fabric facies and HFCs are two key scales for developing conceptual hydrogeologic models of shallow-water platform carbonate aquifers.

- Sixteen rock-fabric facies were identified for the Miami Limestone and Fort Thompson Formation, and these were organized into three depositional facies: (1) shallow shelf, (2) brackish, and (3) freshwater.

- Two types of HFCs are present in the Miami Limestone and Fort Thompson Formation in the Lake Belt area: (1) upward-shallowing brackish- or freshwater-capped cycles and (2) subtidal cycles.

- For young karst platform carbonates, GPR is an effective tool capable of providing a continuous two-dimensional delineation of karst features, cyclostratigraphy, and zones of relatively low and high porosity and permeability.

- Digital borehole images provide opportunities to characterize the size, shape and distribution of vuggy porosity and delineate candidate ground-water flow zones.

- A new hydrogeologic framework has been constructed for the upper part of the Biscayne aquifer that is divided into four ground-water flow classes: (1) a low-permeability peat, muck, and marl ground-water flow class; (2) a high-permeability, horizontal conduit ground-water flow class; (3) a leaky, low-permeability ground-water flow class; and (4) a diffuse-carbonate ground-water flow class.

- The horizontal conduit flow class is characteristic of a major flow zone comprising much of the upper part of the Miami Limestone, and at least, three principal flow zones within HFC3a and HFC2 of the Fort Thompson Formation.

- In the upper part of the Fort Thompson Formation, conduit flow zones are best developed near or at the base of HFCs immediately above the marine flooding surfaces and are associated with dissolution of depositional textures within specific rock-fabric facies.

- A semiconfining zone of low permeability spanning the basal Miami Limestone and upper part of the Fort Thompson Formation is typically leaky due to secondary dissolution and enlargement of cracks, root molds, and associated paleokarstic surfaces.

- Within the upper part of the Fort Thompson Formation, matrix porosity is principally lowest below flooding surfaces.

- Mapping indicates that all principal horizontal conduit flow zones have an extensive sheet-like three-dimensional geometry.

- The presence of the gastropods *Planorbella duryildisstoni*, *Planobella scalaris*, *Physa* sp.(?), *Pomacea paludosa* Say, and *Hydrobidae*(?) is useful in distinguishing freshwater limestone in the Fort Thompson Formation.

- A notable presence of archaiasinid and soritid benthic foraminifers in the peloid wackestone and packstone facies of HFC4 can be useful in distinguishing this cycle from HFC5, both HFCs of the Miami Limestone.

- The paleontology data collected during this study did not result in precise ages and almost entirely range from Pliocene to Holocene.

SELECTED REFERENCES

Abbott, R.T., 1974, American seashells: New York, Van Nostrand Reinhold Company, 663 p.

Annan, A.P., and Davis, J.L., 1976, Impulse radar soundings in permafrost: Radio Science, v. 11, p. 383-394.

Ballard, R.F., 1983, Electromagnetic (radar) techniques applied to cavity detection: U.S. Army Corps of Engineers Water Way Experimental Station Technical Report GL-83-1, Report 5, 90 p.

Barr, G.L., 1993, Applications of ground penetrating radar methods in determining hydrogeologic conditions in a karst area, west-central Florida: U.S. Geological Survey Water-Resources Investigations Report 92-4141, 26 p.

Beck, B.F., and Wilson, W.L., 1988, Interpretation of ground penetrating radar profiles in karst terrane: Proceedings of the Second Conference on Environmental Problems in Karst Terranes and their Solutions, Nashville, Tenn., November 16-18, 1988, p. 347-367.

Benson, A.K., 1995, Applications of ground penetrating radar in assessing some geologic hazards: Examples of groundwater contamination, faults, and cavities: Journal of Applied Geophysics, v. 33, no. 1-3, p. 177-193.

Beres, Milan, Jr., and Haeni, F.P., 1991, Application of ground-penetrating radar methods in hydrogeologic studies: Ground Water, v. 29, no. 3, p. 375-386.

Beres, Milan, Jr., Luester, Marc, and Olivier, Raymond, 2001, Integration of ground-penetrating radar and microgravimetric methods to map shallow caves: Journal of Applied Geophysics v. 46, no. 4, p. 249-262.

Bock, W.D., Lynts, G.W., Smith S., and others, 1971, A symposium of Recent south Florida foraminifera: Miami Geological Society Memoir 1, 245 p.

Broecker, W.S., and Thurber, D.L., 1965, Uranium-series dating of corals and oolites from Bahaman and Florida Key limestones: Science, v. 149, no. 3679, p. 58-60.

Brown and Caldwell Environmental Engineers and Consultants, 1998, Remedial action-plan: Old South Dade Landfill: Report prepared for Miami-Dade County Department of Solid Waste Management, variously paged.

Bruno, M.C., Cunningham, K.J., and Perry, S.A., 2003, Copepod communities from surface and ground waters in the southern Everglades: Southeastern Naturalist, v. 2, no. 4, p. 523-546.

Causaras, C.R., 1987, Geology of the surficial aquifer system, Dade County, Florida: U.S. Geological Survey Water-Resources Investigations Report 86-4126, 240 p., 3 sheets.

Chen, Diazhao, Tucker, M.E., Jiang, Maosheng, and Zhu, Jingquan, 2001, Long-distance correlation between tectonic-controlled, isolated carbonate platforms by cyclostratigraphy and sequence stratigraphy in the Devonian of South China: Sedimentology, v. 48, no. 1, p. 57-78.

Crary, Steve, Dennis, Bob, Denoo, Stan, and others, 1987, Fracture detection with logs: The Technical Review, v. 35, p. 22-34.

Cressler, Alan, 1993, The caves of Dade County, Florida, in Georgia Underground: Dogwood City Grotto, Inc., of the National Speleological Society, Inc., v. 30, no. 3, p. 9-16.

Cunningham, K.J., 2000, Characterization of karst in Pleistocene upward-shallowing carbonate cycles of the upper Biscayne aquifer: Implications for restoration of the Everglades hydroperiod, southeastern Florida, USA (abstract): The International Symposium and Field Seminar on Present State and Future Trends of Karst Studies, September 17-26, 2000, Marmaris, Turkey.

-------- 2004, Application of ground-penetrating radar, digital optical borehole images, and cores for characterization of porosity, hydraulic conductivity, and paleokarst in the Biscayne aquifer, southeastern Florida, USA: Journal of Applied Geophysics, v. 55, p. 61-76.

Cunningham, K.J., and Aviantara, Alexander, 2001, Characterization of the karstic Biscayne aquifer in southeastern Florida using ground-penetrating radar, digital optical borehole images and cores (abstract), in Kuniansky, E.L., ed., U.S. Geological Survey Karst Interest Group Proceedings, St. Petersburg, Florida, February 13-16, 2001: U.S. Geological Survey Water-Resources Investigations Report 01-4011, p. 134.

Cunningham, K.J., Carlson, J.I., and Hurley, N.F., 2004, New method for quantification of vuggy porosity from digital optical borehole images as applied to the karstic Pleistocene limestone of the Biscayne aquifer, southeastern Florida: Journal of Applied Geophysics, v. 55, p. 77-90.

Cunningham, K.J., and Wright, J.M., 1998, Sequence-stratigraphic interpretation and aquifer characterization as critical processes in aquifer management: Local aquifer

remediation in the Biscayne aquifer, southeastern Florida: American Geophysical Union Fall Meeting, San Francisco, Calif., Abstracts volume, p. H242.

Dagallier, Guy, Laitinen, A.I., Malartre, Fabrice, and others, 2000, Ground penetrating radar application in a shallow marine Oxfordian limestone sequence located on the eastern flank of the Paris Basin, NE France: Sedimentary Geology, v. 130, no. 3-4, p. 149-165.

Davis, J.L., and Annan, A.P., 1989, Ground-penetrating radar for high-resolution mapping of soil and rock stratigraphy: Geophysical Prospect, v. 37, no. 5, p. 531-551.

Dunham, R.J., 1962, Classification of carbonate rocks according to depositional textures, in Ham, W.E., ed., Classification of carbonate rocks: American Association of Petroleum Geologists Memoir 1, p. 108-121.

Embry, A.F., and Klovan, J.E., 1971, A late Devonian reef tract on Northeastern Banks Island, N.W.T.: Bulletin of Canadian Petroleum Geology, v. 19, no. 4, p. 730-781.

Enos, Paul, 1977, Holocene sediment accumulations of the south Florida shelf margin, in Enos, Paul, and Perkins, R.D., eds., Quaternary sedimentation in south Florida, part II: Geological Society of America Memoir 147, p. 131-198.

-------- 1989, Islands in the bay—A key habitat of Florida Bay: Bulletin of Marine Science, v. 44, no. 1, p. 365-386.

Evans, C.C., 1984, Development of an ooid sand shoal complex: The importance of antecedent and syndepositional topography, in Harris, P.H. ed., Carbonate sands–A core workshop: Society of Economic Petrologists and Mineralogists Core Workshop no. 5, p. 392-428.

Federal Register Notice, October 11, 1979, v. 44, no. 198.

Fish, J.E., 1988, Hydrogeology, aquifer characteristics, and ground-water flow of the surficial aquifer system, Broward County, Florida: U.S. Geological Survey Water-Resources Investigations Report 87-4034, 92 p.

Fish, J.E., and Stewart, Mark, 1991, Hydrogeology of the surficial aquifer system, Dade County, Florida: U.S. Geological Survey Water-Resources Investigations Report 80-4108, 50 p.

Galli, Gianni, 1991, Mangrove-generated structures and depositional model of the Pleistocene Fort Thompson Formation (Florida Plateau): Facies, v. 25, p. 297-314.

Genereux, David, and Guardiario, Jose, 1998, A canal drawdown experiment for determination of aquifer parameters: Journal of Hydrologic Engineering, v. 3, no. 4, p. 294-302.

Geological Society of America, 1991, Rock color chart: Baltimore, Md., Munsell color.

Goldhammer, R.K., Dunn, P.A., and Hardie, L.A., 1987, High-frequency glacio-eustatic sea level oscillations with Milankovitch characteristics recorded in the Middle Triassic platform carbonates in northern Italy: American Journal of Science, v. 287, no. 9, p. 853-892.

Grasmueck, Mark, 1996, 3-D ground-penetrating radar applied to fracture imaging in gneiss: Geophysics, v. 61, no. 4, p. 1050-1064.

Guardiario, J.D.A., Jr., 1996, Determination of hydraulic conductivity and dispersivity in the Biscayne aquifer, Taylor Slough, Everglades National Park: Miami, Florida International University, M.S. Thesis, 195 p.

Halley, R.B., and Evans, C.C., 1983, The Miami Limestone: A guide to selected outcrops and their interpretation: Miami Geological Society, 67 p.

Heilprin, Angelo, 1887, Explorations on the west coast of Florida and in the Okeechobee wilderness: Philadelphia, Wagner Free Institute of Science, Transactions, v. 1.

Hickey, J.J., 1993, Characterizing secondary porosity of carbonate rocks using borehole video data [abstract]: Geological Society of America, Abstracts with Programs, 25, Southeastern Section, p. 23.

Hoffmeister, J.E., Stockman, K.W., and Multer, H.G., 1967, Miami Limestone of Florida and its recent Bahamian counterpart: Geological Society of America Bulletin, v. 79, no. 2, p. 175-190.

Hunter, M.E., 1968, Molluscan guide fossils in the Late Miocene sediments of southern Florida: Gulf Coast Association of Geological Societies Transactions, v. 18, p. 439-450.

Hurley, N.F., Pantoja, David, and Zimmerman, R.A., 1999, Flow unit determination in a vuggy dolomite reservoir, Dagger Draw Field, New Mexico: Oslo, Norway. Transactions, June edition.

Hurley, N.F., Zimmerman, R.A., and Pantoja, David, 1998, Quantification of vuggy porosity in a dolomite reservoir from borehole images and core, Dagger Draw Field, New Mexico: Society of Petroleum Engineers Annual Technical Conference and Exhibition, New Orleans, La., Paper 49323, p. 789-802.

Jackson, J.A., ed., 1997, Glossary of geology (4th ed.): Alexandria, Va., American Geological Institute, 769 p.

James, N.P., 1979, Shallowing upward sequences in carbonates, Chapter 10, *in* Walker, R.G., ed., Facies models: St. John's, Geological Association of Canada, Geoscience Canada Reprint Series 1, p. 109-199.

Johnson, D.G., 1992, Use of ground-penetrating radar for water-table mapping, Brewster and Harwick, Massachusetts: U.S. Geological Survey Water-Resources Investigations Report 90-4086, 27 p.

Kaufman, R.S., and Switanek, M.P., 1998, Confinement of the Biscayne aquifer in northwest Dade County, Florida: Geological Society of America 47th Annual Meeting Southeastern Section Abstracts with Programs, March 30-31, Charleston, W.V., p. 20.

Kerans, Charles, and Tinker, S.W., 1997, Sequence stratigraphy and characterization of carbonate reservoirs: Society of Economic Paleontologist and Mineralogists Short Course Notes no. 40, 130 p.

Kindinger, Jack, 2002, Lake Belt area: High-resolution seismic reflection survey, Miami-Dade County, Florida: U.S. Geological Survey Open-File Report, 02-325, 24 p.

Klein, Howard, and Sherwood, C.B., 1961, Hydrologic conditions in the vicinity of Levee 30, northern Dade County, Florida: Tallahassee, Florida Bureau of Geology Report of Investigations 24, 24 p.

Kruse, S.E., Schneider, J.C., Campagna, D.J., and others, 2000, Ground penetrating radar imaging of cap rock, caliche and carbonate strata: Journal of Applied Geophysics, v. 43, no. 2-4, p. 239-249.

Lane, J.W. Jr., Buursink, M.L., Haeni, F.P., and Versteeg, R.J., 2000, Evaluation of ground-penetrating radar to detect free-phase hydrocarbons in fractured rocks— Results of numerical modeling and physical experiments: Ground Water, v. 38, no. 6, p. 929-938.

Lovell, M.A., Williamson, Gail, and Harvey, P.K., eds., 1999, Borehole imaging: Applications and case histories: London, Geological Society, Special Publications, no. 159, 296 p.

Lucia, F.J., 1995, Rock-fabric/petrophysical classification of carbonate pore space for reservoir characterization: American Association Petroleum Geologists Bulletin, v. 79, no. 9, p. 1275-1300.

-------- 1999, Carbonate reservoir characterization: Berlin, Springer-Verlag, 226 p.

Lyons, W.G., 1992, Caloosahatchee-age and younger molluscan assemblages at APAC mine, Sarasota County, Florida: Tallahassee, Florida Geological Survey Special Publication No. 36, p. 133-160.

Mansfield, W.C., 1930, Miocene gastropods and scaphopods of the Choctawhatchee Formation of Florida: Tallahassee, Florida Geological Survey Bulletin No. 3, 142 p.

Martinez, Alex, Kruger, J. M., and Franseen, E.K., 1998, Utility of ground-penetrating radar in near-surface, high-resolution imaging of Lansing-Kansas City (Pennsylvanian) Limestone reservoir analogs, *in* Current research in earth sciences: Kansas Geological Survey Bulletin 241, pt. 3, p. 43-59.

McMechan, G.A., Loucks, R.G., Zeng, Xiaoxian, and Mescher, Paul, 1998, Ground penetrating radar imaging of a collapsed paleocave system in the Ellenburger dolomite, central Texas: Journal of Applied Geophysics, v. 39, no. 1, p. 1-10.

Mitchum, Jr., R.M., Vail, P.R., and Sangree, J.B., 1977, Seismic stratigraphy and global changes of sea level, part 6: Stratigraphic interpretation of seismic reflection patterns in depositional sequences, *in* Payton, C.E. ed., Seismic stratigraphy—Applications to hydrocarbon exploration: American Association of Petroleum Geologists Memoir 26, p. 117-133.

Mitterer, R.M., 1975, Ages and diagenetic temperatures of Pleistocene deposits of Florida based on isoleucine epimerization in *Mercenaria*: Earth and Planetary Science Letters, v. 28, p. 275-282.

Multer, H.G., Gischler, Eberhard, Lundberg, Joyce, and others, 2002, Key Largo Limestone revisited: Pleistocene shelf-edge facies, Florida Keys, USA: Facies, v. 46, p. 229-272.

Multer, H.G., and Hoffmeister, J.E., 1968, Subaerial laminated crusts of the Florida Keys: Geological Society of America Bulletin, v. 79, no. 2, p. 183-192.

National Oceanic and Atmospheric Administration, 2002, NOAA's South Florida Ecosystem Research and Monitoring Program: accessed November 19, 2002, at http://www.aoml.noaa.gov/ocd/sferpm/sub.html .

Nemeth, M.S., Wilcox, W.M., and Solo-Gabriele, H.M., 2000, Evaluation of the use of reach transmissivity to quantify leakage beneath Levee 31N, Miami-Dade County, Florida: U.S. Geological Survey Water-Resources Investigations Report 00-4066, 80 p.

Newberry, B.M, Grace, L.M., and Stief, D.D., 1996, Analysis of carbonate dual porosity systems from borehole electrical images: Society of Petroleum Engineers Permian Basin Oil and Gas Recovery Conference, Midland, Texas, Paper 35158, p. 123-125.

Osmond, J.K., Carpenter, J.R., and Windom, H.L., 1965, ^{230}Th/^{234}U age of the Pleistocene corals and oolites of Florida: Journal of Geophysical Research, v. 70, no. 8, p. 1843-1847.

Paillet, F.L., 2000, A field technique for estimating aquifer parameters using flow log data: Ground Water, v. 38, no. 4, p. 510-521.

Paillet, F.L., and Reese, R.S., 2000, Integrating borehole logs and aquifer tests in aquifer characterization: Ground Water, v. 38, no. 5, p. 713-725.

Parker, G.G., 1951, Geologic and hydrologic factors in the perennial yield of the Biscayne aquifer: American Water Works Association Journal, v. 43, no. 10, p. 817-835.

Parker, G.G., and Cooke, C.W., 1944, Late Cenozoic geology of southern Florida with a discussion of the ground water: Tallahassee, Florida Geological Survey Bulletin 27, 119 p.

Parker, G.G., Ferguson, G.E., Love, S.K., and others, 1955, Water resources of southeastern Florida: U.S. Geological Survey Water-Supply Paper 1255, 965 p.

Perkins, R.D., 1977, Depositional framework of Pleistocene rocks in south Florida, *in* Enos, Paul, and Perkins, R.D., eds., Quaternary sedimentation in south Florida, part II: Geological Society of America Memoir 147, p. 131-198.

Poag, C.W., 1981, Ecologic atlas of benthic foraminifera of the Gulf of Mexico: New York, Academic Press, 174 p.

Posamentier, H.W., and Allen, G.P., 1999, Siliciclastic sequence stratigraphy—Concepts and applications: Society of Economic Paleontologists and Mineralogists (Society for Sedimentary Geology) Concepts in Sedimentology and Paleontology no. 7, 204 p.

Reese, R.S., and Cunningham, K.J., 2000, Hydrogeology of the gray limestone aquifer in southern Florida: U.S. Geological Survey Water-Resources Investigations Report 99-4213, 244 p.

Renken, R.A., Ward, W.C., Gill, I.P., and others, 2002, Geology and hydrogeology of the Caribbean Islands aquifer system of the commonwealth of Puerto Rico and the U.S. Virgin Islands: U.S. Geological Survey Professional Paper 1419, 139 p.

Rose, P.R., and Lidz, Barbara, 1977, Diagnostic foraminiferal assemblages of shallow-water modern environments: South Florida and the Bahamas: Sedimenta VI, University of Miami, Florida, 55 p.

Scott, T.M., 1992, Coastal Plains stratigraphy: The dichotomy of biostratigraphy and lithostratigraphy—A philosophical approach to an old problem, *in* Scott, T.M., and Missimer, T.M., eds., Plio-Pleistocene stratigraphy and paleontology of southern Florida: Tallahassee, Florida Geological Survey Special Publication No. 36, p. 21-25.

-------- 2001, Text to accompany the geologic map of Florida: Tallahassee, Florida Geological Survey Open-File Report no. 80, 30 p.

Shinn, E.A., and Corcoran, Eugene, 1988, Contamination by landfill leachate, south Biscayne Bay, Florida: Final report to Sea Grant, University of Florida, 11 p.

Smith, D.G., and Jol, H.M., 1992, Ground-penetrating radar investigation of a Lake Bonneville delta, Provo level, Brigham City, Utah: Geology v. 20, no. 12, p. 1083-1086.

Sonenshein, R.S., 2001, Methods to quantify seepage beneath Levee 30, Miami-Dade County, Florida: U.S. Geological Survey Water-Resources Investigations Report 01-4074, 36 p.

Telford, W.M., Geldart, L.P., and Sheriff, R.E., 1990, Applied geophysics (2d ed.): New York, N.Y., Cambridge University Press, 770 p.

Thrailkill, J.V., 1976, Carbonate equilibria in karst waters, *in* Karst hydrology and water resources, proceedings of the U.S.-Yugoslavian Symposium, Dubrovnik, June 2-7, 1975: Fort Collins, Colorado, Water Resources Publications, p. 745-771.

Vacher, H.L., and Mylroie, J.E., 2002, Eogenetic karst from the perspective of an equivalent porous medium: Carbonates and Evaporites, v. 17, no. 2, p. 182-196.

van Overmeeren, R.A., 1998, Radar facies of unconsolidated sediments in The Netherlands: A radar stratigraphy interpretation method for hydrogeology: Journal of Applied Geophysics, v. 40, no. 1-3, p. 1-18.

Ward, W.C., Cunningham, K.J., Renken, R.A., Wacker, M.A., and Carlson, J.I., 2003, Sequence-stratigraphic analysis of the Regional Observation Monitoring Program (ROMP) 29A test corehole and its relation to carbonate porosity and regional transmissivity in the Floridan aquifer system, Highlands County, Florida: U.S. Geological Survey Open-File Report 03-201, 34 p.

Warmke, G.L., and Abbott, R.T., 1962, Caribbean seashells: Narberth, Penn., Livingston Publishing Company, 348 p.

Wassum, L.D., 2000, Lithostratigraphic and hydrogeologic evaluation of the upper Biscayne aquifer in north-central Miami-Dade County, Florida: Miami, Florida International University, Unpublished M.S. thesis, 170 p.

Williams, J.H., and Johnson, C.D., 2000, Borehole-wall imaging with acoustic and optical televiewers for fractured-bedrock aquifer investigations: Proceedings 7th Minerals and Geotechnology Logging Symposium, Golden, CO, October 24-26, 2000, p. 43-53.